Modeling and Design of Material Recovery Facilities: Genetic Algorithm Approach

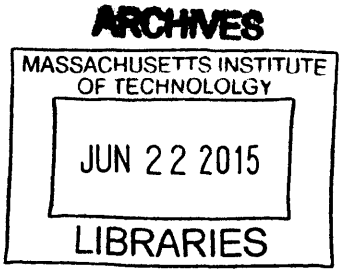

by

Mariapaola Testa

Submitted to the Sloan School of Management
in partial fulfillment of the requirements for the degree of

Master of Science in Operations Research

at the

MASSACHUSETTS INSTITUTE OF TECHNOLOGY

June 2015

Signature redacted

Author .....
Sloan School of Management
May 15, 2015

Signature redacted

Certified by .....
Stephen C. Graves
Abraham J. Siegel Professor of Management Science
Thesis Supervisor

Signature redacted

Accepted by .....
Dimitris Bertimas
Boeing Professor of Operations Research
Co-director, Operations Research Center

Modeling and Design of Material Recovery Facilities: Genetic Algorithm Approach

by

Mariapaola Testa

Submitted to the Sloan School of Management
on May 15, 2015, in partial fulfillment of the
requirements for the degree of
Master of Science in Operations Research

Abstract

In the Organisation for Economic Co-operation and Development (OECD) area, the production of municipal solid waste (MSW) increased by 32% between 1990 and 2011, exceeding 660 million tonnes in 2011; the world-wide production of waste is estimated to grow further due to increasing GDP in developing economies. Given this scenario, effective treatment and recovery of wastes becomes a priority. In developed countries, MSW is usually sent to materials recovery facilities (MRFs), which use mechanical and manual sorting units to extract valuable components.

In this work, we define a network flow model to represent a MRF that sorts wastes using multi-output units with recirculating streams. For each material in the system, we define a matrix to describe the sorting process. We then formulate a genetic algorithm (GA) that generates alternative configurations of a MRF having a given set of sorting units with known separation parameters and selects those with highest profit and efficiency. The GA incorporates a heuristic for personnel allocation to manual units. We code the algorithm in Java and apply it to an existing MRF. The results show a 33.4% improvement in profit and a 1.7% improvement in efficiency with respect to the current configuration without hand sorting; and a 6.7% improvement in profit and a 3.9% improvement in efficiency, with respect to the current configuration with hand sorting.

Thesis Supervisor: Stephen C. Graves
Title: Abraham J. Siegel Professor of Management Science

Acknowledgments

"Getting an education from MIT is like taking a drink from a fire hose."

This quote from Jerome Wiesner summarizes well my experience as a Master's student at MIT: in these two years, I have grown enormously, both professionally and personally. I would never have been able to do this alone, and I am grateful to all the wonderful people that have been on my side.

First, I would like to thank my Advisor, Professor Graves, for his guidance and support. Prof. Graves, I would like to express my immense gratitude for having taken me in your group, for always asking the right questions, and for spending time to correct my work. I hope one day I will be able to guide other people as you guided me in these years.

I would also like to thank Professor Gutowski and Anne, with whom I have worked on this project, and Eli, David, Gonzalo, and Vincente for funding my studies, providing the data, and being always reachable to answer questions.

If MIT is a great place, the ORC is even better. I am grateful to be part of this vibrant community; the co-directors, Dimitris and Patrick, are doing an amazing job in promoting a culture of cooperation in the center. In these years, I have had the opportunity of working closer with Dimitris: I was impressed by the time and attention he dedicates to all his students and by the passion with which he works hard to make the world a better place.

Thanks to all my friends of the ORC, of MITaly, and of GWAMIT, with whom I have shared wonderful moments. A special thanks to my roommates, my extended family: Virgile, Ludovica, and Cecile. Thanks to my friends all over the world. Thanks to Renee and Anita who opened my horizons.

Finally, I would like to thank my family that has been on my side in the most difficult moments, inspired me since I was young, and showed me how to be passionate, strong, and love life.

Contents

List of Figures

List of Tables

Chapter 1

Introduction

1.1 Motivation: the Role of Material Recovery Facilities in Solid Waste Management

The focus of this work is the modeling and the design of Material Recovery Facilities (MRFs), which are facilities responsible for sorting waste streams into their components. Given the increase in waste production and the variety of possible uses of waste, operating effectively and efficiently MRFs is of primary relevance.

1.1.1 Waste Production

In this work, we focus on the treatment of municipal solid waste (MSW) which is nonhazardous solid waste "collected and treated by or for municipalities". MSW "covers waste from households, including bulky waste, similar waste from commerce and trade, office buildings, institutions and small businesses, as well as yard and garden waste, street sweepings, the contents of litter containers, and market cleansing waste if managed as household waste." [6]. The quantity of MSW produced in a country is directly connected to the country's gross domestic product (GDP) and to the rate of urbanization ([6],[4]). Gathering consistent and comparable data about waste production in different countries is complex because of decentralization in waste management practices and of the lack of clear waste classification standards. Taking into account this limit, it is estimated that in 2006 the quantity of waste produced globally exceeded 2.02 billion tonnes [7] and that the quantity of MSW generated in the Organisation for Economic Co-operation and Development

(OECD) area has risen by more than 32% between 1990 and 2011, exceeding 660 million tonnes in 2011 [6]. Figure 1-1 shows the per capita MSW generation in the OECD countries. Interestingly, in recent years waste production has risen at a lower rate than private final consumption and GDP (see Figure 1-2), suggesting a more efficient and responsible use of the resources. In developing countries such as India and China, the per-capita production of waste (less than 0.5 kg/day/capita in India and less than 0.9 kg/day/capita in China) is still far below that of most OECD countries (up to 2.1 kg/day/capita in the USA) [8]; the East Asia Infrastructure Department of the World Bank estimates that by 2030 China and India will both overtake the U.S. waste production [9].

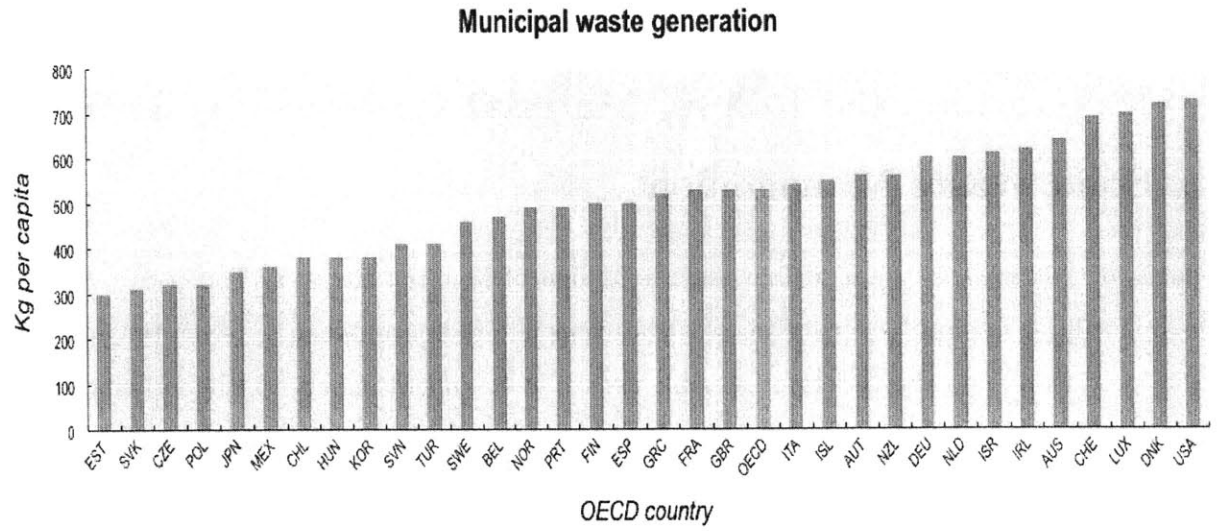

Figure 1-1: Muncipal waste per-capita generation in 2010 or latest available year in the OECD countries. *Source: http://dx.doi.org/10.1787/888933026088*

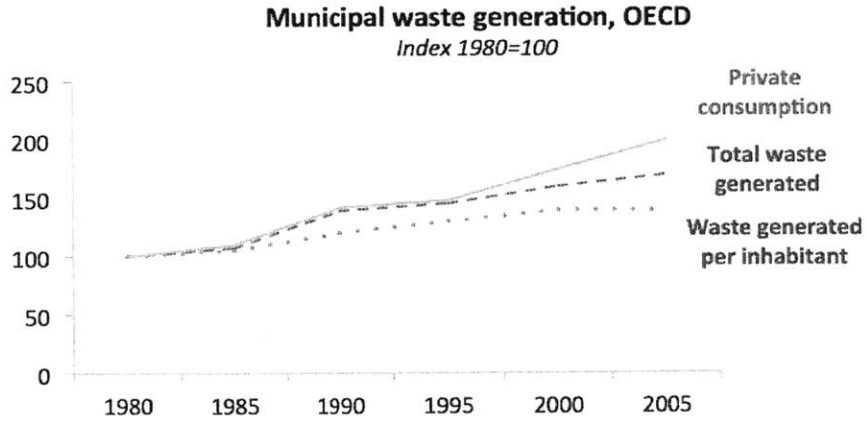

Figure 1-2: Trend in per-capita MSW generation, total MSW generation, and private consumption for the OECD countries. *Source: http://www.oecd.org/environment/indicators-modelling-outlooks/37551205.pdf*

1.1.2 Resource Recovery and Disposal Strategies

Possible uses of MSW include recycling, composting, energy production, and landfill disposal. Looking at aggregated waste management trends in developed countries, in 2012, the U.S. recycled 26% (by weight) of the waste produced, composted 8%, sent to combustion with energy recovery 11%, and sent to landfill or to incineration without energy recovery the remaining 45% [11]. In the OECD E.U. countries, instead, 25% of the waste produced is recycled, 14% composted, 20% sent to combustion with energy recovery, 4% sent to combustion without energy recovery, and 37% sent to landfill [10]. Figure 1-3 shows the quantity of MSW produced in and the disposal strategy adopted by the U.S., Korea, Italy, Germany, and France in 2010. The charts in Figure 1-3 show how Korea has the highest recycling rate (recovering 60% of the total waste produced) and how Germany has substituted landfill with incineration.

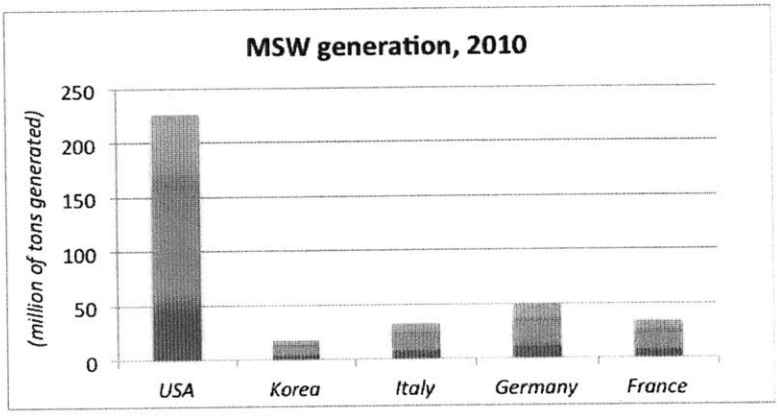

(a) Million of tons produced in selected countries.

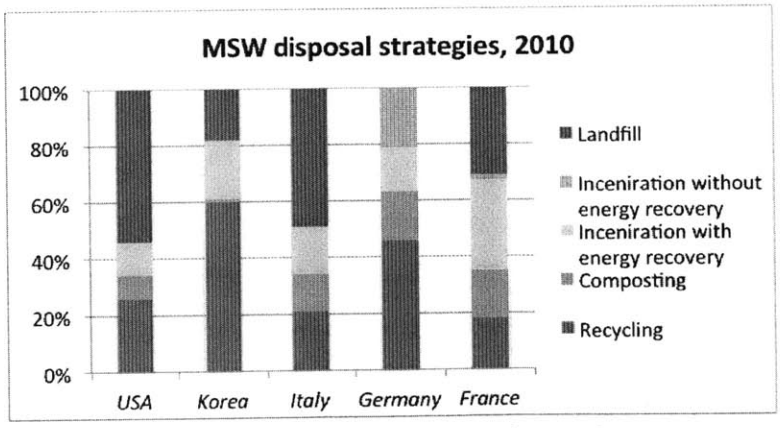

(b) Disposal strategies in selected countries.

Figure 1-3: Municipal solid waste generation data and disposal strategies in the U.S., Korea, Italy, Germany, and France in 2010. Adapted from [10]

Recycling comprises "a series of activities whereby discarded materials are collected, sorted, processed, converted into raw materials, and used in the production of new products"; it "does not include the use of these materials as a fuel substitute for energy production" [15]. Recycling generates consistent savings in energy consumption; for example, the amount of energy necessary to recycle aluminum is approximately 5% of the energy required to produce the virgin metal [15]. Recycling has also greater energy-saving advantages than incineration [15]. For example, paper recycling saves three to four times more energy than the energy captured from the incineration of the same materials [15]. Recyclable materials include metals (e.g., steel, aluminum, copper), plastics (e.g., HDPE, PET), paper, cardboard, and glass. In 2012, the U.S. recovered approximately 34.5% of recyclable materials [3]; figure 1-4 shows the recovery of different product categories.

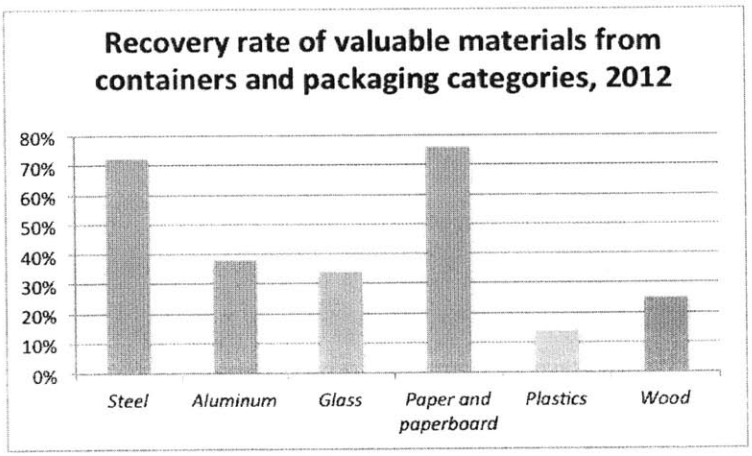

(a) Recovery rate of valuable materials from the light packaging and container categories.

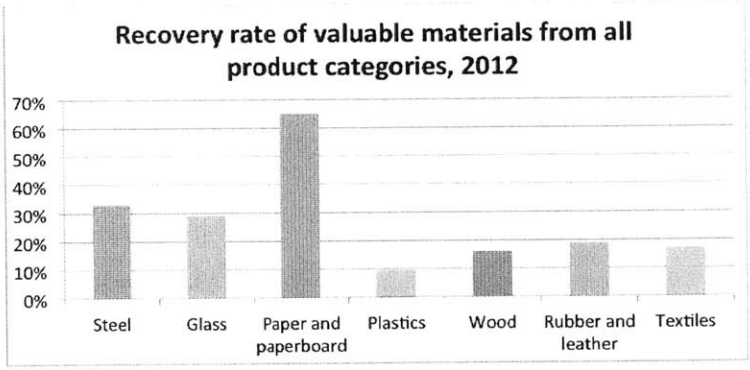

(b) Recovery rate of valuable materials considering durable, non-durable goods, light packaging, and containers.

Figure 1-4: Percentage of material recovered in the U.S. in 2012 by weight. It was not possible to compute the aggregate recovery rate for aluminum because of missing data in the amount of material recovered in the durable goods category. *Source: [3]*

The organic biodegradable component of waste can be used as [3]:

- Soil amendment. Garden and crop debris, animal and human organic wastes (after having properly treated human excreta), and food preparation and processing wastes can be used without further processing as soil amendment for its beneficial effect on the structural characteristics of the soil and for its minor content of fertilizing chemicals, such as nitrogen (N), phosphorous (P), and potassium (K).

- Compost. Composting refers to the "biological decomposition of biodegradable solid waste under controlled predominantly aerobic conditions to a state that is sufficiently stable for nuisance-free storage and handling and is satisfactory matured for safe use in agriculture" [3]. Composting facilities have become one of the most viable options for waste recycling in economically developing countries because of their low equipment and operating costs.

- Feedstock in hydrolysis for ethanol fermentation or for single-cell protein production. Organic waste can be used as the substrate for micro-organisms in the production of single-cell proteins or in the production of ethanol.

MSW also finds application as a source of energy; currently, it can be used [3]:

- Raw. In this case unprocessed waste is directly burnt in incinerators. This procedure allows for the reduction of waste volume as well as the reuse of the heat produced.

- As refuse-derived fuel (RDF). RDF is obtained by shredding waste components with high calorific power. This process usually takes place in a Material Recovery Facility, where MSW is sorted, screened, and shredded.

- As source for biogasification. Biogasification consists in the anaerobic treatment of the organic fraction of waste to produce methane. The production process is also known as "anaerobic digestion".

- As source for thermal gasification. Thermal gasification consists in the fractional distillation of waste under partially O_2-free conditions, in a process that generates gases, liquids (tars), and solids (chars). Both the biodegradable and the non-biodegradable fraction of waste cane bes used for thermal gasification. This process is also known as "waste pyrolysis".

The portion of MSW that is neither recycled nor used as a source of energy is disposed in sanitary landfills. Table 1.1 summarizes the current possible usages of waste components.

Waste component	Destination
Inorganic fraction	Recycling and reuse of valuable materials. Solid refused fuel. Thermal gasification. Incineration with or without energy recovery. Sanitary landfill.
Organic fraction	Soil Amendment. Compost for agriculture. Feedstock in single cell protein and ethanol production. Biogasification and thermal gasification. Incineration with or without energy recovery. Sanitary landfill.

Table 1.1: Destination of waste. Based on [3].

1.1.3 Importance of Material Recovery Facilities

Material Recovery Facilities (MRFs) are facilities responsible for sorting wastes into different components. These may include inorganic materials that can be recycled (e.g., plastics and metals), organic materials that can be composted, or combustible materials that can be used in energy production. For this reason, MRFs represent an important step in solid waste management (SWM). The increasing relevance of these facilities is demonstrated by the fact that, in the U.S., the number of MRFs sites, the revenues generated, and the number of employees in the industry have been growing considerably since 2011 (see Tables 1.2 and 1.3).

	2010	**2011**	**2012**	**2013**	**2014**
Establishments	1,197	1,189	1,239	1,291	1,358
Sales *($millions)*	3,840	4,055	4,495	4,959	5,534
Employment	19,339	19,230	19,991	20,779	21,795

Table 1.2: Number of establishments (MRF sites), revenues generated, and number of employees in MRF industry in the U.S. in 2013. Source [20].

	2010-11	**2011-12**	**2012-13**	**2013-14**
Establishments	-0.7%	4.2%	4.2%	5.2%
Sales *($millions)*	5.6%	10.9%	10.3%	11.6%
Employment	-0.6%	4.0%	3.9%	4.9%

Table 1.3: Percentage change year-to-year in the number of establishments (MRFs sites), revenues generated, and number of employees in MRF industry in the U.S. in 2013. Source [20].

1.2 Overview

The focus of this work is the modeling and the design of MRF sorting operations. As previously done by [46], we use a graphical model to describe the sorting system: nodes represent sorting equipment, and arcs represent material flows. We introduce a set of linear equations that can be solved in matrix form to compute material flows. The conditions under which the system of equations is well defined are discussed. We develop a genetic algorithm to generate different configurations and identify those with higher profit and efficiency (measuring the ability of correctly separating materials). As a part of the genetic algorithm, we define a heuristic to allocate personnel to manual sorting operations. Finally, we apply the model and the genetic algorithm to a real case and discuss the results.

This work is part of a larger project that aims at developing models for MRFs; future research will focus on conducting additional analysis to obtain better estimates of units sorting parameters (i.e., the fraction of material entering into a unit that is diverted to a specific output stream) and to further validate the model.

The structure is the following:

- **Chapter 2.** This chapter introduces MRF operations, describes the pieces of equipment that are most frequently found in the waste sorting industry, identifies the principles that currently guide MRFs design, presents two examples of MRFs configurations, and focuses on the economic performance of MRFs.
- **Chapter 3.** In this chapter, we review the literature on mathematical modeling of MRFs and introduce the proposed model and the metrics used to evaluate MRFs performance.
- **Chapter 4.** In this chapter, we introduce genetic algorithms, formulate the problem, and apply genetic algorithms to find its solution.
- **Chapter 5.** In this chapter, we present a MRF, apply the proposed mathematical model to the facility, and use the genetic algorithm to identify alternative configurations to the one currently adopted.
- **Chapter 6.** Conclusions are drawn.

Chapter 2

Material Recovery Facilities

A key phase in waste management consists in recovering specific materials from municipal solid waste (MSW). In developed countries, this task is primarily conducted in Material Recovery Facilities (MRFs), which sort MSW into different components that can either be used for recycling (e.g., plastics, metals, paper, and glass), composting, energy-production, or disposal. According to a 1995-96 study ([32]) by Governmental Advisory Associates, a MRF is a facility that:

1. Processes a multi-material stream and sells its components to end users, brokers, or value-added resellers.

2. Receives some fraction of this stream as commingled recyclables requiring further sorting. Sorting can be done by any combinations of manual and mechanized approaches.

3. Participates directly or indirectly in municipally structured waste program.

MRFs are usually constituted of a dumping area, a sorting plant, and a storage space, and may incorporate a landfill, a composting facility, and an energy-from-waste facility; they may also work as transfer stations for waste. The waste entering into a MRF is generally collected in a tipping floor or in a bunker, which works as a buffer to stabilize the flow of processed material within the facility. In this work, we focus on the sorting process that is used to extract different materials from the waste stream, without considering additional related operations, such as composting or energy-production from waste.

This chapter addresses MRFs operations, presenting the characteristics of the waste processed, the technologies most widely employed, the main principles regulating MRF design, and the economic scenario.

2.1 What is Sorted: Municipal Solid Waste

Municipal Solid Waste (MSW) is nonhazardous solid waste consisting of "everyday items we use and throw away, such as product packaging, grass clippings, furniture, clothing, bottles, food scraps, newspapers, appliances, paint, and batteries. MSW comes from homes, schools, hospitals, and businesses" [2] and can have a residential (e.g., households), a commercial (e.g.,businesses), or an institutional origin (e.g., schools). Moreover, it can be classified either by material type (e.g, aluminum, ferrous, plastics), or by product category. Different product categories are durable goods (e.g., furniture), non-durable goods (e.g., newspapers), containers and packaging (e.g., milk cartons), and other materials (e.g., food waste and yard trimming). MSW is typically measured by its mass, which is relatively constant except for variations in the moisture content ([34]), or by its volume, especially with applications to landfill design and transportation.

There are several possible ways to classify waste on the basis of the application. At an operational level (e.g., for MRF process design) waste should be classified into as many categories as can be foreseen in order to avoid doing other measurements to respond to market or regulatory changes [12]. Table 2.1 reports Stessel's suggested categorization of waste into its constituent components.

Category	Sub-categories and individual materials
Ferrous metals	Iron, steel, stainless steel. Cast, extruded, forged, rolled.
Non-ferrous metals	Aluminum: cast, extruded, rolled.
	Other metals: copper, brass, nickel, titanium, and magnesium.
Paper	Newspaper, glazed (magazines), office paper, computer paper, card stock: white or colored.
	Corrugated cardboard, kraft paper.
Film plastics	Low-density polyethylene, polypropylene.
Rigid plastics	High-density polyethylene, polyethylene terephthalate, polyvynil chloride, polyurethane.
Food waste	Meat, vegetable.
	Agricultural waste: meat processing, dairy, food crop wastes.
	Fast food: restaurant, institutional.
Yard waste	Tree trimmings, leaves, grass, agricultural waste.
Construction and demolition	Stone products: stone, brick, concrete. Lumber, wallboard.
	Construction materials: paints, solvents, adhesives, and caulks.

Table 2.1: Typical waste categories. Source [12].

The composition and the generation of waste is determined by several factors. According to Stessel (1996) [12], key factors include:

- Climate. Climate affects environmental characteristics, which impact on waste production. For example, in a semi-tropical climate there is a higher generation of yard waste than in a continental one.

- Infrastructure. Infrastructure and urbanization affect the type of waste produced because they affect every day habits of the population. For example, in heavily urbanized areas that are automobile-dependent, there is the tendency of shopping less frequently in great quantities, and this results in more packaging wastes.

- Business and institutions. Certain waste produced by institutions and business is considered MSW, and thus the presence of specific economic activities affects the composition of waste. For instance, a college town or the presence of educational institutions increases the production of paper.

- Socio-economics. Economic and social factors affect MSW because they affect the way in which people consume. For example, very poor people do not have ready cash to buy cost effective large-sized containers and thus they consume a higher quantity of smaller containers, increasing the content of light packaging in waste. As a second example, the presence of older people in an area increases the quantity of medical wastes from home health care.

- Time. Waste composition presents a weekly and yearly seasonality, reflecting both changes in climate as well as changes in people's activities. For example, during weekdays there is a higher quantity of waste generated by businesses and institutions than on the weekends. As a second example, in beach resorts there is a higher production of waste in summer, due to the higher flux of tourists.

Figure 2-1 shows how the material composition of MSW varies in different countries.

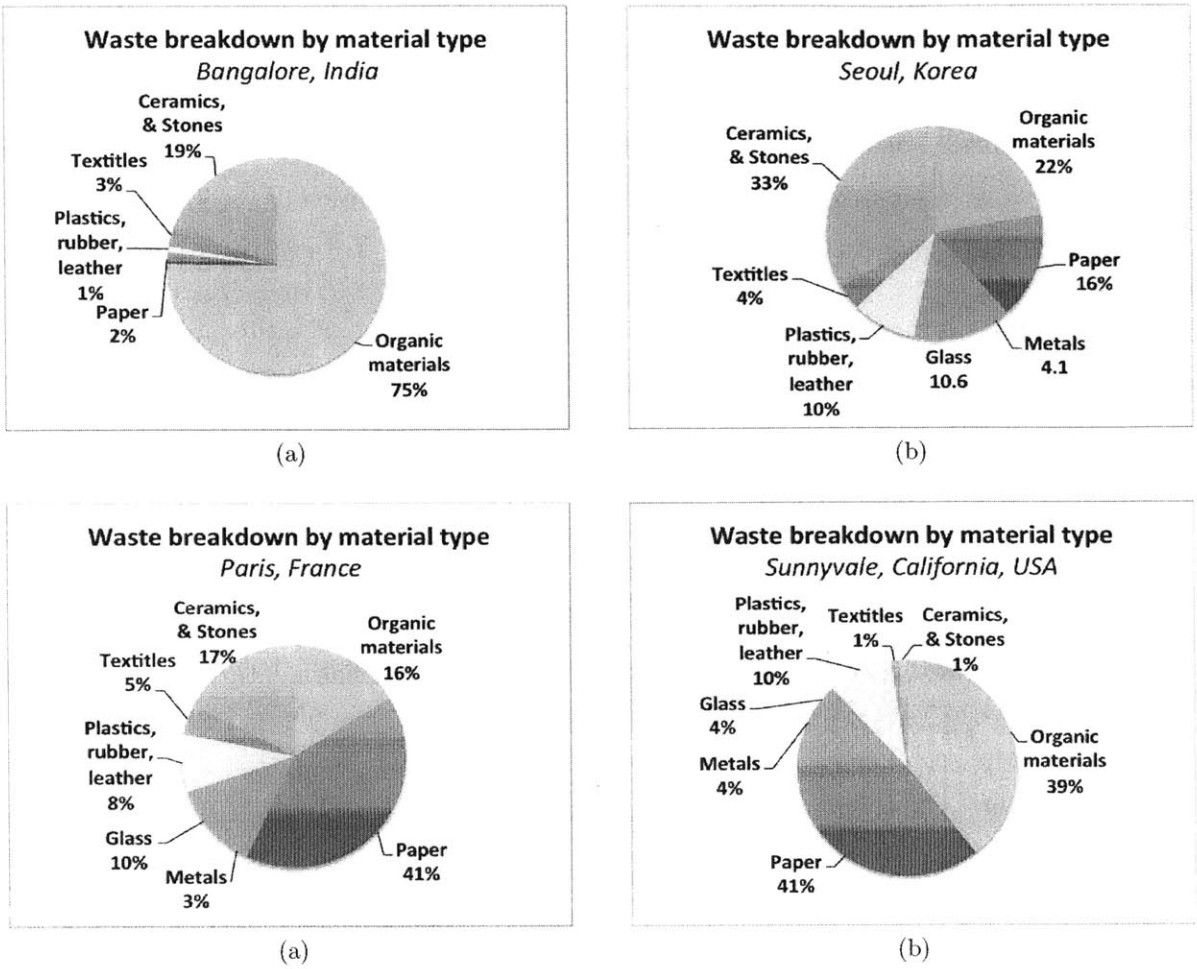

Figure 2-1: Municipal solid waste in different regions of the world. Breakdown by material composition. *Source: [3].*

The composition of waste processed by a MRF is affected by the waste-collection system implemented, which can be classified either on the basis of the collection procedure or on the type of streams generated. There are four major types of waste collection procedures [3]:

- Communal collection. The waste generated is collected in large communal sites; the generator takes care of the transfer from the location of generation to the communal collection center.
- Block collection. The generator brings the waste to the vehicle at the time of collection.
- Kerbside collection (or curbside collection). The generator leaves the waste in containers outside of the location of generation, the collector retrieves the waste leaving the emptied container at the site.

- Door-to-door collection. The generator is not involved in the collection process; the collector enters the premises and retrieves the waste.

If we classify waste-collection systems by stream generated at the origin, we have:

- Single-stream recycling (or "fully commingled", "single-sort" recycling). In this system, MSW is collected in a single stream and is then sent to a MRF for sorting.

- Wet-dry recycling. There are two major ways of applying the wet-dry system. The first consists of two streams: one for "wet" materials (e.g., food waste, yard waste, disposable diapers, and soiled paper) and one for everything else (both recyclables and non-recyclables components). The second system, instead, consists of three streams: one for "wet" compostables, one for "dry" recyclable materials, and one for the rest [16].

- Multi-stream recycling. In this system, waste generators separate waste according to material types. For example, different streams may be generated for paper and cardboard, plastics, glass, biodegradable waste, and other wastes.

When comparing single-stream, wet-dry, and multi-stream recycling, it is necessary to take into account several factors, such as the impact on the collection and transportation systems, the rate of participation of the population, and quantity and purity of material recovered at MRFs. On the one had, single-stream recycling has the advantages of:

- Having low complexity for waste generators;

- Reducing the costs of collection since the trucks used for commingled waste are cheaper to purchase and operate;

- Increasing fleet flexibility and efficiecy in waste collection;

- Having more material sent to MRFs, which may lead to the introduction of new categories of material recovered.

On the other hand, the disadvantages of single-stream recycling are primarily connected to the higher burden placed on MRFs, since separating heterogeneous streams is more complicated than separating homogeneous ones and increases processing costs ([18], [19]). Multi-stream recycling is the opposite of single-stream recycling in that it places the higher burden on the generator

and the collection system, while reducing the complexities of the operations of MRFs. Applying multi-stream recycling does not guarantee that the different streams segregated at the origin are not contaminated. When this happens, either the entire lot is sent to landfill, or a MRF is needed to better separate valuable materials contained in the stream. Moreover, multi-stream recycling also requires constant education of waste generators, who need to be informed about changes in recycling practices and in the material composition of the objects discarded. Wet-dry systems represent an intermediate solution between single-stream and multi-stream recycling, combining a relatively low burden on the waste generator with medium complexity for MRFs. This is primarily a consequence of the fact that the organic fraction of material is one of the major sources of problems in the operations of MRFs, and the wet-dry collection system separates the wet organic fraction from the rest.

2.2 Unit Processes

A MRF is constituted of unit processes that perform one of the following functions:

- Separate materials either on the basis of particles characteristics (e.g., size, shape, and mass), or of material properties (e.g., magnetism or color).
- Change particles characteristics, for example by shredding or compacting material.

The number and the type of units employed vary depending on the nature of the waste stream processed and the specifications on the extracted materials. Unit processes used in a MRF can be either mechanical or manual. Mechanical processes can be classified on the basis of their function into material-handling, separating, size-reducing, environmental control, and other auxiliary processes (e.g., scales). Tables 2.2-2.3 list pieces of equipment often employed in a MRF and their category.

In this section we describe different unit processes used for the handling, size reduction, and separation of MSW in material recovery facilities.

Material Handling				
Type	**Unit**	**Function**	**Material**	**Preprocessing**
Material handling	Feed crane	Collection of material from the tipping floor or the bunker. Placement of the material on the main feeder connected to the rest of the system.	All wastes.	
	Main feeder	Material transportation.	All wastes.	
	Conveyor belt	Materials transportation and support for manual separation.	All wastes.	Removal of large bulky items.

Table 2.2: Function and preprocessing for material-handling equipment. Adapted from [34].

Size Reduction				
Type	**Item**	**Function**	**Material**	**Preprocessing**
Shredder	Hammermill	Size reduction.	All wastes.	Removal of large bulky items and contaminants.
	Flail mill	Size reduction and bag breaking.	All wastes.	Removal of large bulky items and contaminants.
	Shear shredder	Size reduction and bag breaking.	All wastes.	Removal of large bulky items and contaminants.
	Glass crusher	Size reduction of glass.	Glass.	Removal of all non-glass materials.
	Wood grinder	Size reduction of yard trimmings.	Yard waste.	Removal of large items.
Densification	Baler	Compaction into bales.	Paper, cardboard, plastics, textile, aluminum.	Component Separation.
	Can crusher	Compaction into bales and flattening.	Aluminum and tin cans.	Removal of large bulky items.

Table 2.3: Function and preprocessing for size-reducing equipment. Adapted from [34].

Sorting Units				
Type	**Unit**	**Function**	**Material**	**Preprocessing**
Separation by particle properties	Screens	Separation of material by size.	All wastes.	Removal of large bulky items, large cardboard pieces, and glass bottles that may brake during the screening process.
	Air classifier	Separation of light materials on the basis of aerodynamic properties.	All wastes.	Removal of large cardboard and bulky items. Shredding of waste can improve the performance of the unit, at the expenses of following sorting operations.
	Ballistic separation	Separation occur on the basis sorts materials on the basis of particles elsticity and aerodynamic properties.	All wastes.	Removal of large cardboard and bulky items.
Separation by material type	Magnet	Separation of ferrous metal.	Ferrous and magnetic materials.	Removal of large bulky items and large cardboard pieces.
	Eddy-current separator	Separation of non-ferrous metal. Ferrous metals are also separated.	Metals.	Removal of large bulky items and large cardboard pieces.
	Detect-and-route system	Separation of materials on the basis of properties that can be detected by sensors (primarily optic sensors).	Plastics and glass.	Removal of small objects that can interfere with proper material detection. Low bed of the feed to guarantee that objects are well exposed to sensors.

Table 2.4: Function and preprocessing requirements for sorting equipment in a MRF. Adapted from [34].

Conveyors

Material within the facility is moved on conveyors. There are several conveyor systems, the belt conveyor is the most widely used one. Belt conveyors are constituted of a belt moving about drums at either ends of a supporting frame (see Figure 2-2). There are two drums in the conveyor: the tail rotor, which is non-powered and is usually located at the beginning of the conveyor with respect to the direction of material flow, and the head rotor, which is attached to a motor and is located on the other extremity of the belt. The head rotor is responsible for the motion of the conveyor. The frame of the structure on which the belt is located is called support plate. Conveyors are usually operating with a positive angle to the horizontal, and thus flights are used against the slippage of the material. The conveyor belt can either be flat or concave (in the so called "U-shaped" conveyor); flat conveyors require walls to prevent material from falling off the belt, while U-shaped conveyors require the belt to bend more around the rotors thus causing accelerated wear [12].

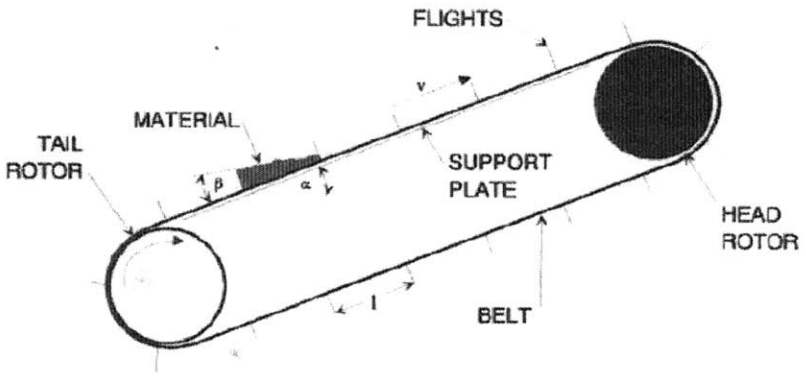

Figure 2-2: Diagram of an inclined belt conveyor. α is the angle of incline of the conveyor with respect to the horizontal, and β is the angle that the surface of the material between flights makes with the longitudinal axis of the conveyor. Source [12].

Size Reduction

There are two major categories of size-reduction processes: compaction and shredding. Compaction (or densification) consists in volume reduction and is primarily employed to facilitate material transportation and has the effect of reducing transportation costs and disposal fees when charged by cubic meter and not by weight. Compactors are often called "balers" because the compacted material is wrapped or tied [3].

Shredding results in particle-size reduction and is primarily used to produce refuse derived fuel and to improve the characteristics of waste prior to landfill because it:

- Increases the exposure to and the passage of air, minimizing odor at the surface;
- Dries the garbage;
- Reduces the attractiveness of waste to insects and rodents when combined with proper aerobic conditions and landfill operations.

Shredding should not be employed in the initial stages of waste separation processes, because uniform reduction of all materials may compromise the effectiveness of specific unit operations. This is the case, for example, of detect and route systems, which use sensors to classify materials and need big-enough objects to operate on. An exception are shredders employed as bag openers that should be placed as one of the first units in the system since they assure that all waste is properly treated. Shredders may have the effect of drying wastes by reducing the content of moisture, increasing the value of RDF, reducing transportation costs, and limiting unpleasant smells [12]. There are three major types of shredding techniques:

1. Shear. Blades rotate in different directions as in the action of scissors.
2. Grinding. Friction is applied to the surface of an object, as when stone-polishing a drum.
3. Crushing. A force is directly applied to the surface of an object, as in can-crushers used in household recycling where a load is directly applied to the cans.

There is a wide variety of technologies employed for shredding. The most used in waste management are [12]:

- Tub grinders. These are semi-circular containers, equipped with arms tipped with wheels that rotate against the side of the tub. The arms perform a combination of crushing, grinding, and shearing. Tub grinders are primarily used for relatively homogeneous waste composed of large materials, such as yard waste containing tree trunks, or construction and demolition debris. Tub grinders act fairly slowly, turning at less than 100 rpm, and consume less than 200 kW [12].

- Shear-shredders. Shear-shredders can be either constituted of counter-rotating blades or by a bank of scissors pointed upwards, aligned at their pivot. These units are often positioned off-line and are fed with bulky material. They require the use of sensors or other control-systems to avoid jamming [12]. Figure 2-3 shows an example.

- Flail mills. Flail mills are constituted of a rotor equipped with either blades or articulated arms. These units require low-maintenance and low energy; typical power is 50 kW, with rotor speeds up to 1500 rpm. They are often employed as bag-breakers, with the function of releasing, rather than size-reducing, bag contents [12].

- Hammermills. Hammermills are the most widely used shredder in MRFs. They are constituted of a rotor with hammers and can be either vertical or horizontal (see Figure 2-4). These units operate at 1000 rpm and require high power (often operating at 700 kW) and maintenance, since hammers and walls are subject to high wear [12].

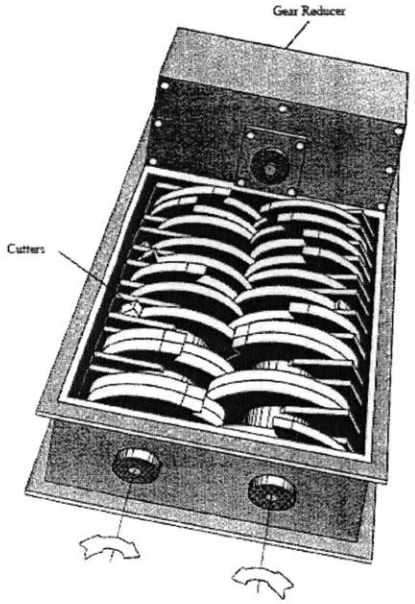

Figure 2-3: Shear shredder. Source [12].

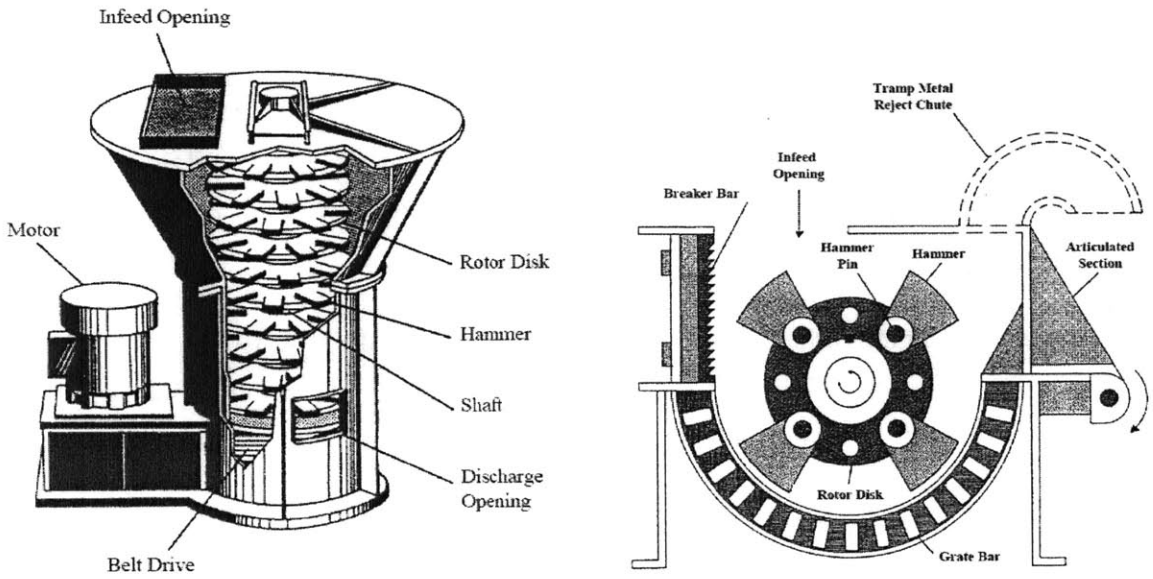

(a) Vertical hammermill.

(b) Horizontal hammermill.

Figure 2-4: Representation of vertical and horizontal hammermills. Source [12].

Screening

Screening consists in the separation of waste by size. It is usually employed at the initial stages of the sorting process in order to remove fine organic materials and large objects that can harm following units. Additionally, it is employed towards the end of the process to remove broken glass [35]. When referring to screening operations, it is common to distinguish between under-size ("unders") and over-size material ("overs"), the first being the fraction of material going through the holes of the screen. Screening of MSW may be difficult because MSW is constituted of irregular objects; it is conceivable that some long and thin objects pass trough small holes and that flat two-dimensional objects (e.g., newspaper, plastic sheets) occlude the holes and prevent unders to be properly separated. Another problem is represented by moisture, which causes waste to agglomerate in a phenomenon called bridging (see Figure 2-5).

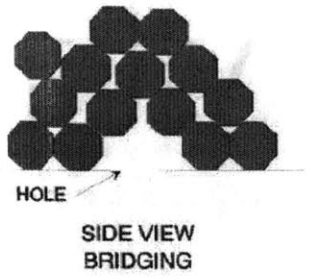

Figure 2-5: Representation of the bridging phenomenon. Source [12] p.186.

There are two major types of screens employed in material recovery facilities [12]: flat screens (primarily shaker and disc screens) and trommels. Trommels are the most widely used in the field. Flat screens are the best choice when: i) the under-size material is more dense than the over-size material; ii) the over-size material does not have a flat shape that could obstruct the holes of the screen (e.g., removing dirt from glass bottles); or iii) it is necessary to avoid breakage of material components (e.g., high content of glass that could break and affect the performance of subsequent units). Shaker screens (shown in Figure 2-8 a) are the simplest screens adopted in MRFs; they are constituted of a walled inclined screen connected to a motor which imposes an oscillation in the direction of material flow. Material is loaded from the top of the unit, and the oscillation favors the movement of the material towards the direction of the flow and mixes the waste stream. Disc screens (shown in Figure 2-8 ba) are constituted of several small disks, spinning on common shafts; material is fed onto the disks, it advances in the unit because of disks rotation and falls through the openings. Disk screens permit a change to the screen-size during regular operations because the openings between the discs can be adjusted by sliding the shafts towards or away from one-another within a defined range. Disc screens have the disadvantage that the specific motion and the geometry of the discs make it more difficult to separate long and thin objects, as they can easily find their way through the holes.

Trommels are constituted of an inclined and rotating drum covered by a perforated screen (see Figure 2-6). The material advances in the trommel primarily thanks to the initial feed rate at which it is introduced in the drum, the inclination of the drum with respect to the horizontal, and the rotatory speed that dictates a spiral movement on the material.

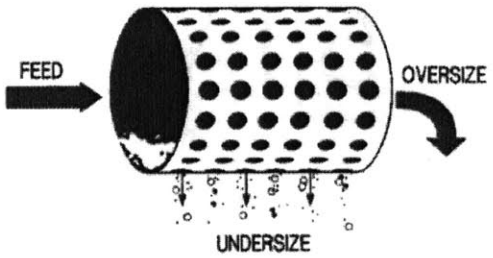

Figure 2-6: Representation of a trommel. Source [24].

The main parameters that impact the screening process of a trommel are the area of the holes in the screen, the hole-density (i.e., ratio between the area covered by holes and the total area of the screen,), the inclination of the drum with respect to the horizontal, the rotatory speed, the length, the volumetric feed rate (i.e., volume of material per unit of time that is fed into the trommel), the radius, the presence of lifting bars to increase the flight of the particles. The existing literature examines the effects of these parameters on the screening efficiency ([27] [26]). The area of the holes and the hole-density affect the probability of a particle to pass through the screen: for a spherical particle of diameter smaller than the diameter of the holes, the bigger the screen and the higher the hole-density, the more likely the particle will fall through the screen. The inclination of the trommel and the length of the drum primarily affect the residency time (i.e., the time for which the material stays in the drum): the higher the angle and the shorter the trommel, the lower the residency time ([27]). The radius of the trommel and the feed rate determine the time of residency, the volumetric capacity of the trommel, and the thickness of the material in the trommel. The rotatory speed affects both the time of residency (the higher the speed, the shorter the time) and the movement of the particles within the trommel, imposing a "corkscrew" motion on material flow [12]. Figure 2-7 shows material movement within the trommel at different rotational speeds.

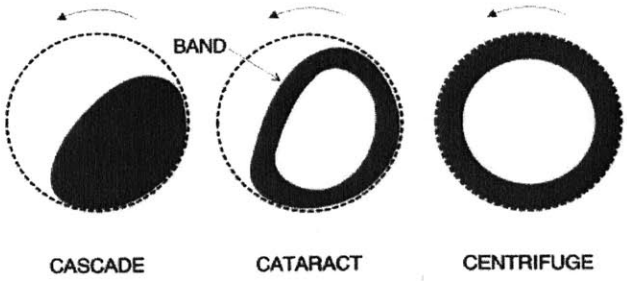

Figure 2-7: Particles motion within the trommel. Rotational velocity increases from left to right. Source [12].

In particular, at low rotational velocities, the material has a "cascading" behavior in which the mixing action is insufficient to adequately present the tumbling mass to the openings. When the speed increases, the corresponding increase in the centrifugal force produces a "cataracting" behavior: first, the material rises on the surface of the screen, and, when the gravitational force opposes the centrifugal force, the material falls and impinges on the holed surface. This impingement of the material onto the screening surface determines the passage of the particles. At the highest rotational speed, the centrifugal reaction holds the particles against the entire section of the drum and the material assumes a "centrifuging" behavior; in this situation no impingement occurs. Since the screening efficiency is primarily determined by the impingements of the material on the screening surface, the highest screening efficiency is achieved when the material has a cataracting behavior ([26]). Performance can be improved by introducing longitudinal flights running along the interior of the drum. Flights increase the angle at which particles depart from the interior of the trommel to tumble on the screening surface, increasing the number of particles impinging on the surface [12].

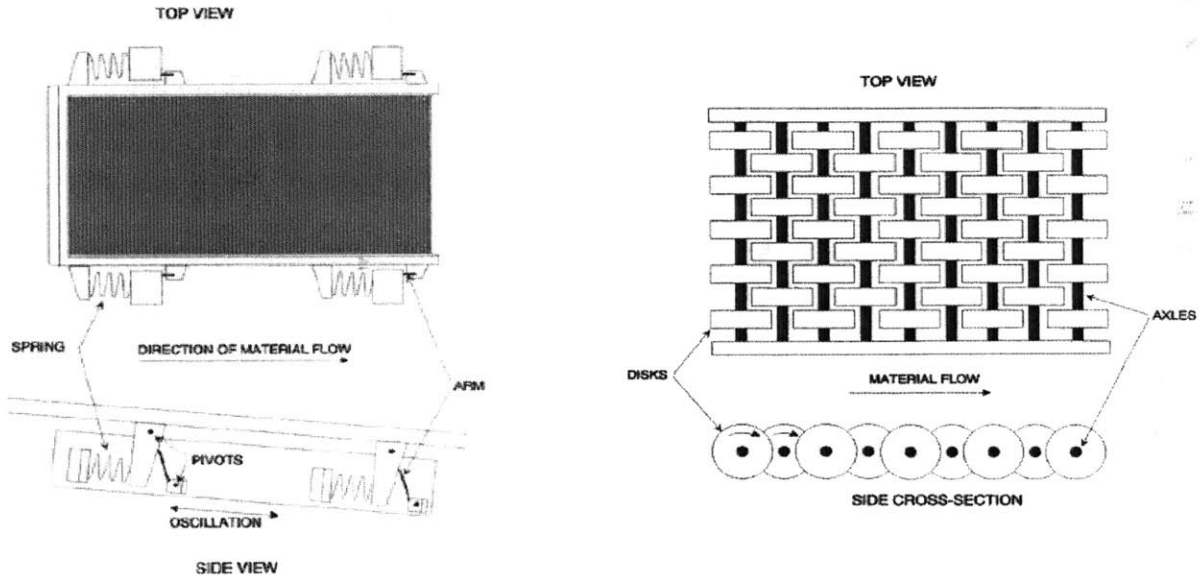

(a) Vibrating Screen.

(b) Disc screen.

Figure 2-8: Representation of vibrating screen and disc screen. Source [12].

Fluid-based Separation

Materials can be separated by exploiting their behavior in a fluid; different particles may rise, float, move, or sink depending on their relative density to the fluid. Air is the most widely used fluid in MRFs because it dries the material, but other fluids can be also employed. Wet separation systems (i.e., all fluid-based systems that do not use air) reduce putrefaction and odor arising from organic waste in bulk shipment of materials[12]. They are not usually employed in MRFs because they require a drying phase or otherwise the increased weight of material due to higher moisture content would negatively impact on transportation costs. Examples of fluid separators are the following:

- Heavy media. Heavy media exploit the difference between particle and fluid densities to achieve separation, employing flotation alone, without fluid motion. Different fluid densities can be obtained using specific chemical mixtures or colloidal preparations.

- Water elutriators. These units use pumps to produce a rising current in water to facilitate particles separation.

- Froth flotation. In froth flotation air is injected at the bottom of a tank filled with a liquid and, due to surface tension, it adheres to the particles of materials. This changes the apparent density of particles, allowing for the separation of material. Froth flotation works well with fine particles and can be used to remove grit from a stream of shredded metal fines.

- Jigs. Jigs (see Figure 2-9 a) use a piston to impose a vertical oscillation in the liquid; this accentuates the differences between particle densities.

- Air knives. Air knives (shown in Figure 2-9 b) are the simplest type of air classifier; they use a blower to produce a breeze which separates waste according to differences in the aerodynamic behavior of the particles.

- Air classifiers - general. Air classifiers (shown in Figure 2-9 c-d) differ from air knives in that they use specific closed units to perform separation, increasing the control on the process. They can be either horizontal or vertical and have different shapes to exploit different aerodynamic properties of the materials. Straight vertical and zig-zag air classifiers are the most widely used in waste management; the former for its simplicity and the latter for its effectiveness.

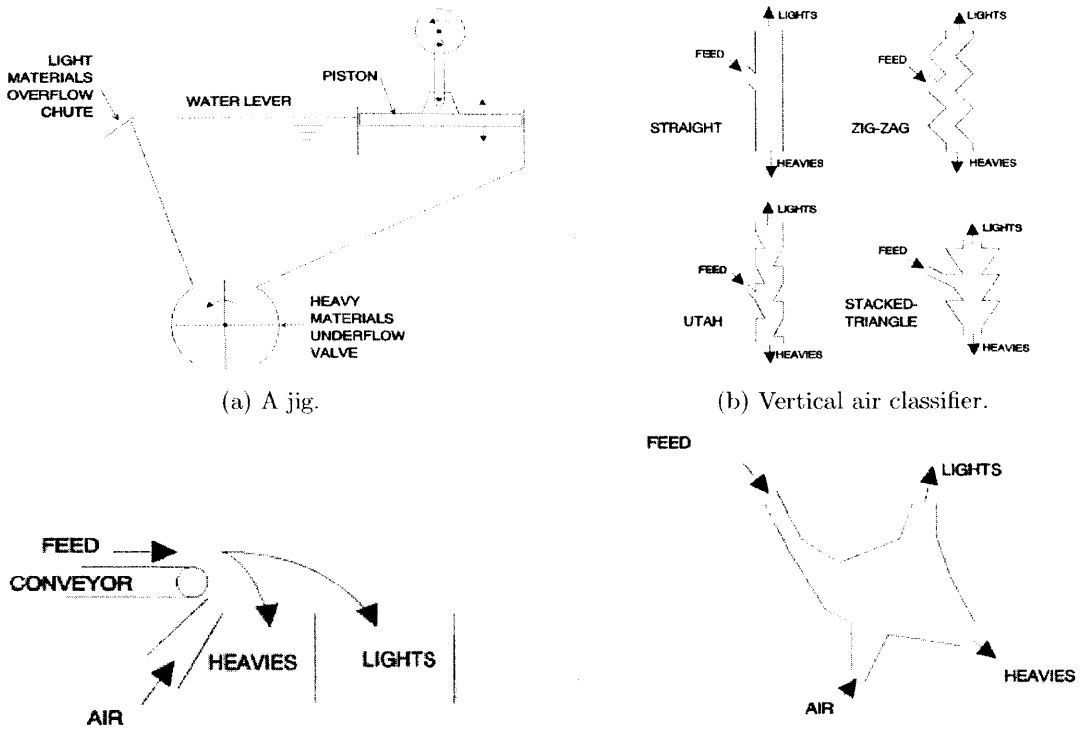

(a) A jig.

(b) Vertical air classifier.

(c) Air knife.

(d) Horizontal air classifier.

Figure 2-9: Different fluid separation technologies. Source [12] p.151 and p.156.

Ballistic Separators

Ballistic separators use inclined conveyors that follow an elliptical movement to cause material to bounce: light and flat materials go to the top of the ballistic, while heavy and rounded materials go to the bottom (see Figure 2-10). Elastic and aerodynamic particle properties play a role in this process [28]. Conveyors are activated with a crankshaft and a fixed shaft as a second support. Conveyors may have holes that act as filters to separate undersized materials. Figures 2-10 and 2-11 illustrate ballistic separation operations.

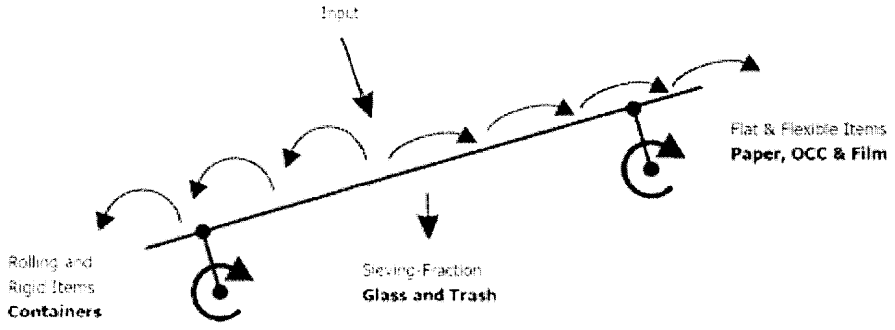

Figure 2-10: Representation of ballistic separator operations. Source [29].

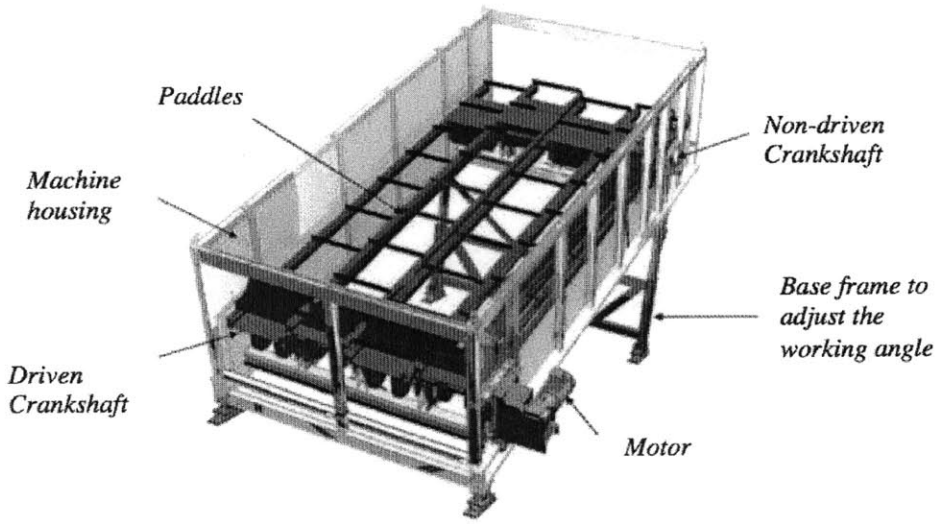

Figure 2-11: Representation of a ballistic separator. Adapted from [29].

Ferrous Metals Separation

Ferrous materials are defined by their magnetic properties, which allow them to be easily separated from the general waste stream when exposed to a magnetic field. Magnetic separators are classified according to the position of the magnet and the type of magnet used: the magnet can either be located above or below the conveyor carrying the waste stream, and it can either be a permanent or an electro-magnet. Electro-magnets are usually stronger than permanent magnets, as they employ extra power to generate the magnetic field. The two most common magnetic separators are the overhead-belt magnet and the tail-rotor magnet [12].

The major problems associated with magnetic separation relate to the entrainment of non-ferrous particles with ferrous metals; to increase the performance of the system it is common to employ dual-sequential magnets or to add air classifiers to clean the feed.

Overhead-belt magnets (shown in Figure 2-12) normally use an electro-magnet which is placed above the feed conveyor carrying the waste stream. Separation occurs as ferrous materials are attracted by the magnet, while non-ferrous materials remain on the conveyor due to gravity force. The space between the magnet and the conveyor allows entrained non-ferrous materials to fall back onto the conveyor belt. A second flighted conveyor surrounds the magnet and has the function

of preventing ferrous particles to remain attached to the magnet, as it moves them towards a region with lower magnetic field; the extracted particles then fall onto a third conveyor belt or in a properly designated container. The air gap between the feed conveyor and the magnet requires a strong magnetic field, and thus electro-magnets are preferred. In order to maximize the utilization of the magnet, the overhead belt magnet should not be placed in line with the feed conveyor (i.e., the conveyor belt should end before the magnet ends to guarantee that non-magnetic particles fall before magnetic ones).

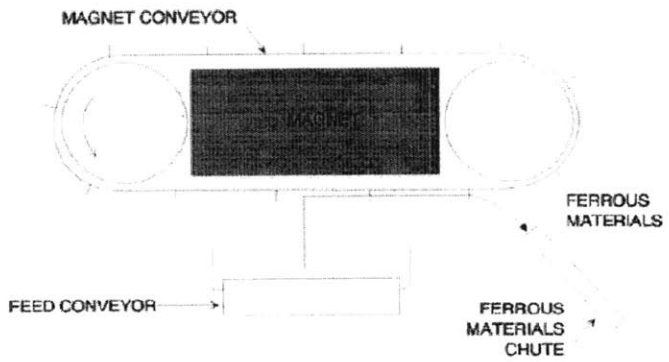

Figure 2-12: Representation of overhead magnet operations. Source [12].

Tail-rotor magnets (shown in Figure 2-13) are below-the-belt magnets that are widely used because of their advantages in price and operation. The magnet is located in the tail-rotor of the main feeder, and thus no additional conveyor and support structure is required. The proximity of the magnet to the feed permits the use of permanent magnets, without need of extra electric power. Separation occurs as ferrous materials remain attached to the main feeder, while non-ferrous materials leave the tail-rotor. Hence, different materials leave the tail-rotor at different angles, and a chute can be employed to facilitate the separation of the material and avoid contamination of falling streams. Tail-rotors are effective when the feed stream has a low content of sheet material (e.g., plastic film and paper) and when the bulk densities of the particles are such that the falling behavior of non-ferrous materials is similar.

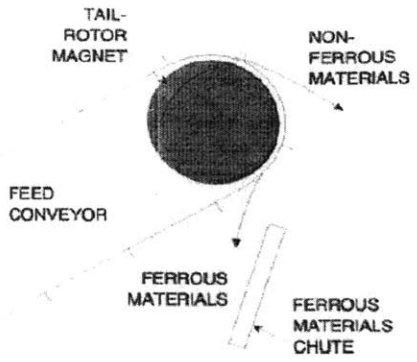

Figure 2-13: Representation of tail-rotor magnet operations. Source [12].

Non-ferrous Metals Separation

Non-ferrous metals include valuable materials, such as aluminum, copper, and some stainless steels, and non-valuable materials such as lead. Aluminum is one of the most targeted materials, and it can be found in the form of light foil, packaging, lawn furniture, and castings [21]. Lead is usually targeted to facilitate disposal, digestion, or combustion of waste [12]. There are three major types of non-ferrous metals separation processes: high-tension electrostatic separators, heavy media separators (seen in Section 2.2), and eddy-current separators, the last being the most widely used [3], [12].

High-tension electrostatic separators induce strong static charges in the incoming feed of MSW. Since metals have higher conductivity than plastics and most other materials, they loose the induced charge sooner and can be separated by using a properly charged metal drum or magnet. This process is primarily used to sort aluminum from a plastic mix.

As seen in Section 2.2, heavy media separators sort materials by density and, given their high-cost, are not particularly used in non-ferrous metals separation[12].

Eddy-current separators (ECSs) use powerful magnetic fields to generate eddy currents in non-magnetic metals. Their working principle is based on Lenz's Law, according to which an induced current sets up a magnetic field that opposes the inducing field. In ECSs, magnets generate induced currents in non-magnetic particles, and the induced currents subsequently generate opposing magnetic fields which make the particles be repelled from the initial magnets. ECSs provide a path

by which particles can exit the flow of materials. The effectiveness of ECSs and the specific effect on non-magnetic materials depends on conductivity and density; conductivity affects the strength of the eddy-current induced, while density determines the force required to affect the direction of the particle. The higher the ratio of conductivity to density, the easier the extraction of the particle from the stream. Table 2.5 shows ECS separation properties of various non-ferrous metals. Ferrous materials tend to become hot inside an eddy current field; for this reason they should be removed from the waste stream entering an ECS.

Metal	**Conductivity** σ $10^{-8}\frac{mho}{m}$	**Density** ρ $10^{3}\frac{kg}{m^3}$	$\frac{\sigma}{\rho}$ $10^{-13}\frac{mho\ m^2}{kg}$
Aluminum	0.35	2.7	13.1
Copper	0.59	8.9	6.6
Silver	0.63	10.5	6.0
Zinc	0.17	7.1	2.4
Brass	0.14	8.5	1.7
Tin	0.09	7.3	1.2
Lead	0.05	11.3	0.4

Table 2.5: ECS separation properties of various non-ferrous metals. Source [12].

Detect-and-route Systems for Glass and Plastic Sorting

Detect-and-route (DAR) systems are based on a two-step process that first uses sensors to determine the type of material (in the so called "detect" phase), and then uses air jets to direct the material to the desired stream (in the so called "route" phase). Figure 2-14 shows the generic configuration of a DAR unit. In the "detect" phase, several sensors screen the object and an internal CPU compares the results to specific tables that contain data about different materials. For this phase to be effective, the material must be well exposed to sensors, and thus it should be as spread as possible on the conveyor, contaminating fine materials should be previously removed, and the bed of the feed should be one-object deep. In the "route" phase, information concerning the type and destination of the material, its position, and the speed of the conveyor, is used to activate air jets that send the material to the desired stream. The air jets may be located in a wall on the side of the conveyor or below the conveyor itself depending on the case. Small size of the materials may reduce separation efficiency.

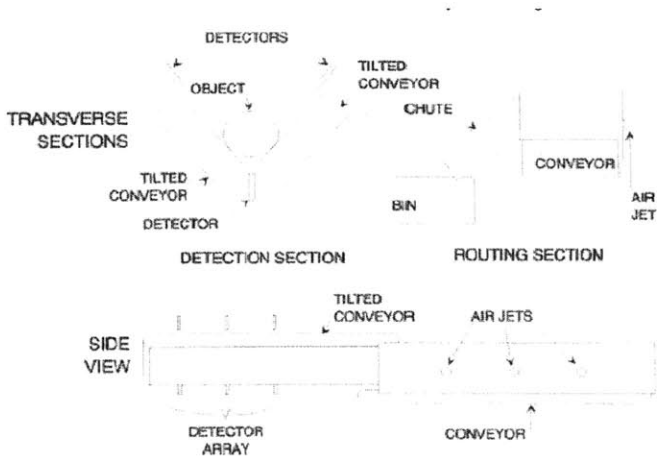

Figure 2-14: Generic configuration in a detect-and-route system. Source [12] p231.

DAR systems have historically been used to sort glass, categorizing it by color into flint, emerald, and amber glass by using visible-light spectrophotometry ([22], [23]). Figure 2-15 shows the difference in the wavelength spectra of different colors of glass. The contamination in the glass stream is potentially caused by different kinds of glass, such as plat glass, or ceramic objects. Currently, DAR systems are used to sort plastics by the use of near infrared spectrophotometry. Plastic materials sorted include high and low density polyethylene (HDPE, LDPE), polypropylene (PP), polyvinyl chloride (PVC), polyethylene terephthalate (PET), and polystyrene (PS).

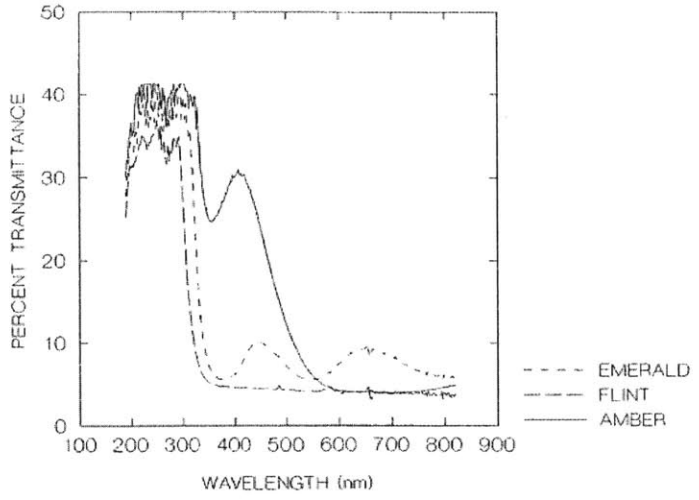

Figure 2-15: Ultraviolet-to-visible light spectra for bottle glass. Source [12] p234.

Hand Sorting

Manual sorting is primarily used to:

- Remove bulky items (e.g., appliances, furniture, large containers) and contaminants (e.g, hazardous waste) [3] from the initial stream entering the facility.
- Remove contaminants from desirable material streams in quality control operations.
- Extract desirable material for which there is no mechanical sorting unit available in sorting cabins.

There are two types of hand-sorting:

- Positive sorting, in which desirable material is removed.
- Negative sorting, in which undesirable material is removed.

Manual sorting usually requires workers ("sorters") to station on one or both sides of a conveyor belt or a table carrying the mixture of materials to be separated. The design of manual sorting units requires determining the belt width and speed and the burden depth, which is the average thickness of waste on the belt [33]. The conveyor speed should range between 4.6 to 27 m/min, with higher speeds possible when negatively sorting [33]. Effective picking is possible at burden depths up to 15 cm [34]. Table 2.6 provides sorting rates (i.e., amount of materials that can be sorted by a worker per unit of time) and recovery efficiencies (i.e., amount of material correctly identified and separated) for hand sorting.

Material	**Sorting rate** $(\frac{kg}{hr\,sorter})$	**Recovery efficiency** (%)
Newspaper[a]	700 to 4,500	60 to 95
Glass containers[b] *(mixing colors)*	400 to 800	70 to 95
Glass containers[b] *(by colors)*	200 to 400	80 to 95
Plastic containers[b] *(PET, HDPE)*	140 to 200	80 to 95
Aluminum cans[b]	45 to 55	80 to 95

Table 2.6: Manual sorting rates and efficiencies. Source [3].
a) From a paper stream of predominantly one or two paper grades.
b) From a processing stream of predominantly metal, glass, and plastics.

2.3 Design Principles

Designing a MRF requires a thorough understanding of the characteristics of the waste stream and the material market. With regards to the characteristics of MSW, it is necessary to know the quantity and the frequency in which material is collected and delivered to the facility, its composition, the type of waste collection systems that is implemented (i.e., whether is commingled, wet-dry, or source-separated), and the transportation system [3]. It is important to know for what materials there exists a secondary market and how the market is designed (i.e, how the prices are set, who are the players, what the volatility is). The understanding of the waste management system and market characteristics allows determining the expected throughput of the facility and identifying target materials. Other elements to consider are processing flexibility to accommodate changes in technology and the protection of the workers and the environment. After this preliminary analysis, it is possible to focus on the actual MRF design, by properly determining:

- The degree of automation;
- The pieces of equipment to use;
- The size and characteristics of material storing locations;
- The sequence and layout of the system.

It is also important to take into account the desired availability and redundancy of the system [3]. "Availability is the percentage of the time that a particular piece of equipment (or a system) is "available" to perform the task for which it is intended" [3]. Redundancy is a concept related to availability, "as it consists in defining possible alternative routes, or alternative processes (also by repeating the same unit) that guarantee the execution of a certain tasks. Redundancy is connected to capital costs, and in waste processing is often minimized in order to reduce costs" [3].

Finally, to guarantee the correct operations of a MRF, there is the need for staff that takes care of hand-sorting, operation of fixed and rolling equipment, and maintenance. MRFs also require office staff, such as plant managers, weight masters, bookkeepers, clerks, and custodians. Table 2.7 shows typical staffing requirements for MRFs processing source-separated materials.

Personnel	Facility throughput (Mg/wk)		
	550	1,000	2,000
Office	2 to 30	3 to 4	5 to 6
Operational			
-Foreman/machine operator	1 to 2	2 to 3	3 to 4
-Sorters	8 to 16	10 to 18	15 to 26
-Forklift operators	2 to 3	3 to 4	5 to 6
-Maintenance	1	2	4
Total	14 to 25	20 to 31	32 to 46

Table 2.7: Typical staffing requirements for facilities that process source-separated materials. Source [3].

2.4 Examples of Configurations

In this section, we examine two examples of MRFs, which have been adapted from [3].

2.4.1 Facility Processing Source Separated Waste

In the first case we consider a MRF that processes source-separated waste, sorting corrugated paper (OCC), newspapers,and magazines, glass, and tin, aluminum, HDPE, PET. The input stream is received in the form of commingled wastes (i.e., a stream for mixed paper, and one for mixed containers) and in the form of source separated waste (i.e., an independent stream from each material category). Figure 2-16 presents the design of the entire facility, while Figure 2-17 shows how different paper and container processing lines work and provides a mass-balance graph of the flows. The mass-balance graph of a MRF shows how the mass of input material is diverted through the system. In this example, (see Figure 2-17.a) paper is separated by hand-sorting and then sent to trailers or to balers. In Figure 2-17.b, glass input stream first goes through a magnet and an air classifier (A/C) to remove contaminants and other valuable materials, and then it is hand-sorted by color. Segregated containers go first through a magnetic separator before being hand-sorted into different components (i.e., PET green, PET clear, HDPE from milk, HDPE not from milk, and aluminum). Mixed containers go through magnetic separation, vibratory screens and air classifiers. Looking at the overall design (see Figure 2-16), the facility follows the principles of redundancy in the lines. This can be seen, for example, by the fact that the tipping floor for the paper fraction has two receiving pits, each of which serves a processing line that could process either the entire anticipated input of mixed paper, or the entire anticipated input of segregated paper.

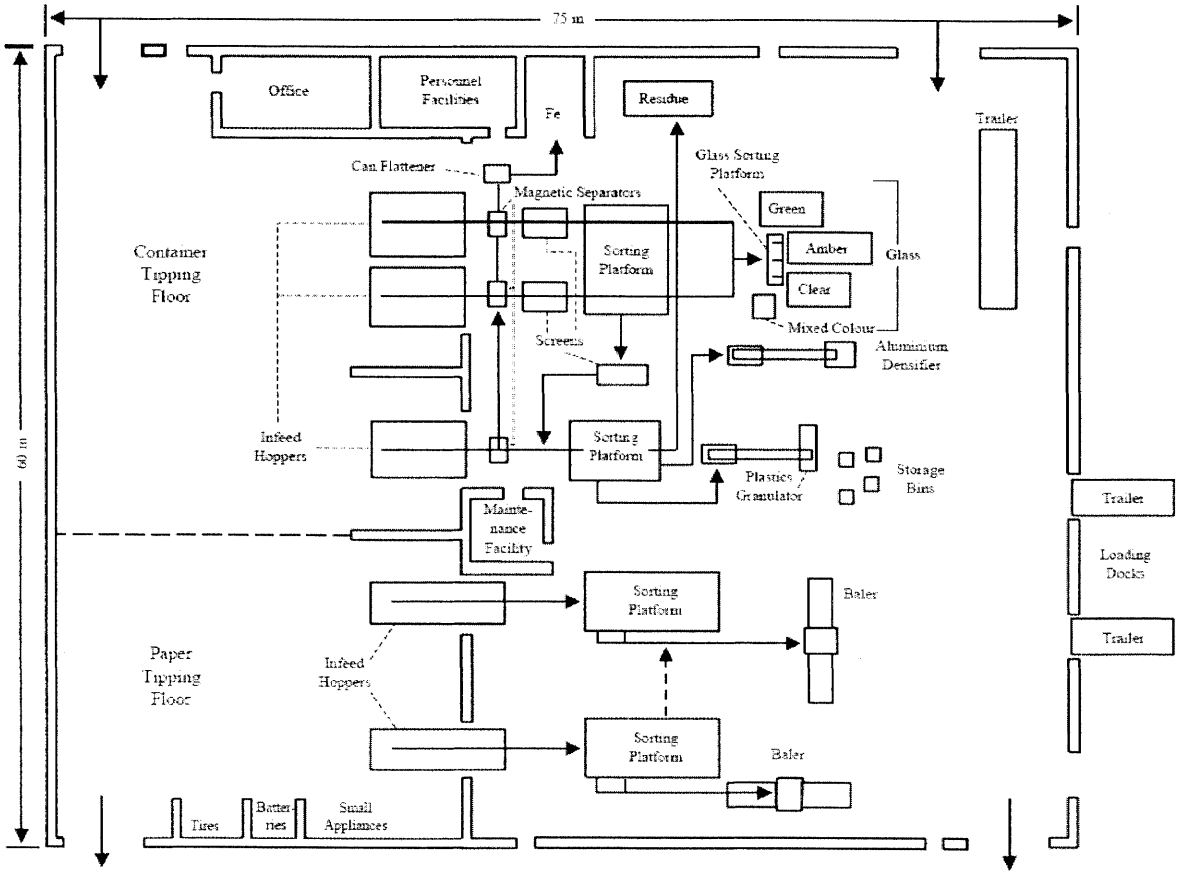

Figure 2-16: Example plan view of facility that processes source-separated materials. Source [3].

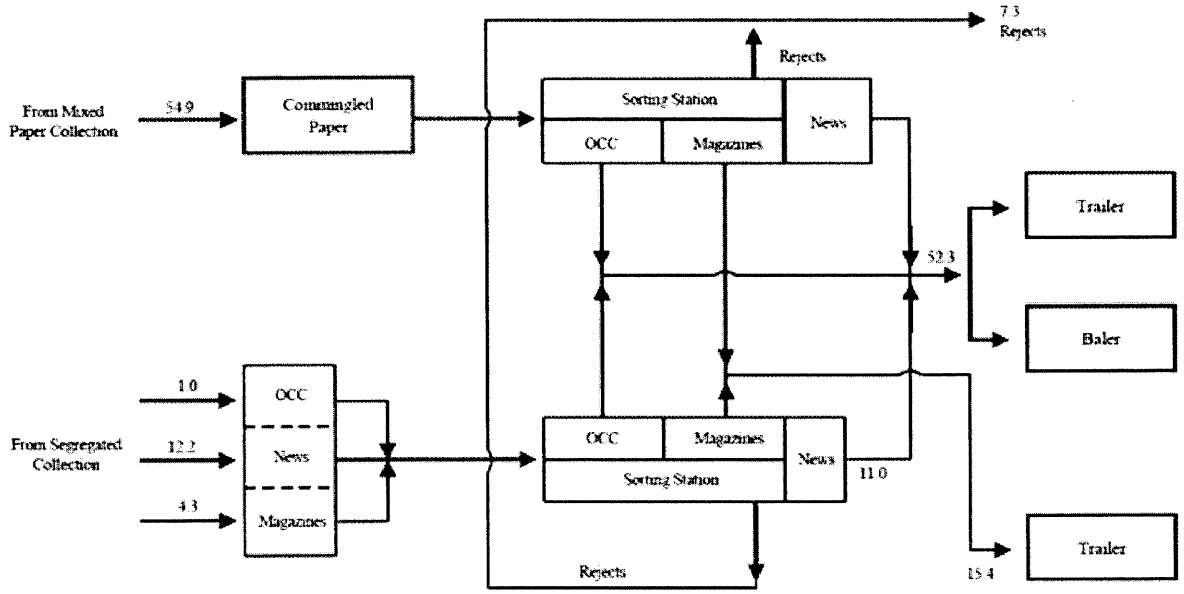

(a) Paper processing line, the numbers express the flow of material in ton/day.

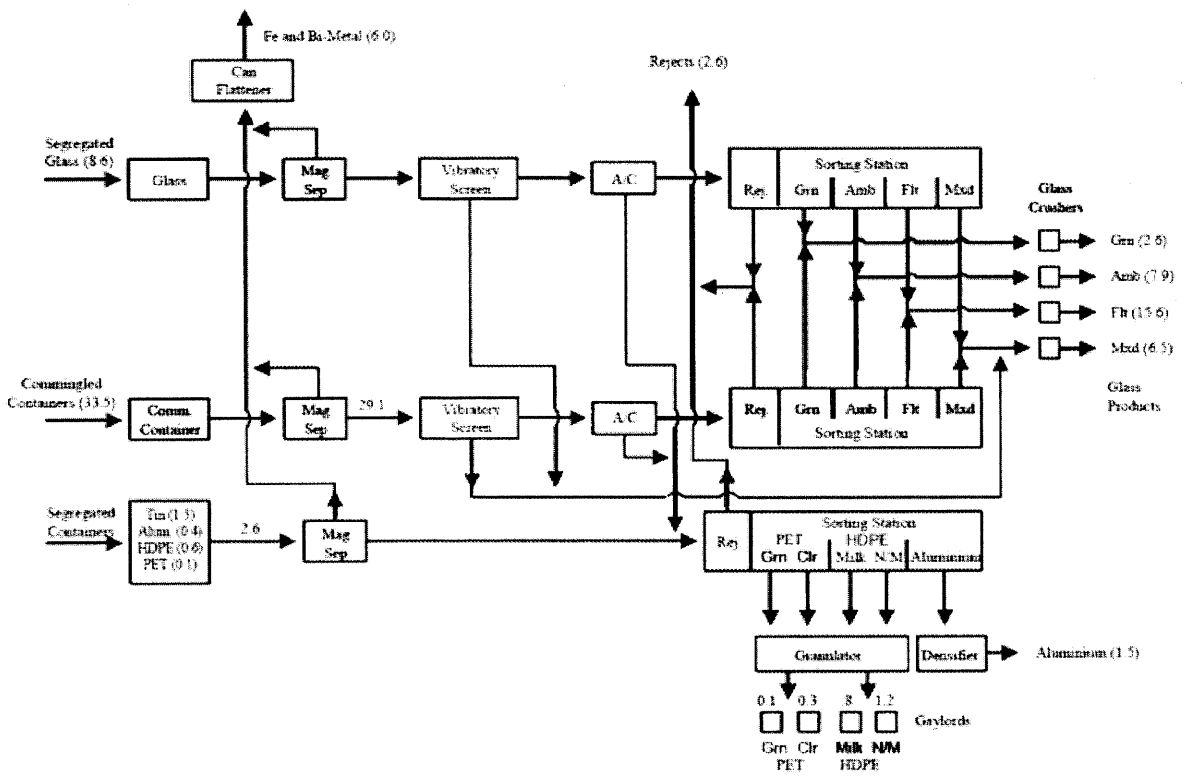

(b) Container processing line.

Figure 2-17: Paper and container processing lines at a source-separated processing facility, quantities in ton/day. Source [3].

2.4.2 Facility Processing Commingled Waste

An example of a MRF processing mixed municipal solid waste is depicted in Figure 2-18. The capacity is assumed to be 50 ton/day. The facility employs both manual and mechanical sorting to recover ferrous, aluminum, glass, plastics (HDPE and PET), and paper (fines, news, and other). In this system, a trommel initially sorts waste into three streams of different size, each of which goes through a magnet. Larger ferrous items are hand-sorted to extract cans from the rest of the ferrous materials. Larger non-ferrous material is manually sorted in two different hand-sorting units, while under size material is rejected. In the example shown, approximately 15% of the waste stream is recycled.

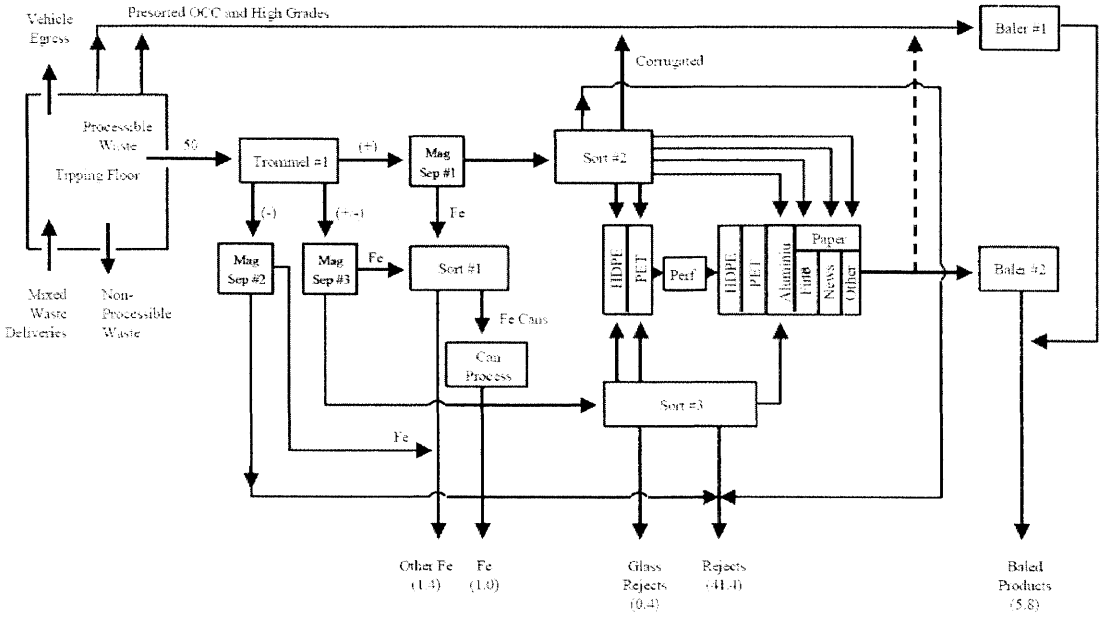

Figure 2-18: Example flow diagram for a mixed waste processing facility. The numbers represent the mass of material in a stream measured in ton/day. Source [3] p163.

2.5 Economic Performance of MRFs

Material Recovery Facilities (MRFs) are usually for-profit enterprises, even though some countries may subsidize part of the operations. Policy-makers have placed a lot of effort on designing financing systems that shift the burden of waste disposal from the government to the product producers. This practice, known as extended producer responsibility (EPR), internalizes the costs of waste management into the cost of the product and is based on the principle that since producers have got the greatest power on the recoverability of a good, they should be charged with the costs of product disposal. EPR may take the form of a reuse, buy-back, or recycling program. In some countries, EPR has led to the formation of recycling corporations that guarantee a stable market for recovered materials. This is the case, for example, of the Green Dot Corporation in Europe, which consists of a network of industry-funded systems for recycling packaging materials of consumer goods.

When assessing the economic performance of a MRF, the revenues generated by selling separated materials are compared against the costs of operations and other costs, including capital costs and the costs of financing [45]. In some cases, the MRF may receive an income for processing the waste.

2.5.1 Valuation of Waste

There are different systems to evaluate waste. In some countries like the U.S., recovered material is sold in secondary resource markets and its price fluctuates with the price of the corresponding pure material [45]. In other countries like Spain, the market is stabilized by the presence of organizations that guarantee a minimum selling price for recovered materials.

[45] focuses on the U.S. market and shows how prices are defined for specific purity levels of the recycled material with possibly many several purity grades for a given material; for example, there are over 40 grades of aluminum scrap [48]. [45] proposes a continuous price-purity curve for scrap materials in which the prices of recovered materials are defined with respect to the price of the corresponding pure material as:

$$p = \begin{cases} p_{pure}(2c-1) & \text{if } c > 0.5 \\ 0 & \text{if } c \leq 0.5\ . \end{cases} \tag{2.1}$$

Here, p is the selling price of the recovered material, p_{pure} is the price of the corresponding pure material, and c is the concentration of the material in the stream. This relationship is suggested on the basis of Figure 2-19, where each data point is the ratio between the secondary price and the price for the pure material.

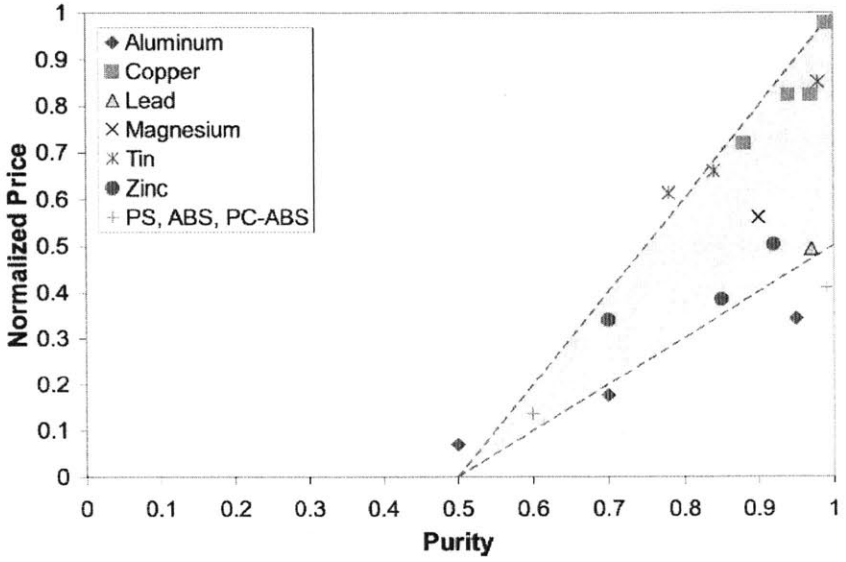

Figure 2-19: Normalized price purity curve for secondary materials market. Source [45].

In this work, we consider a valuation of waste based on discrete price levels as the one implemented in Spain; the data and the valuation model have been obtained by working with a company operating MRFs in Spain. According to this model, a material m meeting concentration requirements is sold at a total price given by a market-based component p_m^{mkt} and a recovery-based component p_m^{rec}. The total selling price of material m, p_m is given by:

$$p_m = p_m^{mkt} + p_m^{rec}, \tag{2.2}$$

Defining the recovered ratio ρ_m of material m to be the ratio of the total amount of material m collected in one year over the total amount of all materials processed in the same period, the recovery-based component is given by:

$$p_m^{rec} = \begin{cases} p_{m,1} & \text{if } \rho_m \geq \overline{\rho_m} \\ p_{m,2} & \text{Otherwise ,} \end{cases} \tag{2.3}$$

where $\overline{\rho^m}$ is a defined threshold. Approximate recovered ratios are computed at the end of

every month taking into account the cumulative amount of material collected and processed since the month of January of the same year. At the end of the year, the actual recovered ratio ρ_m is computed and corrective factors are applied to the valuation.

For example, PET can be sold if the collected stream meets the following concentration requirements (percentages are expressed with respect to material weight):

- Minimum concentration of PET in the stream of 92.00%.
- Maximum concentration of PVC of 0.50%.
- Maximum concentration of metals of 0.50%.
- Maximum concentration of the sum of other plastic materials and impurities of 7.00%.

To compute the selling price of PET is necessary to determine the market-based and the recovery-based components. In the Spanish market, the market price is $p_{PET}^{mkt} = 170\frac{€}{ton}$. If in one calendar year the MRF extracts less PET than $\overline{\rho}_{PET} = 0.2\%$ of the total mass of material processed, then the recovery-based component of the price for all the PET recovered in that year is $118\frac{€}{ton}$ otherwise it is $150\frac{€}{ton}$. In summary, the price of PET meeting the specified concentration requirements is given by:

- Market-based fraction:

$$p_{PET}^{mkt} = 170\frac{€}{ton};$$

- Recovery-based fraction:

$$p_{PET}^{rec} = \begin{cases} 150\ \frac{€}{ton} & \text{if } \rho_m \geq 0.2\% \\ 118\ \frac{€}{ton} & \text{Otherwise .} \end{cases}$$

2.5.2 Evaluating Costs

The costs of MRFs depend on the specific installation; Table 2.8 reports some of the potential sources of costs [45].

Cost	Description
Equipment	Capital cost of owning separation equipment.
Installation	Installation and support equipment.
Facility Space	Ownership or leasing of workspace.
Financing	Financing costs for equipment and workspace.
Taxes	Property and business taxes.
Labor	Equipment operators wages and benefits.
Utilities	Electricity, water, and other utilities.
Shipping	Packaging, hauling, and other shipping costs.
Waste Disposal	Disposal fees for non-salable materials

Table 2.8: Potential cost sources of a separation system facility. Source [45].

Table 2.8 does not include all possible costs and does not provide a way of allocating these costs. The allocation methodology depends on the metric used to evaluate the economic performance and on the context of application. Generally speaking, when assessing MRFs operations, costs can be computed considering hourly operational costs, cost per mass of material processed, or fixed capital costs [45].

Chapter 3

Mathematical Models for Material Recovery Facilities

To evaluate the performance of a Material Recovery Facility (MRF), we formulate a quantitative model to trace how material flows in the system. In the proposed model, multi-stage MRFs composed of multi-output units sorting material mixtures are represented through a directed graph and the performance of a configuration is evaluated in terms of its ability of correctly sorting material and of its profitability.

In this section, we first review the major contributions to the field of MRF modeling, we then introduce the proposed mathematical model, discussing the constraints on the system and the estimation of the parameters, and we finally present the metrics adopted to evaluate the facility performance.

3.1 Literature Review

MRF modeling exists in both industry and academia [45] and focuses on finding representations of single-unit and system sorting processes to guide facility design. In industry, this is achieved using flow-sheets that describe the way in which materials are diverted in the system, and facility design is primarily guided by already existing installations [45]. In academia, MRFs modeling was originally inspired to sorting processes in mineral processing, chemical industries, and food processing, and only recently has developed as an independent field of research (see, for example, [26], [34], [40] [41]).

The current literature can be divided into two main areas: deterministic and probabilistic modeling [45]. Deterministic modeling (also called physical modeling) aims at developing detailed models of sorting units, describing the forces acting on material particles. For example, deterministic models for eddy-current separators involve the calculation of the Lorentz force and take into account the magnetic field, the aerodynamic drag, the gravity force, and particle to particle and belt interactions ([36], [37], [38], [39]). [45] argues that the use of physical models to determine the way in which waste is sorted requires detailed knowledge of the input particles, which is rarely available in MRF operations. Probabilistic models instead do not try to capture the physical principles causing the sorting process, but rather describe each unit in terms of mass-balance equations. The terminology "deterministic" and "probabilistic" does not refer to the actual use of stochasticity in the model; that is, both deterministic and probabilistic models may or may not incorporate stochasticity in the formulation. We adopt this terminology to be consistent with the current literature, but we believe that a better taxonomy should be developed to avoid confusion. Probabilistic and deterministic models are not in contrast, but rather complement each other; probabilistic models should be used to describe how material flows in the system, whereas deterministic models should be used to determine how each unit sorts the material under given operational settings and input composition.

In the following sections we review the major results in MRF probabilistic modeling at both single-unit and sorting-facility levels.

3.1.1 Unit Models

Binary Bayesian Model

To the best of our knowledge, the first model formally describing unit operations in a MRF through probabilistic modeling is the Bayesian separation model proposed by [40]. The Bayesian model represents the operations of a unit dividing an input stream composed of target materials and non-target materials into two streams: the primary output stream collecting target materials and the secondary output stream collecting non-target materials. The performance of each unit is described through two parameters expressing the quantity of material that is sent to the desired output stream: parameter $r \in [0, 1]$ representing the percentage of the target material correctly sent to the primary stream, and parameter $q \in [0, 1]$ representing the percentage of the non-target material correctly sent to the secondary stream.

According to this model, each separation unit can be seen as a Bayesian test. Defining the following events:

$$A = \{Target\ material\ in\ the\ input\}$$

$$B = \{Material\ sent\ to\ the\ primary\ output\ stream\},$$

then we have:

$$P(B|A) = r, \tag{3.1}$$

$$P(B^c|A) = 1 - r, \tag{3.2}$$

$$P(B^c|A^c) = q, \tag{3.3}$$

$$P(B|A^c) = 1 - q. \tag{3.4}$$

The composition of the output streams generated by the unit is then determined by applying Bayes' theorem. In particular, the concentration of the target material in the primary output stream is the probability $P(A|B)$ and is computed as:

$$P(A|B) = \frac{P(B|A)P(A)}{P(B|A)P(A) + P(B|A^c)P(A^c)}. \tag{3.5}$$

The prior probabilities $P(A)$ and $P(A^c)$ are taken as the fraction of target and non-target materials in the input stream. By combining the sorting probabilities of each unit with the information on the composition of the input stream, it is possible to derive the composition of the material in each stream of the system.

The Bayesain separation model can be applied to any unit that generates two output streams. The material entering the process does not have to be constituted of two homogeneous material types; different materials are grouped into two major categories of target and non-target materials [45]. Figure 3-1 shows a graphical representation of the Bayesian model. In this case, the input material is composed by a mass m_t of target material and a mass m_n of non-target material. Thus:

$$P(A) = \frac{m_t}{m_t + m_n},$$
$$P(A^c) = \frac{m_n}{m_t + m_n}.$$

Applying Bayes' theorem, the probability of having target material in the primary output stream is:

$$P(A|B) = \frac{P(B|A)P(A)}{P(B|A)P(A) + P(B|A^c)P(A^c)} = \frac{r\frac{m_t}{m_t+m_n}}{r\frac{m_t}{m_t+m_n} + (1-q)\frac{m_n}{m_t+m_n}} = \frac{rm_t}{rm_t + (1-q)m_n},$$

and the probability of having non-target material in the secondary output stream is:

$$P(A^c|B^c) = \frac{P(B^c|A^c)P(A^c)}{P(B^c|A)P(A) + P(B^c|A^c)P(A^c)} = \frac{q\frac{m_n}{m_t+m_n}}{(1-r)\frac{m_t}{m_t+m_n} + q\frac{m_t}{m_n+m_n}} = \frac{qm_n}{(1-r)m_t + qm_n}.$$

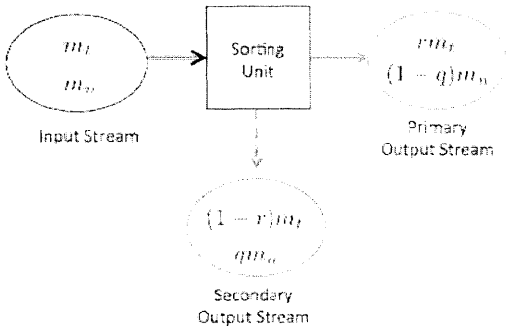

Figure 3-1: Scheme of a binary unit sorting an input mixture with a mass m_t of target materials and a mass m_n of non-target materials. In this example, $r \in [0, 1]$ is the fraction of target material sent to the primary stream and $q \in [0, 1]$ is the fraction of non-target material sent to the secondary stream.

Multi-output Bayesian Model

As seen in Chapter 2, MRFs are composed of units that sort a complex mixture of materials into multiple output streams to extract more materials. For this reason, the Bayesian model could have a limited applicability to real world systems. [45] and [46] extend the Bayesian separation model to the generic case of a unit sorting a mixture of M materials into K output streams. The sorting

process is described through a sorting matrix $Q \in [0,1]_{M\times K}$, in which each element $q_{i,j}$, called separation parameter, represents the fraction of material i sent to output stream j. Since the mass of material is conserved, we have that $\sum_j q_{i,j} = 1$. For example, a matrix of a unit sorting four materials into three output streams, could be:

$$Q = \begin{bmatrix} 0.1 & 0.1 & 0.8 \\ 0.05 & 0.75 & 0.2 \\ 0.03 & 0.9 & 0.07 \\ 0.82 & 0.08 & 0.1 \end{bmatrix}$$

Figure 3-2 shows the corresponding graphical representation of a multi-output unit sorting a mixture of M materials into K output streams.

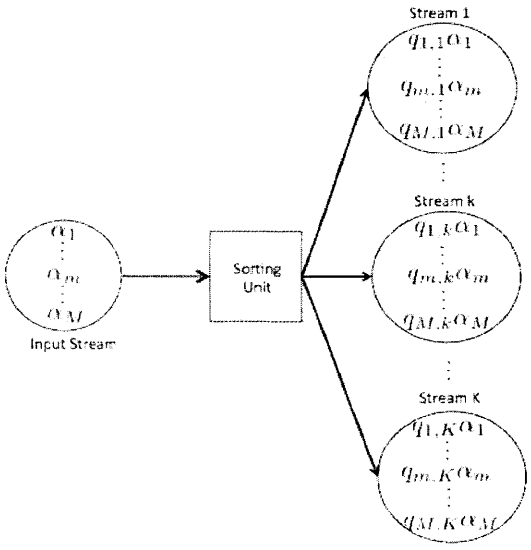

Figure 3-2: Scheme of a multi-output unit sorting an input mixture of M materials, each with concentration $\alpha_m \in [0,1]$ into K output streams. The sorting parameters associated to each stream are $q_{m,k} \in [0,1], \forall m = 1,...M,\ \forall\ k = 1,...,K$, satisfying $\sum_{k=1}^{K} q_{m,k} = 1,\ \forall m = 1,...,M$.

3.1.2 System Models

Given the complexity of municipal solid waste, MRFs combine single units in multi-stage sorting systems. Units may be connected in several ways, the simplest case being a train of sequential operations as shown in Figure 3-3. This situation is considered, for example, by [33].

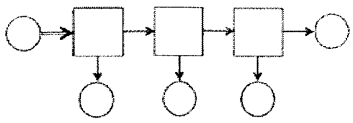

Figure 3-3: Scheme of a train of binary sorting units.

More complex configurations are possible; in many cases MRFs employ branching and recirculation to improve system performance. When recirculation is adopted, one of the output streams of a unit is directed upstream. [43], [42], [44], and [45] analyze multi-stage systems composed of binary identical units using recirculation (see Figure 3-4).

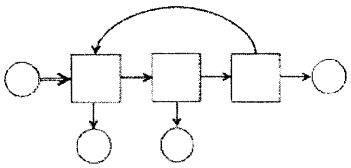

Figure 3-4: Scheme of a system of binary sorting units with recirculation.

More recently, [46] has considered systems composed of multi-output units with recirculation. [46] proposes a network flow model in which there is a set of nodes $\mathcal{S}$ for the units in the process, a set of input nodes $\mathcal{I}$, and a set of output nodes $\mathcal{Z}$ (see Figure 3-5 for a schematic representation of the system). The topology of the system is described by a set of directed arcs (i, j), representing a flow of material from unit i to unit j:

$$\mathcal{E} = \{(i,j) \mid \forall\, i \in \mathcal{S} \cup \mathcal{I}\ \exists\, j \in \mathcal{S} \cup \mathcal{Z}\}. \tag{3.6}$$

The system sorts M materials, and each stage i sees an incoming flow of material $F_i \in \mathcal{R}_{M\times 1}$, in which each element $f_{i,1}, ..., f_{i,M}$ represents the quantity of material in the stream. The model distinguishes different units in the system, depending on their function:

- *Comminution units.* These units change the size distribution of material by shredding the components; they leave the mass of material unchanged. Thus:

$$F_i^{out} = F_i. \tag{3.7}$$

The set of comminution units in the system is $\mathcal{C} \subseteq S$.

- *Separation units.* These units divert the input stream into K_i output streams, changing the relative concentration of material in each stream. To define these stages it is necessary to provide the sorting matrix associated to a unit. As seen in section 3.1.1, the element at position (m, k) of a sorting matrix $Q_i \in [0,1]_{M \times K}$, corresponds to the quantity of material m that i sends to output stream k. We have:

$$F_{i,k}^{out} = diag(F_i)\ Q_i\ \mathbf{one}_k, \tag{3.8}$$

where $F_{i,k}^{out}$ is the material vector associated to the k^{th} output stream of separation unit i, $diag(F_i)$ is the matrix having on the diagonal the elements of F_i (i.e., $diag(F_i)_{m,m} = f_{i,m}$), and $\mathbf{one}_k$ is a vector with all zeros except for the k^{th} element equal to one. The set of separation units in the system is $\mathcal{SEP} \subseteq S$

- *Mixing units.* These units merge incoming material flows into one single flow, thus:

$$F_i^{out} = \sum_{(j,i) \in \mathcal{E}} F_j. \tag{3.9}$$

The set of mixing units in the system is $\mathcal{MIX} \subseteq S$.

- *Splitting units.* A splitting unit i divides the flow of input material into K_i output streams; each output stream generated has the same material composition of the original input stream. P_i is a vector whose element $p_{i,k} \in [0,1]$ defines the fraction of input stream that is sent to stream $k \in K_i$, and thus $\sum_{k \in K_i} p_{i,k} = 1$. Defining $F_{i,k}^{out}$ to be the material vector in the k^{th} output stream of splitting unit i, we have:

$$F_{i,k}^{out} = p_{i,k} F_i, \tag{3.10}$$

where $p_{i,k}$ is a scalar expressing the fraction of material sent to stream k. The set of splitting units in the system is $\mathcal{SP} \subseteq S$.

[46] defines mass-balance equations at each node $i \in \mathcal{S} \cup \mathcal{Z}$:

$$\begin{aligned} F_i = \quad & \sum_{(j,i)\in\mathcal{E}, j \in \mathcal{C} \cup \mathcal{I} \cup \mathcal{MIX}} F_j \\ & + \sum_{(j,i)\in\mathcal{E}, j\in\mathcal{SEP}} diag(F_j)\ Q_j\ \mathbf{one}_i \\ & + \sum_{(j,i)\in\mathcal{E}, j\in\mathcal{SP}} \sum_{(j,i)\in\mathcal{E}} p_{j,i} F_j. \end{aligned} \tag{3.11}$$

This equation states that the material vector at unit $i \in \mathcal{S} \cup \mathcal{Z}$ is given by the sum of the material in the output streams of mixing, separation, splitting, and comminution units that are incoming to unit i. For a given set of external input flows (i.e., $F_i\ \forall i \in \mathcal{I}$), [46] computes the flow of material in each output, splitting, separation, mixing, and comminution unit by solving the linear system of $|\mathcal{S} \cup \mathcal{Z}|$ mass-balance equations, one for each unit in the process. According to [46], the model requires that i) each separation process in the system is on a directional path that starts at an input node and ends at an output node and ii) no separation process is self-feeding, that is, the output of a process is not directly fed into its input.

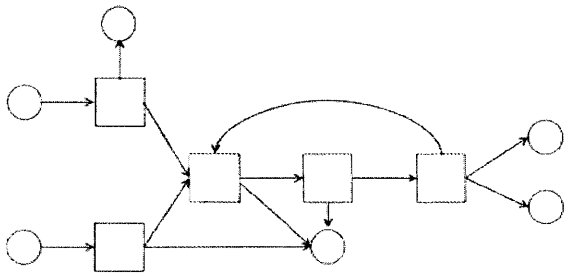

Figure 3-5: Scheme of a MRF using multi-output units to sort material. Squares represent comminution, mixing, separation, and splitting units, circles represent input and output nodes, and the arcs represent flows of material.

3.1.3 Metrics Used in Configuration Analysis

In this section, we discuss the main metrics used in MRF modeling. In the literature, authors have used metrics to evaluate the material performance (i.e., the ability of a configuration to properly sort material), the economic performance, and the energy requirements [45].

Material Performance Metrics

To measure the ability of a system to correctly sort material, binary output and multi-output Bayesian models use the metrics of recovery and grade. Recovery measures the fraction of a material that is correctly sent to the desired output stream, and grade measures the concentration of a material in a stream.

For a single unit processing M materials and sending material m to output stream k, the recovery of material m is:

$$R_m = \frac{f_{k,m}}{\mu_m}, \tag{3.12}$$

and the grade of material m in output stream k is:

$$G_{k,m} = \frac{f_{k,m}}{\sum_{m=1}^{M} f_{k,m}}. \tag{3.13}$$

Here, $f_{k,m}$ is the mass of material m in stream k and μ_m is the mass of material m in the input stream.

For example, let's consider a unit receiving an input stream containing a $\mu_{Al} = 2\frac{ton}{hour}$ of aluminum and a $\mu_{Other} = 3\frac{ton}{hour}$ of other materials; the unit sends aluminum to stream 1 and other materials to stream 2 (see Figure 3-6). Let's also assume that 90% of aluminum is correctly sent to stream 1 and 80% of other materials is correctly sent to stream 2. Then we have:

$$R_{Al} = \frac{0.9 \cdot 2}{2} = 90.00\%,$$

$$G_{1,Al} = \frac{0.9 \cdot 2}{0.9 \cdot 2 + 0.2 \cdot 3} = 75.00\%,$$

$$G_{2,Al} = \frac{0.1 \cdot 2}{0.1 \cdot 2 + 0.8 \cdot 3} = 7.69\%.$$

We can proceed in the same way to compute R_{Other}, $G_{1,Other}$, and $G_{2,Other}$.

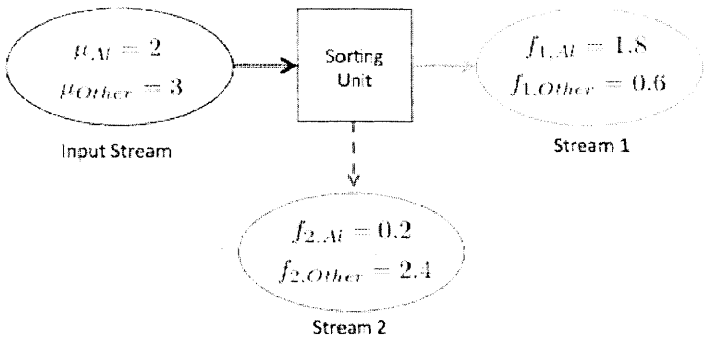

Figure 3-6: Representation of a single unit sorting aluminum and other materials into two streams. Quantities in tons/hour.

For a multi-stage MRF, recovery and grade are computed considering the stream composition at the output units where material is ultimately collected. Taking μ_m to be the mass of material m in input to the facility, unit i to be the output unit collecting material m, and $f_{i,m}$ to be the mass of material m in unit i, the recovery for material m is:

$$R_m = \frac{f_{i,m}}{\mu_m}, \tag{3.14}$$

and the grade of material m in unit i, $G_{i,m}$, is:

$$G_{i,m} = \frac{f_{i,m}}{\sum_{j=1}^{M} f_{i,j}}. \tag{3.15}$$

For example, let's consider a MRF using four sorting units to separate a mixture of aluminum, PET, and other materials to collect aluminum in output unit 1, PET in output unit 2, and other materials in output unit 3. Figure 3-7 reports the results. We can compute:

$$R_{Al} = \frac{1.8}{2} = 90.00\%,$$

$$R_{PET} = \frac{0.95}{1} = 95.00\%,$$

$$R_{Other} = \frac{2.8}{3} = 93.33\%,$$

$$G_{1,Al} = \frac{1.8}{1.8 + 0.03 + 0.1} = 93.26\%.$$

We can proceed in the same way to obtain $G_{2,Al}$, $G_{3,Al}$, $G_{1,PET}$, $G_{2,PET}$, $G_{3,PET}$, $G_{1,Other}$, $G_{2,Other}$, and $G_{3,Other}$.

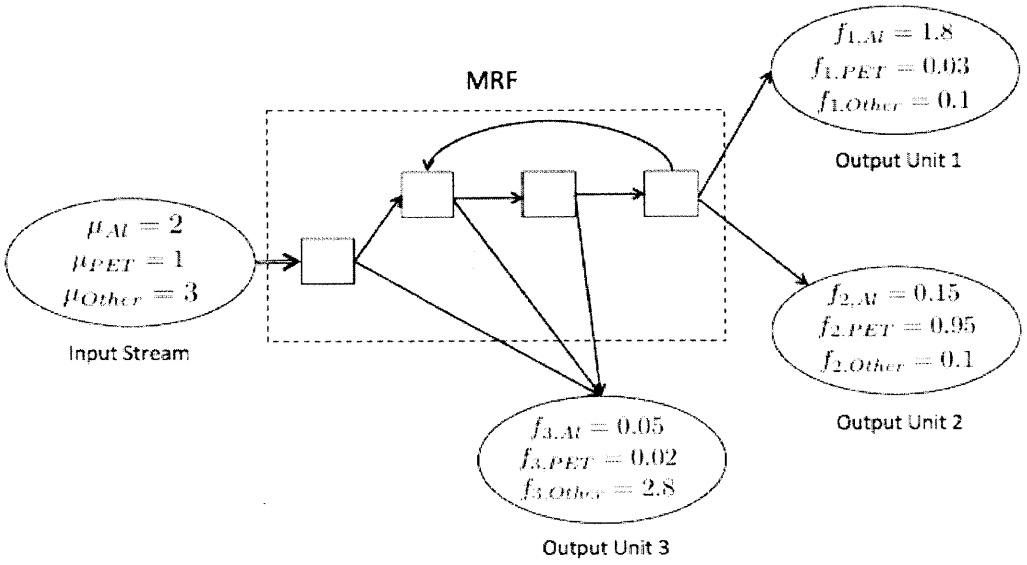

Figure 3-7: Representation of a multi-stage MRF sorting a mixture of aluminum, PET, and other materials. Quantities in tons/hour.

To capture the material performance of a MRF with a single metric, [12] and [33] propose to combine the recoveries of different materials into the efficiency ϵ, given by:

$$\epsilon = \prod_{m \in \mathcal{M}} R_m^{1/M}. \tag{3.16}$$

Proceeding with the example of the multi-stage MRF in Figure 3-7, we have:

$$\epsilon = R_{Al}^{\frac{1}{3}} \, R_{PET}^{\frac{1}{3}} \, R_{Other}^{\frac{1}{3}} = 92.75\%.$$

Alternatively, [45] proposes to evaluate multi-material processes in terms of the weighed sums of recovery and grade:

$$Sum_R = \sum_{m \in \mathcal{M}} R_m \beta_m, \tag{3.17}$$

and:

$$Sum_G = \sum_{m \in \mathcal{M}} G_m \beta_m. \tag{3.18}$$

$\beta_m \in [0,1], \sum_{m \in \mathcal{M}} \beta_m = 1$ are weights that express the relative importance of each collected material and could be computed considering either the value or the quantity of a material in the input stream.

Economic Metrics

In the literature, a variety of metrics has been considered to measure the profitability of a facility; these metrics consider the revenues generated from recovered materials and the costs of material processing and capital costs. Depending on the decision-making scenario, the metrics considered include the net cash flow, the net present value, the benefit/cost ratio, and the payback time. For example, [45] considers two examples of decision-making processes:

- As a first case, different configurations of a MRF obtained by rearranging the same set of sorting equipment are compared. In this case, the author argues that rearranging the units has a minor impact on costs; and thus different options are compared exclusively in terms of revenues generated.
- As a second case, the author analyzes the installation of a processing line to recover plastics for the secondary resource market in an energy-to-waste system. In this case, the metric chosen to evaluate the investment is the payback time, computed considering the revenues from selling plastics and from energy production, the costs of capital and installation, of operators, and energy consumption.

Environmental Metrics

In the literature, MRFs have been evaluated with respect to the environmental impact of the facility. For example, [45] measures energy savings derived from recycling materials, by taking into account the energy consumption associated with transportation, processing, and landfilling. Additionally, [45] argues that the environmental impact of a facility could be measured by evaluating all utility and support inputs, such as electricity, water, cleaning agents, and consumable machines parts, and assigning greenhouse gas and pollutants to each separation unit.

3.1.4 Optimization of MRFs Configurations

Finding the configuration (i.e., the set of connections $\mathcal{E}$ introduced in 3.6) with the highest recovery and grade is one of the most treated optimization problems in the literature. Considering the case of multi-output multi-stage configurations and defining $\mathcal{T}_z \subseteq \mathcal{M}$ to be the set of materials collected at output unit z, [46] formulates three optimization problems to find the best-performing configuration:

1. *Recovery maximization.* In this case, the objective is that of maximizing the recovery under certain minimum grade requirements $G^{obj}_{z,m}$. That is:

$$\begin{aligned} \max_{E} \quad & \sum_{z \in \mathcal{Z}} \sum_{m \in \mathcal{T}_z} R_{z,m} \\ \text{subject to} \quad & G_{z,m} \geq G^{obj}_{z,m}, \ \forall\, z \in \mathcal{Z}, \ \forall m \in \mathcal{T}_z. \end{aligned} \tag{3.19}$$

2. *Grade maximization.* Here, the objective is that of maximizing the grade under certain minimum recovery requirements $R^{obj}_{z,m}$. That is:

$$\begin{aligned} \max_{E} \quad & \sum_{z \in \mathcal{Z}} \sum_{m \in \mathcal{T}_z} G_{z,m} \\ \text{subject to} \quad & R_{z,m} \geq R^{obj}_{z,m}, \ \forall\, z \in \mathcal{Z}, \ \forall m \in \mathcal{T}_z. \end{aligned} \tag{3.20}$$

3. *Total mass flow minimization.* In this case, the objective is that of minimizing the total flow of material subject to satisfying certain grade and recovery requirements (i.e., $R^{obj}_{z,m}$ and $G^{obj}_{z,m}$). The author suggests that this problem may be addressed when the amount of processed material is taken as an indicator of the energy consumption of the material. The formulation is:

$$\begin{aligned} \min_{E} \quad & \sum_{i \in \mathcal{S}} \sum_{m \in \mathcal{M}} f_{i,m} \\ \text{subject to} \quad & G_{z,m} \geq G^{obj}_{z,m}, \ \forall\, z \in \mathcal{Z}, \ \forall m \in \mathcal{T}_z \\ & R_{z,m} \geq R^{obj}_{z,m}, \ \forall\, z \in \mathcal{Z}, \ \forall m \in \mathcal{T}_z. \end{aligned} \tag{3.21}$$

Solution techniques

To the best of our knowledge, in the literature these optimization problems have been approached by full enumeration of the possible configurations ([46], [44]). If we have a configuration with K connections and N units, there are $\mathcal{O}(N^K)$ possible configurations. Enumerating all possible solutions becomes quickly prohibitive, and probably for this reason the instances evaluated in the literature consider configurations composed of at most three units. Real world MRFs may have a large number of units (on the order of one or two dozens), and thus the full enumeration of the configurations is not applicable.

3.2 Proposed Mathematical Model

In this work, we model the sorting process of a MRF as a directed graph in which each unit is a node and each material flow is a directed arc between two nodes. We evaluate a configuration with respect to its material performance, measured by the efficiency ϵ, and to its economic performance, measured by the profit π. Even though MRF operators are primarily concerned with the economic performance of the facility, it is important to account for the material performance as well. In fact, there could be situations in which not all output streams of a configuration meet the concentration requirements (this could be due for example to the limited availability of sorting equipment). In these cases, the efficiency can be taken as an indicator measuring how close the output units of a facility are to the required concentration. For example, let's consider a case in which we have two configurations with different efficiencies and identical profits, and let's assume that there is at least one of the output streams that does not meet the concentration requirements and cannot be sold on the market. The fact that a configuration has a higher efficiency than another means that it sends more materials to the desired output streams, and thus its output streams that do not meet the concentration requirements are probably closer to meeting them. In this case, we can obtain output streams that meet the concentration requirements with a smaller effort, for example by adding one extra unit or adding personnel.

To evaluate the performance of a specific configuration, we proceed sequentially: first, we compute the flow of material going through each unit in steady state (i.e., when the process is operating at full regime and, under the assumption of constant input, each unit is processing a positive constant flow of material), and then, we compute the metrics of the configuration.

In this section, we illustrate the mathematical model of the sorting process, how to compute the flow of material in the system, how to incorporate constraints, how to estimate the sorting parameters, and how to compute efficiency and profit.

3.2.1 Computation of Material Flows in Steady State Operations

To compute the flow of material in the system, we build on the model proposed by [46] and represent a MRF as a directed graph in which each node i is a unit and each arc (i, j) is a directed flow of material from unit i to unit j. Differently from [46], we do not consider mixing, splitting, and comminution units, but we focus only on sorting units. This choice is motivated by the fact that sorting units are quite general and can represent all other units with proper connections and parameter settings. Splitting units can be seen as a specific case of sorting units in which the sorting matrix has the same value on all the elements of a column (i.e., all materials are sorted equally within the system). Mixing units can be modeled using appropriate connections between units. Comminution units do not affect stream mass and thus are not relevant in a flow model in which sorting parameters depend only on material type and not on the granularity of the material. Figure 3-8 shows how we represent splitting, mixing, and comminution units in terms of sorting units and system connections.

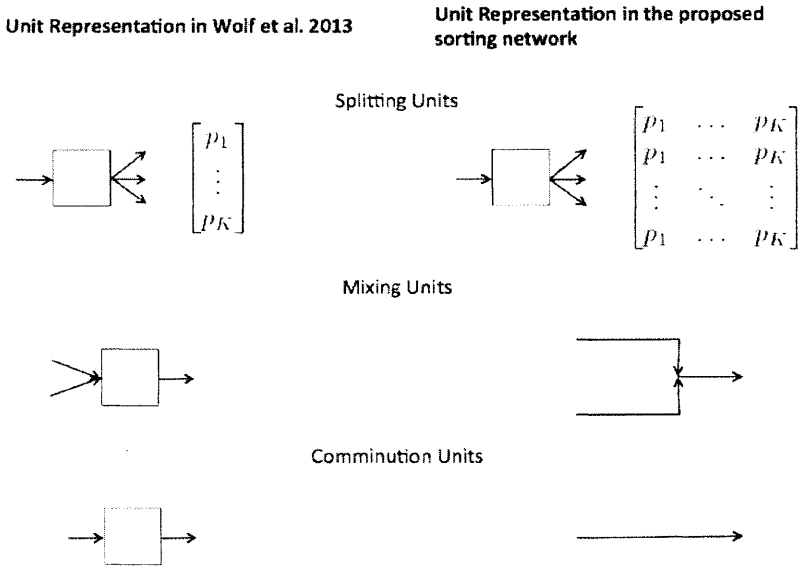

Figure 3-8: Comparison of units representation in [46] and in this work.

We use system-level equations for each material, rather than unit-level equations for all materials as in [46]. That is, we do not define a sorting matrix for each unit, but we define a system-level sorting matrix for each material. In these system-level matrices, each row is an origin node i, each column a destination node j, and each element at position (i, j) equals the fraction of a material that unit i sends to unit j. This leads to a more compact formulation that allows solving the generalized mass balance equations in matrix form.

We define the following:

- $\mathcal{M}$: Set of materials in the system, $\mathcal{M} = \{1, ..., M\}$.
- $\mathcal{N}$: Set of units (or nodes) in the system, $\mathcal{U} = \{1, ..., N\}$. The units in the system are either sorting units, input units, or output units.
- $\mathcal{S} \subset \mathcal{N}$: Set of sorting units in the system. Each sorting unit in the system has at least one outgoing arc exiting the unit and one incoming arc entering the unit.
- $\mathcal{I} \subset \mathcal{N}$: Set of units receiving external input in the system. Each input unit in the system has exactly one outgoing arc.
- $\mathcal{Z} \subset \mathcal{N}$: Set of output collection units in the system. Each output unit in the system has no outgoing arcs.

We have that $\mathcal{N} = \mathcal{S} \cup \mathcal{I} \cup \mathcal{Z}$ and $\mathcal{S} \cap \mathcal{I} \cap \mathcal{Z} = \emptyset$.

As a first step to evaluate the performance of a MRF, we compute the steady state flow rates for each material going through each unit. The flows entering the system are assumed to be stationary, the units to have no storage capacity, the processes to operate under steady operating conditions, the value of the separation parameters to be constant and independent from the input composition, and all the parameters to be known deterministically.

We introduce the following:

- $Q^m \in [0, 1]_{NxN}, \forall\ m \in \mathcal{M}$: System-level sorting matrix for material m. This matrix contains the separation parameters for material m, expressing how the flow of material is

sorted by each unit. Each element of the matrix $q_{i,j}^m$ is the fraction of material m that unit i receives in input and sends to unit j. For all input and sorting units i:

$$\sum_{j \in \mathcal{N}} q_{i,j}^m = 1, \ \forall i \in \mathcal{I} \cup \mathcal{S}, \ \forall m \in \mathcal{M}.$$

Whereas, for all output units i:

$$q_{i,j}^m = 0, \ \forall i \in \mathcal{Z}, \ \forall j \in \mathcal{N}, \ \forall m \in \mathcal{M}.$$

For example, if we have a simple system of three units, one input unit (unit 0), one sorting unit (unit 1), and one output unit (unit 2), carrying one single material, we get:

$$Q = \begin{pmatrix} 0 & 1 & 0 \\ 0 & 0 & 1 \\ 0 & 0 & 0 \end{pmatrix}$$

Figure 3-9: Representation of the connections of a unit processes through a system-level sorting matrix.

- $\bar{\mu}^m \in \mathcal{R}_{Nx1}, \ \forall \ m \in \mathcal{M}$: Input vector for material m. μ_i^m is the quantity of external input of material m entering the system at unit i; $\mu_i^m = 0 \ \forall i \notin \mathcal{I}$. The flow of material in input is measured in $\frac{ton}{hour}$.
- $\bar{f}^m \in \mathcal{R}_{Nx1}, \ \forall \ m \in \mathcal{M}$: Flow vector for material m. These vectors contain the steady state flow rates of material m processed by each unit. That is, each element f_i^m represents the quantity of material m going through unit i at steady state. Material flows are expressed in $\frac{ton}{hour}$.

Knowing the configuration of the facility, the quantity of material in input, and the sorting efficiencies of each unit, we can compute the steady state flow rates of materials through each unit. In steady state, we can write the mass balance equation for each unit i; where the quantity of material m going through unit $i \in \mathcal{I} \cup \mathcal{S} \cup \mathcal{Z}$ is given by:

$$f_i^m = \sum_{j \in \mathcal{I} \cup \mathcal{S}} f_j^m q_{j,i}^m. \tag{3.22}$$

For each input unit $i \in \mathcal{I}$ we have:

$$f_i^m = \mu_i^m. \tag{3.23}$$

In order to compute the flow of material going through each unit, we need to solve the system of linear equations given by the mass-balance equations 3.22 for all units in the system. We can write this in matrix notation, obtaining:

$$\bar{f}^m = (Q^m)^T \bar{f}^m + \bar{\mu}^m, \tag{3.24}$$

thus:

$$(I - (Q^m)^T)\bar{f}^m = \bar{\mu}^m. \tag{3.25}$$

Here, $(Q^m)^T$ is the transpose of matrix Q^m and I is the identity matrix. Assuming a positive flow of material in input (i.e., $\bar{\mu}^m > \bar{0}$) and defining $A = (I - (Q^m)^T)$, the system of equations has a solution given by:

$$\bar{f}^m = A^{-1}\bar{\mu}^m, \tag{3.26}$$

$(A)^{-1}$ is the inverse of matrix A. This system of equations is well defined if and only if A is non-singular.

Theorem 1. *$det(A) \neq 0 \iff$ there is a directed path from every node $i \in \mathcal{I} \cup \mathcal{S}$ to an output node $z \in \mathcal{Z}$.*

Proof. We define a recirculating subsystem REC_r, as $REC_r = \{i, j \in \mathcal{I} \cup \mathcal{S} \mid \exists$ a path from i to i via $j\}$.

We substitute the recirculating subsystems of a graph with single nodes obtaining a new graph having a set of nodes $\widetilde{\mathcal{N}}$. When generating the new graph, we maintain the external arcs of the subsystem. That is, we maintain all connections $\{(i, j) \mid (i \notin REC_r \cap j \in REC_r) \cup (i \in REC_r \cap j \notin REC_r)\}$.

Figure 3-10 provides a graphical example of the procedure. The sorting process corresponding to the new system is represented by the system sorting matrix $\widetilde{Q}$. The new graph allows computing all flows of the original system except those of the arcs within recirculating subsystems.

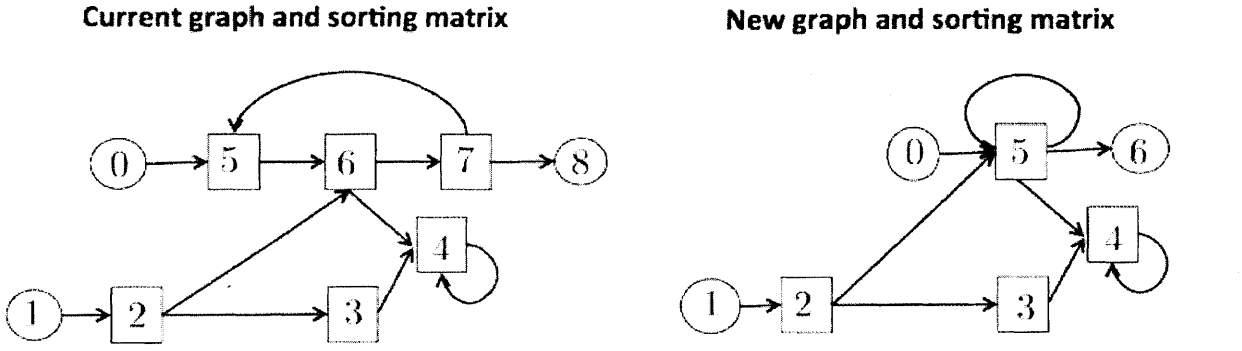

Figure 3-10: Graphical example showing how to convert the original graph into a new graph having only downstream connections or self-reentrant loops..

The corresponding sorting matrices are:

$$Q = \begin{pmatrix} 0 & 0 & 0 & 0 & 0 & q_{0,5} & 0 & 0 & 0 \\ 0 & 0 & q_{1,2} & 0 & 0 & 0 & 0 & 0 & 0 \\ 0 & 0 & 0 & q_{2,3} & 0 & 0 & q_{2,6} & 0 & 0 \\ 0 & 0 & 0 & 0 & q_{3,4} & 0 & 0 & 0 & 0 \\ 0 & 0 & 0 & 0 & q_{4,4} & 0 & 0 & 0 & 0 \\ 0 & 0 & 0 & 0 & 0 & 0 & q_{5,6} & 0 & 0 \\ 0 & 0 & 0 & 0 & q_{6,4} & 0 & 0 & q_{6,7} & 0 \\ 0 & 0 & 0 & 0 & 0 & q_{7,5} & 0 & 0 & q_{7,8} \\ 0 & 0 & 0 & 0 & 0 & 0 & 0 & 0 & 0 \end{pmatrix} \quad \text{and} \quad \widetilde{Q} = \begin{pmatrix} 0 & 0 & 0 & 0 & 0 & \tilde{q}_{0,5} & 0 \\ 0 & 0 & \tilde{q}_{1,2} & 0 & 0 & 0 & 0 \\ 0 & 0 & 0 & \tilde{q}_{2,3} & 0 & \tilde{q}_{2,5} & 0 \\ 0 & 0 & 0 & 0 & \tilde{q}_{3,4} & 0 & 0 \\ 0 & 0 & 0 & 0 & \tilde{q}_{4,4} & 0 & 0 \\ 0 & 0 & 0 & 0 & \tilde{q}_{5,4} & \tilde{q}_{5,5} & \tilde{q}_{5,6} \\ 0 & 0 & 0 & 0 & 0 & 0 & 0 \end{pmatrix}$$

The new graph obtained has only downstream connections or self-reentrant loops, and thus the entries of $\widetilde{Q}$ can be ordered by performing elementary row and column operations to obtain an upper triangular matrix $\widetilde{Q}^{\Delta}$. We reorder the elements of matrix $\widetilde{Q}$, assigning index i' to unit i in a way that

$$i' < j' \iff \text{there is no directed path from } j \text{ to } i.$$

In this example, we invert unit 4 and unit 5 as shown in Figure 3-11.

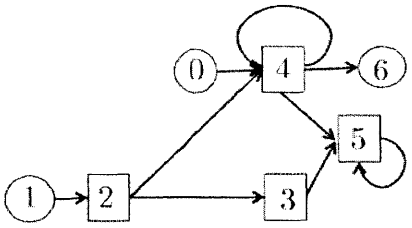

Figure 3-11: Graphical example showing how to change the index of the units (which corresponds to doing elementary row operations on the matrix).

The corresponding upper triangular matrix $\tilde{Q}^{\Delta}$ is given by:

$$\tilde{Q}^{\Delta} = \begin{pmatrix} 0 & 0 & 0 & 0 & \tilde{q}_{0,4} & 0 & 0 \\ 0 & 0 & \tilde{q}_{1,2} & 0 & 0 & 0 & 0 \\ 0 & 0 & 0 & \tilde{q}_{2,3} & 0 & \tilde{q}_{2,5} & 0 \\ 0 & 0 & 0 & 0 & 0 & \tilde{q}_{3,5} & 0 \\ 0 & 0 & 0 & 0 & \tilde{q}_{4,4} & \tilde{q}_{4,5} & 0 \\ 0 & 0 & 0 & 0 & 0 & \tilde{q}_{5,5} & \tilde{q}_{5,6} \\ 0 & 0 & 0 & 0 & 0 & 0 & 0 \end{pmatrix}.$$

We can compute system flows using $\tilde{Q}^{\Delta}$, and since $\tilde{Q}^{\Delta}$ is upper triangular, matrix A is lower triangular. Thus,

$$det(A) = \prod_{i \in \tilde{\mathcal{N}}} a_{i,i}$$

and

$$det(A) \neq 0 \iff a_{i,i} \neq 0 \; \forall i \in \tilde{\mathcal{N}}.$$

Since $a_{i,i} = 1 - \tilde{q}_{i,i}$, we have

$$det(A) \neq 0 \iff \tilde{q}_{i,i} < 1 \; \forall i \in \tilde{\mathcal{N}}. \tag{3.27}$$

This is always true for output collection units, which have no output streams and thus $q_{i,i} = 0 \; \forall \; i \in \mathcal{Z}$. For the other units in the system, equation 3.27 implies that A is non-singular if and only if there are no subsystems recirculating their entire output flow, which is equivalent to requiring that each input or sorting unit is connected to an output node.

□

Example

Let's consider the system in Figure 3-12, sorting a mixture of three materials. The system is composed of one input unit, two sorting units, and three output collection units (i.e., $\mathcal{M} = \{0,1,2,3,4,5\}$, $\mathcal{N} = \{0,1,2,3\}$, divided into $\mathcal{I} = \{0\}$, $\mathcal{S} = \{1,2\}$, and $\mathcal{Z} = \{3,4,5\}$).

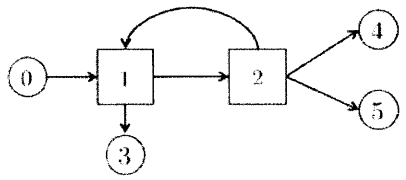

Figure 3-12: System representation.

The input streams are given by (quantities in $\frac{ton}{hour}$):

$$\bar{\mu}^0 = \begin{pmatrix} 20 \\ 0 \\ 0 \\ 0 \\ 0 \\ 0 \end{pmatrix} \quad \bar{\mu}^1 = \begin{pmatrix} 30 \\ 0 \\ 0 \\ 0 \\ 0 \\ 0 \end{pmatrix} \quad \bar{\mu}^2 = \begin{pmatrix} 15 \\ 0 \\ 0 \\ 0 \\ 0 \\ 0 \end{pmatrix}.$$

The sorting matrices are:

$$Q^0 = \begin{pmatrix} 0 & 1 & 0 & 0 & 0 & 0 \\ 0 & 0 & 0.1 & 0.9 & 0 & 0 \\ 0 & 0.8 & 0 & 0 & 0.15 & 0.05 \\ 0 & 0 & 0 & 0 & 0 & 0 \\ 0 & 0 & 0 & 0 & 0 & 0 \\ 0 & 0 & 0 & 0 & 0 & 0 \end{pmatrix} \quad Q^1 = \begin{pmatrix} 0 & 1 & 0 & 0 & 0 & 0 \\ 0 & 0 & 0.8 & 0.2 & 0 & 0 \\ 0 & 0.05 & 0 & 0 & 0.85 & 0.1 \\ 0 & 0 & 0 & 0 & 0 & 0 \\ 0 & 0 & 0 & 0 & 0 & 0 \\ 0 & 0 & 0 & 0 & 0 & 0 \end{pmatrix}$$

$$Q^2 = \begin{pmatrix} 0 & 1 & 0 & 0 & 0 & 0 \\ 0 & 0 & 0.85 & 0.15 & 0 & 0 \\ 0 & 0.1 & 0 & 0 & 0.15 & 0.75 \\ 0 & 0 & 0 & 0 & 0 & 0 \\ 0 & 0 & 0 & 0 & 0 & 0 \\ 0 & 0 & 0 & 0 & 0 & 0 \end{pmatrix}.$$

In this example, output collection unit $z = 3$ collects material $m = 0$, output collection unit $z = 4$ collects material $m = 1$, and output collection unit $z = 5$ collects material $m = 2$. Here, we compute explicitly only $\bar{f}^0$ (i.e., the flow of material $m = 0$); the same computation can be carried out for any other material in the system. Thus:

$$\bar{f}^0 = (I - (Q^0)^T)^{-1}\bar{\mu}^0,$$

that is:

$$\bar{f}^0 = \begin{pmatrix} 1 & 0 & 0 & 0 & 0 & 0 \\ -1 & 1 & -0.8 & 0 & 0 & 0 \\ 0 & -0.1 & 1 & 0 & 0 & 0 \\ 0 & -0.9 & 0 & 1 & 0 & 0 \\ 0 & 0 & -0.15 & 0 & 1 & 0 \\ 0 & 0 & -0.05 & 0 & 0 & 1 \end{pmatrix}^{-1} \begin{pmatrix} 20 \\ 0 \\ 0 \\ 0 \\ 0 \\ 0 \end{pmatrix}.$$

This leads to:

$$\bar{f}^0 = \begin{pmatrix} 20.0000 \\ 21.7391 \\ 2.1739 \\ 19.5652 \\ 0.3261 \\ 0.1087 \end{pmatrix}.$$

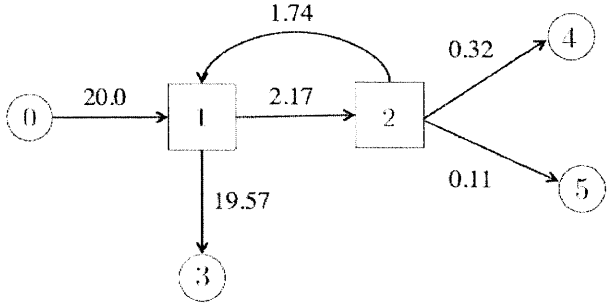

Figure 3-13: System representation with the flows of material $m = 0$. Quantities in $\frac{ton}{hour}$.

3.2.2 Constraints

All configurations of a MRF must satisfy the following:

1. Connection to an output node. To guarantee that $det(I - (Q^m)^T) \neq 0$, we require the existence of a directed path with positive flow from each node $i \in \mathcal{I} \cup \mathcal{S}$ to an output node $z \in \mathcal{Z}$.

2. Respect of unit capacity. Each unit $i \in \mathcal{I} \cup \mathcal{S} \cup \mathcal{Z}$ has a capacity of $f_i^{max}\left(\frac{ton}{hour}\right)$, and thus:

$$\sum_{m \in \mathcal{M}} f_i^m \leq f_i^{max}, \quad \forall i \in \mathcal{Z}. \tag{3.28}$$

3. Positive flow. To guarantee full utilization of each piece of equipment, we require that each sorting unit processes a positive material flow. This corresponds to having a directed path from an input node to each sorting and output node in the system.

4. Precedence constraints. Certain units should precede others. For example, trommels are usually placed at the beginning of the sorting operations to guarantee that a majority of the organic material and the large components of MSW are removed from the material flow. Even though there are some general guiding principles behind MRF configurations, these constraints depend on the specific MRF considered.

3.2.3 Separation Parameters

The computation of steady-state flows relies on the knowledge of the separation parameters $q_{i,j}^m$. These parameters depend on the characteristics of the material entering the unit, on the material feed rate, and on the operational settings of each unit. In the literature, two possible estimation approaches have been proposed [12]:

1. Obtain a detailed understanding of the equipment operating principles and calibrate it with field data.

2. Conduct empirical characterizations to determine how the sorting parameters vary by varying operational settings.

The first approach, adopted in physical modeling, requires a detailed knowledge of the input stream composition. The second approach is usually preferred in probabilistic modeling ([45], [46]), where separation efficiencies are determined empirically via waste sampling, possibly under varying conditions. In this context, defining $x_{i,j}^m$ to be the quantity of material m flowing from unit i to unit j, the separation parameter $q_{i,j}^m$ representing the fraction of material m that unit i sends to unit j is given by [46]:

$$q_{i,j}^m = \frac{x_{i,j}^m}{\sum_k x_{i,k}^m} \tag{3.29}$$

The obtained parameters may depend on the specific input composition, feed rate, and operational settings used during the measurements. In this thesis, we assume unit operational parameters to be fixed, and thus we do not consider the effect of these parameters on separation efficiencies. [45] considers the dependency of sorting parameters on changing input material composition. This could be the case, for example, of inter-particle interference due to particle overlapping or entanglements. Concentration dependence is an important issue when investigating systems of multiple separation stages, since the composition of the flow varies within the process. [45] suggests that applying appropriate separation efficiencies for different stages may require prior knowledge of the expected concentration at each stage or a numerical analysis of those concentrations. In this work, we assume sorting parameters to be constant and independent from input composition.

3.2.4 Performance Metrics: Efficiency and Profit

As seen in Section 3.1.3, there are several possible metrics that have been used to evaluate the performance of MRFs. In this thesis, we measure the material and economic performance of a MRF in terms of efficiency ϵ and profit π. When performing design-optimization in Section 4, these two metrics are combined to obtain a single objective function.

Efficiency

As proposed by [12] and [33], the efficiency ϵ is a single metric that measures the ability of a MRF to recover different materials. Before defining this metric, we need to specify further the topology of the graph, introducing:

- $\mathcal{T}_z \subset \mathcal{M}$: Set of materials collected at output unit z, $\forall z \in \mathcal{Z}$. $\mathcal{T}_z$ may be a single material, as in the case of an output stream collecting only PET, or a material mixture, as in the case of an output stream collecting textiles, plastic films, and other combustibles to produce refuse-derived fuel.

- $l \in \mathcal{Z}$: Landfill output collection unit. The landfill output collection unit collects all those materials that are not collected by any other output collection unit, that is:

$$\mathcal{T}_l = \mathcal{M} \setminus \bigcup_{z \in \mathcal{Z}, z \neq l} \mathcal{T}_z. \tag{3.30}$$

- $\mathcal{Z}_m \subseteq \mathcal{Z}$: Set of output collection units collecting material m, $\forall\ m \in \mathcal{M}$.

- R_m: Recovery of material m, $\forall m \in \mathcal{M}$. As seen in Section 3.1.3, the recovery of a material represents the fraction of the material that is sent to the designated output stream. In the case of multi-material systems this is:

$$R_m = \frac{\sum_{z \in \mathcal{Z}_m} f_z^m}{\sum_{i \in \mathcal{I}} \mu_i^m}. \tag{3.31}$$

[33] proposes the following expression of the efficiency 3.16:

$$\epsilon = \prod_{m \in \mathcal{M}} R_m^{1/M},$$

where R_m is the recovery rate of material m. This formulation has the drawback of taking value zero if one of the efficiencies is zero. Thus, we adopted the efficiency proposed by [45]:

$$\epsilon = \sum_{m \in \mathcal{M}} \beta_m R_m, \tag{3.32}$$

where $\beta_m \in [0, 1]$ is the relative weight of the recovery of material m, such that $\sum_m \beta_m = 1$. We use weights proportional to the mass of a material in the input stream. That is:

$$\beta_m = \frac{\sum_{i \in \mathcal{I}} \mu_i^m}{\sum_{m \in \mathcal{M}} \sum_{i \in \mathcal{I}} \mu_i^m}. \tag{3.33}$$

Profit

In this work, we consider the profit that a MRF generates in one hour of operations. As seen in Section 2.5, we account for the revenues generated by processing materials (i.e., the facility perceives a fixed income per ton of material processed) and by selling recovered materials. Recovered materials meeting the concentration requirements can either be sold to recyclers, used to produce compost, or marketed as refuse-derived fuel. Concentration requirements are expressed as upper and lower bounds on the concentration of a given material in the stream. If the concentration requirements are met, the collected output stream is sold at a price p_k , otherwise it is sent to landfill at a cost c_l. We consider the costs of personnel and the cost of landfill. We define:

- $\alpha_{i,m} \in [0,1],\ \forall i \in \mathcal{S} \cup \mathcal{I} \cup \mathcal{Z},\ \forall\ m \in \mathcal{M}$: Concentration of material m in the flow going through unit i. We have that $\sum_{m \in \mathcal{M}} \alpha_{i,m} = 1$. The concentration of a material is computed from the flow of material in the unit as:

$$\alpha_{i,m} = \frac{f_i^m}{\sum_{m \in \mathcal{M}} f_i^m}. \tag{3.34}$$

- $\alpha_{z,m}^{min},\ \alpha_{z,m}^{max} \in [0,1],\ \forall m \in \mathcal{M},\ z\ \in\ \mathcal{Z}$: Concentration requirements for material m for output stream z.

- $\mathcal{Z}^+ \subseteq \mathcal{Z}$: Subset of the output collection units whose streams meet the purity requirements. That is:

$$\mathcal{Z}^+ = \{z \in \mathcal{Z} \mid \alpha_{z,m}\ \in\ [\alpha_{z,m}^{min},\ \alpha_{z,m}^{max}]\ \forall\ m\ \in\ \mathcal{M}\}. \tag{3.35}$$

- $\mathcal{Z}^-\ \subseteq\ \mathcal{Z}$: Subset of the output collection units whose streams do not meet the purity requirements. That is:

$$\mathcal{Z}^- = \mathcal{Z} \setminus\ \mathcal{Z}^+. \tag{3.36}$$

- $p_z,\ \forall\ z\ \in\ \mathcal{Z}$: Price of output stream z expressed in $\frac{\$}{ton}$. As seen in Section 2.5.1, the selling price p_z is given by $p_z = p_z^{mkt} + p_z^{rec}$; where p_z^{mkt} is the market-based portion and p_z^{rec} is the

recovery-based portion of the selling price. p_z^{rec} is given by:

$$p_z^{rec} = \begin{cases} p_{z,1} & \text{if } \rho_z \geq \overline{\rho_z} \\ p_{z,2} & \text{otherwise,} \end{cases} \tag{3.37}$$

where ρ_z is the ratio of the total amount of desired material recovered at output unit z and the amount of total material processed and $\overline{\rho_z}$ is a designated threshold. Usually ρ_z is computed on a yearly-basis. In this work, we assume that the composition of input material and the model parameters are constant over time, and thus we compute ρ_z with respect to the amount of material processed during one hour of operations. That is:

$$\rho_z = \frac{\sum_{m \in \mathcal{T}_z} f_z^m}{\sum_{m \in \mathcal{M}} \sum_{i \in \mathcal{I}} \mu_i^m}. \tag{3.38}$$

- V_z: Value of materials collected at output collection unit $z \in \mathcal{Z}$, expressed in $\frac{\$}{hour}$. $\forall\, z \in \mathcal{Z}$.

$$V_z = \begin{cases} p_z \sum_{m \in \mathcal{M}} f_z^m & \text{if } z \in \mathcal{Z}^+ \\ 0 & \text{otherwise.} \end{cases} \tag{3.39}$$

- V_p: Revenue generated for processing material. For every ton of material processed, the MRF receives p_p ($\frac{\$}{ton}$), then:

$$V_p = p_p \sum_{m \in \mathcal{M}} \sum_{i \in \mathcal{I}} \mu_i^m. \tag{3.40}$$

- C_l: Cost of landfill. Every ton of material that is sent to landfill costs to the MRF c_l $\frac{\$}{ton}$.

$$C_l = c_l \Big(\sum_{m \in \mathcal{M}} f_l^m + \sum_{z \in \mathcal{Z}} \sum_{m \in \mathcal{M}} f_z^m \Big). \tag{3.41}$$

- C_p: Total cost of personnel expressed in ($\frac{\$}{hour}$). This cost considers the hourly cost of the personnel assigned to manual operations in regular time and in overtime. For a plant operating with nR hand-sorters in regular time at a cost of c_r ($\frac{\$}{hour\ person}$) and nO hand-

sorters in overtime at a cost of c_o ($\frac{\$}{hour\ person}$), the hourly cost of personnel is given by:

$$C_p = c_r\ nR + c_p\ nO. \tag{3.42}$$

Thus, the hourly profit π of a MRF is given by:

$$\pi = \left(V_p + \sum_{z \in \mathcal{Z}} V_z\right) - \left(C_l + C_p\right). \tag{3.43}$$

3.2.5 Applicability to Real Systems

The proposed mathematical model can be applied to MRFs constituted of unit processes sorting a material mixture into multiple output streams. The model makes three major assumptions that could affect its applicability to real world systems. These assumptions are that: i) units sort only by material type; ii) the input stream is stationary and known deterministically; and iii) the separation parameters are independent from the input composition.

Units sorting by material type

First, the model assumes that the sorting process occurs exclusively by material type and not by other characteristics of the material stream (e.g., material size and density). It is possible to extend the model to incorporate units that sort material on the basis of other properties. Let's consider, for example, a unit that sorts material on the basis of a generic property P into N output streams. The property P can be continuous (e.g., size) or discrete (e.g., type); if the property is continuous we identify a finite number of categories corresponding to the output streams generated by the unit. The material categories identified are such that we can define a one-to-one mapping between the material in input and the categories of the property. If we consider, for example, a trommel separating particles of less than 80mm from particles above 80mm, we can map the input material into two categories, one for the fraction of material less than or equal to 80mm (unders) and one for the fraction of material greater than 80mm (overs). In the general case of a unit sorting a flow of material into N output streams with respect to a property P composed of C categories, we define:

- A mapping matrix $\Phi \in [0,1]_{M \times C}$, where each elemement $\phi_{i,j}$ represents the fraction of material i mapped to category j.

- A unit-level sorting matrix $\bar{Q} \in [0,1]_{C \times N}$ where each separation parameter $q_{i,j}$ corresponds to the fraction of material of category $i \in P$ that is sent to stream j.

To determine how different material types are diverted by the unit into each output stream, we compute $Q \in [0,1]_{M \times N}$ given by $Q = \Phi\ \bar{Q}$. Thus, using a proper material mapping we can incorporate into the model units operating on the basis of a generic property. The limit of this approach is that it is necessary to know the mapping Φ at different stages of the process.

Stationary flow of material in input

Second, the model assumes stationary input flow. In reality, material volume and composition fluctuate over time with yearly and weekly seasonality. To relax this assumption, we can:

- Define a function capturing the actual behavior of input material and evaluate the overall performance of the MRF over time.
- Consider the input as the average of the input composition over time.
- Assign a probabiltiy distribution to the input.

Independence of the separation parameters from input composition

Finally, the model assumes that the separation parameters are known and independent from material composition. This is a strong assumption especially given that the composition of the input entering a unit varies with the configuration considered. This problem can be solved by:

- Assigning a distribution to the sorting parameters that depends on the probability that the processed material has a given composition.
- Conducting a scenario analysis considering different values of the sorting parameters.

Chapter 4

A Genetic Algorithm for MRF Design and Personnel Allocation

4.1 Literature Review

Genetic Algorithms (GAs) were originally proposed by Holland in 1975 and investigated by his students (see, for example, [51]) as a technique to solve optimization problems using biological-evolution criteria. In these models, chromosome-like data structures are used to encode potential solutions to a problem. GAs are global search methods that do not use gradient information and have found many applications in non-linear and combinatorial optimization [52]. For example, in operations management (OM) GAs have been used in loading, scheduling, facility layout design, line balancing, production planning, and supply-chain design [53]. In the Artificial Intelligence community, these methods are known as "weak methods" because they make relatively few assumptions on the problem that is being solved [52]. In the literature, there are several different implementations of GAs; the original interpretation is the one proposed by Holland and his students and is referred to as the "canonical genetic algorithm". Currently, GA is applied in a broad sense to describe any population-based model that uses selection and recombination operators to generate new sample points in a search space [52]. In this work, we adopt this broad definition of GAs and refer primarily to [52], which proposes a genetic algorithm tutorial, and to [53], which reviews the major applications of genetic algorithms to OM.

4.1.1 Principles of Genetic Algorithms

A GA starts with a population of individuals (representing the potential solutions to the problem), each carrying genetic material mapping to a unique point in the solution space. Usually, genes are constituted of an array of binary or integer numbers, and the specific mapping adopted depends on the type of problem analyzed. The algorithm explores the solution space by applying mechanisms similar to the evolution of the fittest in nature. Individuals mutate and combine genetic material through reproduction; this is modeled with two types of operations, mutation and crossover. Mutation involves the variation of the genetic material of a single individual, while crossover involves the combination of the genetic materials of two individuals. Only a limited number of individuals contribute to the following generation and they are chosen through a selection process, based on: i) a probabilistic approach in which each individual has a given probability of survival; or ii) an elitist approach in which only the fittest survive. Each individual is assigned a fitness function, expressing the goodness of an individual with respect to the rest of the population.

A general GA works as follows [53], [60]:

- **Step 1 - Initialization:** Set $t = 1$. Randomly generate N solutions to form the first population $\mathcal{P}_1$. Evaluate the fitness of solutions in $\mathcal{P}_1$.
- **Step 2 - Crossover:** Generate an offspring population $\mathcal{Q}_t$ as follows:
  Step 2.1. Choose two individuals x and y from $\mathcal{P}_t$. This could be done randomly or based on the fitness values.
  Step 2.1. Using a crossover operator, generate offspring and add them to $\mathcal{Q}_t$.
- **Step 3 - Mutation:** Mutate each solution $x \in \mathcal{Q}_t \cup \mathcal{P}_t$ with a predefined mutation rate. Keep the original individual and add the mutant to $\mathcal{Q}_t$
- **Step 4 - Fitness assignment:** Evaluate and assign a fitness value to each solution $x \in \mathcal{Q}_t$, discard infeasible solutions.
- **Step 5 - Selection:** Select N solutions from $\mathcal{Q}_t \cup \mathcal{P}_t$ based on their fitness and copy them to $\mathcal{P}_{t+1}$.
- **Step 6 - Iteration:** If the stopping criterion is satisfied, terminate the search and return the current population, else, set $t = t + 1$ and go to Step 2.

This general approach may present variations, the most relevant being whether only the individuals in $\mathcal{Q}_t$ or also the individuals in $\mathcal{P}_t$ contribute to the following generation.

In this section, we discuss the constitutive elements of a GA: solution encoding, measure of fit, initial population, mutation, crossover, selection criterion, and stopping criterion.

Solution Encoding

Potential solutions to the problem are codified through arrays of values. The array encoding a solution is called *genotype* or *chromosome* [50]. Each element of the array is called *allele*; a sequence of alleles encoding the value of a decision variable is called *gene*.

In canonical genetic algorithms, the genotype of an individual is composed of binary digits, and the values taken by each variable are encoded in binary numbers. For example, in the case where a solution is identified by two variables, $x \in \{0, 1, 2, 3, 4, 5, 6, 7\}$ and $y \in \{0, 1\}$, a binary encoding requires a chromosome of four alleles: three encoding the value of x and one encoding the value of y (see Figure 4-1). With this representation, a gene of K alleles can encode 2^K values.

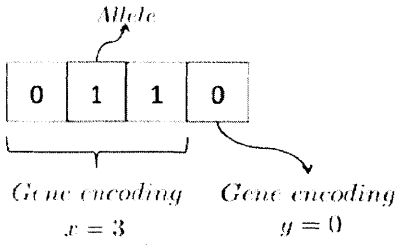

Figure 4-1: Representation of a chromosome using binary encoding.

Other encodings are also possible; for example, in operations management encodings based on integer numbers are often used [53]. The mapping between the gene and the solution impacts on the performance of the algorithm: a poorly structured mapping has often been responsible for errors in the algorithm [54]. One of the major challenges in designing GAs is that of preserving solution feasibility after mutation and crossover; a possible way of solving this problem is represented by random keys [55]. Random keys are based on a soft encoding of the solution that guarantees feasibility; for example, this could be done by encoding the value of the variables in the relative order of the alleles [55].

Measure of Fit

Each gene has a *measure of fit* or *figure of merit* expressing the goodness of an individual with respect to other individuals in the population. As in [52], we distinguish between the objective function (or evaluation function) and the fitness function: the objective function depends only on the value of the decision variables of a solution and measures the performance of the individual in absolute terms; the fitness function is a monotonic function of the objective function that measures the goodness of an individual with respect to other individuals in a population. For example, if the objective value of individual i is ξ_i, the measure of fit ϕ_i can be given by [52]:

$$\phi_i = \frac{\xi_i}{\bar{\xi}}, \tag{4.1}$$

where $\bar{\xi}$ is the average of the objective values of the individuals in the population. This measure is defined only if $\bar{\xi} \neq 0$.

Often, the optimization requires the evaluation of multiple objectives. In these cases, there are two major approaches [60]:

- *Consider a single objective function.* This is achieved either by taking all objectives but one as constraints of the problem, or by combining all objectives into one metric through a utility function or a weighed sum. The former approach is limited by the difficulties in properly defining proper bounds to incorporate the objectives as constraints; the latter approach is limited by the fact that it is difficult to set proper weights or utility functions.

- *Consider a set of Pareto-optimal solutions.* A Pareto optimal set is a set of solutions that are non dominated with respect to each other. While moving from one Pareto solution to another, there is always a certain amount of sacrifice in one objective(s) to achieve a certain amount of gain in the other(s). Examples of applications of Pareto-optimal GAs are given by [56], [57], [58], [59]. This approach may not work well if the Pareto frontier is sparse, with solutions that propose significant trade-offs with respect to different objectives. In this case, there may be a set of well performing dominated solutions, clustered in proximity of the Pareto frontier, that are not considered.

The measure of fit used in this work is the weighed sum of the objectives of the individual. Defining ξ_i^j to be the j^{th} objective of the i^{th} individual in the population and $\alpha_j \in [0,1]$ the weight of the j^{th} objective such that $\sum_j \alpha_j = 1$, the measure of fit is given by:

$$\phi_i = \sum_j \alpha_j \frac{\xi_{max}^j - \xi_i^j}{\xi_{max}^j - \xi_{min}^j}. \tag{4.2}$$

Here, ξ_{max}^j is the maximum value of the j^{th} objective in the population, and ξ_{min}^j is the minimum value of the j^{th} objective in the population. This measure is well defined only if $\xi_{max}^j - \xi_{min}^j \neq 0 \; \forall j$; if this condition is not satisfied, it means that there is at least one objective j for which $\xi_{max}^j = \xi_{min}^j$ and thus the j^{th} objective does not allow discriminating between individuals.

Initial Population

The initial population $\mathcal{P}_1$ is usually randomly generated. In some situations it is possible to incorporate domain specific knowledge and include individuals with desired characteristics. The size of the population affects the efficiency of the algorithm; in fact, the larger the number of the individuals, the greater the number of mutations and crossovers at each iteration.

Crossover

Crossover consists in an exchange of genetic material between two individuals. At every iteration, pairs of individuals may be selected randomly with respect to their measure of fit. The chosen parents interchange their genetic material on the basis of different possible crossover operations, each one having a probabiltiy of occurrence p_i (i.e., in the case of I possible crossover operations, we have $\sum_{i=1}^{I} p_i = 1$, with $p_i \in (0,1), \; \forall \; i = 1, ..., I$):

- One-point crossover: An index is chosen at random and the parents exchange all alleles up to and including the allele at the chosen index.
- Two-point crossover: Two indexes are chosen at random, and the material between and including the two alleles is exchanged.
- Mask crossover: A sequence of zeros and ones is randomly generated, and the parents exchange the alleles corresponding to the positive values of the mask.

Figure 4-2 shows how different crossover operations are applied.

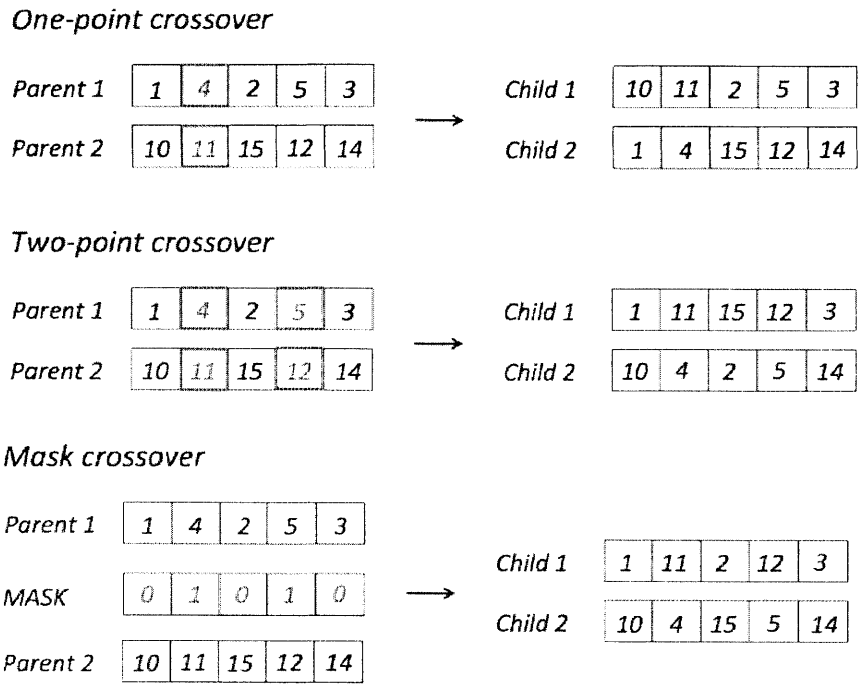

Figure 4-2: Representation of crossover operations on chromosomes of integer numbers.

Mutation

Mutation consists in the variation of the chromosome of an individual. It can be achieved, for example, by:

- Changing the values of a subset of the alleles. Both the mutating alleles and the new value taken are chosen randomly. [53] considers mutations in which only one-single allele is changed, but more disruptive situations are possible.

- Alleles swap. Pairs of alleles are chosen randomly according to a uniform distribution and their values are exchanged. [53] considers swap mutations in which one-single pair of alleles is changed, but more disruptive situations can be considered.

As with crossover, each type of mutation occurs with probability p_i. Figure 4-3 shows how different crossover operations are applied.

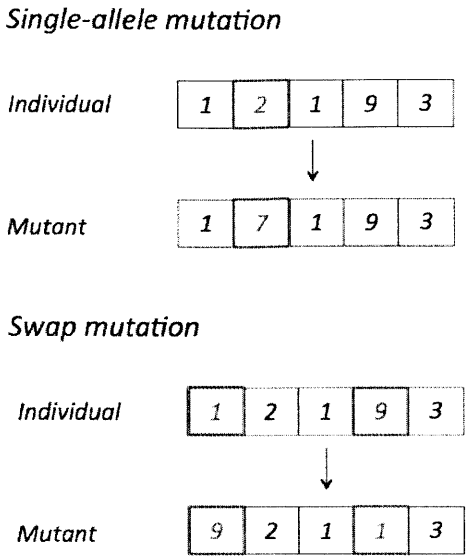

Figure 4-3: Representation of mutation operations on chromosomes of integer numbers.

Selection Criterion

Only a subset of the individuals contributes to the next generation. There are several selection strategies, such as the roulette strategy, the tournament strategy, and the elitist strategy. The roulette strategy assigns a probability of survival to each individual proportional to the measure of fit of that individual; the tournament strategy picks $k \geq 2$ individuals to compete against each other and selects the fittest individual out of the k; the elitist strategy preserves the fittest individuals out of the entire population.

Stopping Criterion

The algorithm stops either after a certain number of iterations, or when the improvement in the measure of fit falls below a specified value.

Parameters Selection

GAs rely on the definition of the population size, stopping criterion, probability of mutation and crossover. There is no definitive process adopted to select these parameters; in the literature parameters are primarily chosen on the basis of pilot run and ad-hoc selection [53].

4.1.2 Applications of GAs to Facility Design

In the literature, GAs have been applied to several operations management (OM) problems, such as machine and personnel scheduling (e.g.,[61], [62], [63]), single-product and multi-product line balancing (e.g., [64], [65], [66]), lot sizing and production system planning (e.g., [67], [68]), and supply chain management (e.g , [69], [70]). [53] proposes a comprehensive review of these models.

GAs have also been applied to facility design, such as to cell formation problems for cellular manufacturing and to facility layout problems. Cell formation problems involve the grouping of different machines into cells responsible for producing families of similar parts. Facility layout problems focus on determining the optimal positioning of cells to minimize material flow costs between cells. These problems are different from MRF design, but their study can show possible applications of GAs. For example, in cell formation problems, [71] proposes a nested GA in which an outer loop solves a GA to assign machines to cells, and an inner loop solves another GA to determine part routing between cells. As a second example, [72] adopts a double encoding scheme to assign parts in cellular manufacturing with alternative process plans. In the proposed encoding, each gene refers to a part number, and the information stored in the gene is converted into a process plan number and a manufacturing cell number by evaluating two different functions.

The application of GAs to facility design is predominantly characterized by integer encodings of solutions and termination is usually reached after a maximum number of iterations [53]. Even though traditional crossover and mutation are widely used, several authors have created specialized operations with certain properties. For example, [73] proposes a GA for cell formation that preserves the feasibility of offspring under specific constraints: for example, certain machines must be placed in the same cell because they share a common resource and certain machines must be kept separate because they produce interferences. To preserve feasibility in crossover, as a first step, the pieces of equipment that are assigned to the same cells in both parents are assigned to the same cell also in the children. As a second step, the pieces of equipment that are placed in different cells in the parents are reproduced in a way that one child inherits the assignment of one parent and the other child inherits the assignment of the other parent. This child-parent assignment is done randomly. Finally, the remaining pieces of equipment are randomly assigned to feasible cells.

In summary, the literature offers many examples of applications of GAs to facility design, each formulation being highly dependent on the specific application.

4.2 Problem Formulation

In this work, we apply GAs to determine the configuration of a MRF and to assign personnel to manual operations. We consider a MRF that has a set of predefined pieces of equipment with known sorting parameters and personnel that can be assigned to manual operations. We then want to find the facility configuration and the personnel assignment maximizing efficiency and profit.

Configuration

We refer to the model introduced in Section 3.2, representing a MRF in terms of nodes for input, sorting, and output collection units and arcs for material streams. Sets $\mathcal{I}$, $\mathcal{S}$, and $\mathcal{Z}$ are the sets of input, sorting, and output nodes respectively. A specific configuration e is defined in terms of connections between units as:

$$e = \{(i,j) | i \in \mathcal{I} \cup \mathcal{S}, j \in \mathcal{S} \cup \mathcal{Z}\}. \tag{4.3}$$

The number of existing arcs and their origin node are known; the destination node is to be determined.

As seen in Section 3.2.2, a configuration e is feasible if:

1. There is a directed path from each node $i \in \mathcal{I} \cup \mathcal{S}$ to an output node $z \in \mathcal{Z}$.
2. The flow capacity of each unit is met.
3. There is a directed path from an input node $i \in \mathcal{I}$ to each sorting and output nodes in the system $j \in \mathcal{S} \cup \mathcal{Z}$.
4. Precedence constraints are met.

The set of feasible configurations is the set $\mathcal{E}$.

Personnel Assignment

MRFs use two types of manual operations: hand-sorting (HS) and quality-control (QC). HS units remove desired material from a stream and can be located at any stage in the process. For example, personnel in HS units may remove large cardboard and plastic containers from the waste stream. QC units are located at the end of the process, in correspondence of output collection units, and the personnel removes undesired material from the stream. For example, personnel in QC units may remove wood and inert materials from a stream collecting aluminum. Since the location of QC units is predefined (i.e., they are always located after specific output collection units), these units are not considered as sorting units that need to be located when determining a configuration of a MRF (i.e., QC units are not considered in the set $\mathcal{S}$).

Let's define the set MAN to be the set of manual units in the system, x_i^{min} and x_i^{max} to be the minimum and maximum number of workers that can be assigned to manual unit i, $\bar{x}^{max}$ to be the total number of workers available, and x_i to be the decision variable corresponding to the number of workers assigned to manual unit i,. Then the set of feasible personnel assignments is given by:

$$\mathcal{X} = \{x \in \mathcal{N}_0^{|MAN|} |\ x_i^{min} \leq x_i \leq x_i^{max}\ \forall i \in MAN,\ \sum_{i \in MAN} x_i \leq \bar{x}^{max}\}. \tag{4.4}$$

Objective Function

As introduced in Section 3.2.4, MRFs are evaluated in terms of efficiency and profit, with $\epsilon_{e,x}$ and $\pi_{e,x}$ being the efficiency and the profit of configuration e with personnel assignment x. We compare different configurations and personnel assignments with respect to both objectives.

Problem Formulation

The problem is given by:

$$\begin{aligned} \max_{e,x} \quad & (\pi_{e,x},\ \epsilon_{e,x}) \\ \text{s.t.} \quad & e \in \mathcal{E} \\ & x \in \mathcal{X}. \end{aligned} \tag{4.5}$$

4.3 Proposed Genetic Algorithm

In this section, we discuss how to apply GAs to solve problem 4.5. As seen in Sections 3.2 and 4.2, MRF are defined in terms of nodes representing input, sorting, and output collection units and arcs representing material streams. Arcs are directed and can be *outgoing* if exiting a unit or *incoming* if entering a unit; for example, an arc from node i to node j is outgoing for i and incoming for j. The set of units and their output streams that need to be connected is predefined; input units have one outgoing arc, sorting units have at least two outgoing arcs, and output units have no outgoing arc. Each unit has a number of outgoing arcs that are initially "dangling", that is, the destination node of the arc is not specified and is to be determined in the decoding phase of the algorithm. The only destination nodes that are assigned since initialization are those directed to output collection units. In fact, there are only specific sorting units that collect materials; for example, eddy-current separator collects aluminum while magnet collects ferrous.

The proposed GA works as follows:

- **Step 0 - Preprocessing:** In this phase we assign all arcs directed to output collection units; these connections are predetermined and given as an input to the model. Landfill unit is the only output collection unit that after this step does not have an incoming arc.

- **Step 1 - Initialization:** Set $t = 1$. Randomly generate N individuals to form the first population $\mathcal{P}_1$. Each individual is defined by a chromosome, which is an array of $L + I + 1$ integer numbers, where L is the number of dangling arcs and I the number of input nodes. Each allele can take values in $[1, L]$. At initialization, the alleles are independently generated from a uniform distribution in $[1, L]$. All solutions have different genetic material; we keep track of the genetic material of all individuals in the "history" set $\mathcal{H}$, containing the chromosomes of all individuals generated in the population.

- **Step 2 - Crossover:** Generate an offspring population $\mathcal{Q}_t$ as follows:

  Step 2.1. Choose at random two individuals x and y from $\mathcal{P}_t$. All individuals are chosen exactly once to reproduce, and all of them are equally likely to be selected among the individuals that have not reproduced yet.

Step 2.1. Using a crossover operator, generate two children; if their genetic material is not in $\mathcal{H}$, add them to $\mathcal{Q}_t$ and add their chromosomes to $\mathcal{H}$, otherwise discard them. The parents exchange the genetic material via one-point crossover with probabiltiy p_1, two-point crossover with probability p_2, and mask crossover with probability p_3, with $p_i \in [0,1]$ and $\sum_{i=1}^{3} p_i = 1$.

- **Step 3 - Mutation:** Mutate each solution $x \in \mathcal{Q}_t \cup \mathcal{P}_t$. If the mutant has new genetic material, add the mutant to $\mathcal{Q}_t$ and its chromosome to $\mathcal{H}$, otherwise discard the mutant. With probability $p'_1 \in [0,1]$ the mutation involves the random change of an allele: the mutating allele is chosen uniformly out of the alleles of the chromosome, and its new value is selected uniformly out of the possible values taken by that allele. With probability $p'_2 \in [0,1]$ the mutation involves the swap between two alleles: two alleles are chosen uniformly out of the alleles in the chromosome and their values are swapped. We have $p'_1 + p'_2 = 1$.

- **Step 4 - Fitness assignment:** Determine the measure of fit of each solution $x \in \mathcal{Q}_t \cup \mathcal{P}_t$, discard infeasible solutions.

- **Step 5 - Selection:** Since we are solving a maximization problem, select the N individuals with the highest measure of fit from $\mathcal{Q}_t \cup \mathcal{P}_t$ and copy them to $\mathcal{P}_{t+1}$.

- **Step 6 - Iteration:** If $t = T^{max}$, terminate the search and return the current population. Otherwise, set $t = t + 1$ and go to Step 2.

The fitness assignment is the specialized part of the GA; it incorporates the decoding of the chromosome, the personnel assignment, and the computation of the objective function and the measure of fit for each solution. Following [55], we propose a GA based on soft-encoding. Given a set of sorting units, input units, and output units with defined sorting parameters, the decoding algorithm finds a configuration that guarantees that each sorting unit is located on a directed path between an input node and an output node. Once a configuration is determined, additional constraints are enforced; these may include the respect of flow capacity and precedence between units.

We now illustrate the procedure to compute the measure of fit of an individual.

- **Step 1 - Compute the objective value for each individual $x \in \mathcal{Q}_t$:**

  Step 1.1 - Decode the chromosome and verify constraints: The information contained in the chromosome is decoded to determine a configuration in which each sorting unit is located on a directed path from an input node to an output node. User-defined constraints regarding the sequence of units in the system are verified. Solutions violating the constraints are discarded.

  Step 1.2 - Compute material flows: As seen in Section 3.2, once the configuration of a MRF is determined, it is possible to compute the flow of material through each unit using equation 3.26. In this phase, the sorting efficiencies of all manual sorting units are computed assuming that the minimum required number of operators is assigned to that unit. The modeling of manual units and the heuristic used to allocate personnel are explained in Section 4.3.3.

  Step 1.3 - Assign personnel, update material flows, and verify capacity constraints: Personnel operating in regular time and in overtime is assigned to manual units. Personnel assignment affects the sorting efficiencies of manual units and impacts on the overall flow of material. Thus, it is necessary to recompute material flows with equation 3.26. Capacity constraints on the flow of material going through each unit are verified. Solutions violating the constraints are removed from the population.

  Step 1.4 - Compute efficiency and profit: In this phase, the recovery rate of each material is computed and used to determine the efficiency ϵ_x of individual x. The revenues form recyclable output streams and from processed materials, and the costs of landfill and personnel are considered to compute the profit π_x of individual x.

- **Step 2 - Compute the measure of fit for each individual $x \in \mathcal{Q}_t \cup \mathcal{P}_t$:.**

  The measure of fit ϕ_x of each individual $x \in \mathcal{P}_t \cup \mathcal{Q}_t$ is given by:

$$\phi_x = \alpha_1 \frac{\pi^{max} - \pi_x}{\pi^{max} - \pi^{min}} + (1 - \alpha_1) \frac{\epsilon^{max} - \epsilon_x}{\epsilon^{max} - \epsilon^{min}}, \tag{4.6}$$

  where π^{max} and π^{min} are the maximum and minimum profits in $\mathcal{P}_t \cup \mathcal{Q}_t$, ϵ^{max} and ϵ^{min} are the maximum and minimum efficiencies in $\mathcal{P}_t \cup \mathcal{Q}_t$, and $\alpha_1 \in [0, 1]$ is the weight assigned to the profit. If $\pi^{max} = \pi^{min}$ or $\epsilon^{max} = \epsilon^{min}$ that specific metric is not considered because all individuals in the population perform in the same way with respect to it.

4.3.1 Decode the Chromosome

The notation used in this section is the same as the notation introduced in Section 3.2, with S indicating the number of sorting units, I the number of input units, Z the number of output units in the system including the landfill output unit. Each unit is identified by an integer number i:

- For sorting units: $i \in [1, S]$;
- For landfill unit: $i = S + 1$;
- For input units: $i \in [S + 2, S + I + 1]$;
- For other output collection units: $i \in [S + I + 2, S + I + Z]$.

For each unit we define:

- $\mathcal{A}_i$: Set of outgoing arcs. Each arc is identified by two numbers (i, a), where i is the identification of the origin unit and a is the arc number $a = 1, ..., |\mathcal{A}_i|$. The arcs of a unit can either be *dangling* or *assigned*.

  Each arc has:

  - A destination unit $dest_{(i,a)}$, which is determined once the arc is *assigned*.
  - A weight array $W_{(i,a)} \in [0, 1]_{1 \times M}$, where each element $w^m_{(i,a)}$ is the fraction of material entering unit i that is sent to connection a.
  - A descendants set $Descendants_{(i,a)}$, containing the identification numbers of sorting and output units j in the system for which there is a directed path from i to j via (i, a).

- $Dangling_i \subset \mathcal{A}_i$: Set of outgoing arcs of unit i that do not have a destination node.
- $Assigned_i \subset \mathcal{A}_i$: Set of outgoing arcs of unit i that have a destination node. At initialization, it contains all arcs directed to output collection units.
  That is: $Assigned_i = \{(i, a) \mid dest_{(i,a)} \in \mathcal{Z}\}$.
- $Ancestors_i$: Set containing all units j for which there is a directed path from j to i.

We introduce the list of dangling arcs, $\mathcal{L}$, containing arcs (i, a) that do not have a destination node assigned. That is:

$$\mathcal{L} = \bigcup_{i \in \mathcal{S}} Dangling_i.$$

The l^{th} element of $\mathcal{L}$ is referred to as $(i,a)_l$. The list changes size as the algorithm proceeds: we indicate with L the initial size of the list and with $|\mathcal{L}|$ the size of the list at a given iteration. Finally, we define the *Root* set to be the set of sorting units directly connected to input units. At initialization $Root = \emptyset$.

The chromosome c of an individual is an array of $L + I + 1$ integer numbers, each taking values in $[1, L]$. The first S alleles contain information regarding sorting units; allele $S + 1$ contains information regarding landfill units; the following I alleles contain information regarding input units; the remaining alleles contain information regarding dangling arcs.

We proceed as follows: first, we determine the elements in the *Root* set; second, we identify a graph structure in which each sorting unit is on a directed path originating from an input node; third, we assign the remaining dangling connections ensuring that each sorting unit is on a directed path from an input node to an output node.

Phase 1. Determine the root set.

The information to assign the outgoing arcs of input nodes is contained in the alleles from position $S + 2$ to position $S + I + 1$. Let c_k be the allele at position k of chromosome c.

For $k = S + 2, ..., S + I + 1$:

- Assign the destination node of the outgoing arc $(k, 1)$ to sorting unit i,

$$i = (c_k \% S) + 1;$$

- Add i to *Root* set.

Here, % is the remainder operator, returning the remainder of two numbers. For example, 10%3 returns 1, because 10 divided by 3 leaves a remainder of 1.

Every time that we assign the destination node of an arc, we update the information of all units affected by the assignment. In the case of arc (i, a) connected to unit j:

- Update the information of the assigned arc:
  - Set $dest_{(i,a)} = j$;
  - Add j and $\bigcup_{a \in \mathcal{A}_j} Descendants_{(j,a)}$ to $Descendants_{(i,a)}$.

- Update the information of the origin node i:
  - Remove (i, a) form $Dangling_i$ and add it to $Assigned_i$.

- Update the information of the destination node j:
  - Add i and $Ancestors_i$ to $Ancestors_j$.

- Update the information of ancestor and descendant nodes:
  - Add i and $Ancestors_i$ to $Ancestors_k$, $\forall k \in \bigcup_{\bar{a} \in \mathcal{A}_j} Descendants_{(j,\bar{a})}$;
  - Add $Descendants_{(i,a)}$ to $Descendants_{(k,\bar{a})}$ for $k \in Ancestors_i$ such that $i \in Descendants_{(k,\bar{a})}$, $\forall\, \bar{a} \in \mathcal{A}_k$.

Phase 2. Generate a graph in which each sorting unit is on a directed path originating from an input node.

We iterate through the first $S+1$ alleles of chromosome c to determine the incoming connections of sorting and landfill units in the system.

For $j = 1, ..., S+1$, $j \notin Root$:

- *Step 1:* Set $l = 1 + c_j\%|\mathcal{L}|$.

- *Step 2:* Pick $(i, a)_l$, the l^{th} arc in $\mathcal{L}$.

- *Step 3:* If $i \neq j$ and $i \notin Descendants_{(j,\bar{a})}$, $\forall \bar{a} \in \mathcal{A}_j$:

  - Set $dest_{(i,a)_l} = j$.
  - Update the information in the system.
  - Remove $(i, a)_l$ from $\mathcal{L}$.
  - If $j = S+1$: Stop. Otherwise: increment $j = j + 1$ and go to Step 1.

  Otherwise:

  - Move to the following arc in $\mathcal{L}$. That is, if $l = |\mathcal{L}|$, set $l = 0$, otherwise, set $l = l + 1$.
  - Go to Step 2.

Theorem 2. *For a system in which each input unit has exactly one dangling arc and each sorting unit has at least one dangling arc, the proposed algorithm always finds a feasible graph (i.e., the algorithm does not iterate indefinitely).*

Proof. First, we recall that we can assign a dangling arc l originating from node i to be incoming to node j only if:

- $i \neq j$;
- i is not a descendant of j. That is, there is no directed path from j to i.

Let's consider a graph with $\mathcal{I}$ input nodes, $\mathcal{S}$ sorting nodes and $\mathcal{L}$ dangling arcs originating from the sorting nodes only, and let $\mathcal{K} \subset \mathcal{S}$ be the set of sorting nodes for which we need to find an incoming arc after *Phase* 1 of the algorithm. We have that $\mathcal{K} \subset \mathcal{S}$ because there is at least one root node with an incoming arc originating at an input node.

If $\mathcal{K} = \emptyset$, then we only need to assign an incoming arc to the landfill unit, and this assignment is always feasible.

Let's consider instead the case in which $\mathcal{K} \neq \emptyset$. Since each sorting unit has at least one dangling arc, at the beginning of *Phase* 2 there are at least $|\mathcal{S}|$ dangling arcs; that is:

$$|\mathcal{L}| \geq |\mathcal{S}| > |\mathcal{K}|. \tag{4.7}$$

Let $k \in \mathcal{K}$ be the first unit for which the algorithm seeks to find an incoming arc. At the first iteration none of the units in $\mathcal{S}$ has descendants; and therefore any arc $l \in \mathcal{L}$ that originates from unit $i \neq k, i \in \mathcal{S}$ can be the incoming arc to unit k.

Now, we can merge unit i and unit k considering them as if they were one single unit having dangling arcs corresponding to the dangling arcs of both units. This situation can be seen as the beginning of a new *Step* 2′ of the algorithm, with sets $\mathcal{S}'$, $\mathcal{K}'$, and $\mathcal{L}'$ (clearly, $|\mathcal{S}'| = |\mathcal{S}| - 1$, $|\mathcal{K}'| = |\mathcal{K}| - 1$, and $|\mathcal{L}'| = |\mathcal{L}| - 1$). As we noted previously, none of the units in $\mathcal{S}'$ has descendants; and therefore we can assign any arc $l \in \mathcal{L}$ that originates from unit $i \neq k$ to be the incoming arc to unit k.

We can iterate this procedure until all units $k \in \mathcal{K}$ have an incoming arc, and there is at lease one dangling arc left (i.e., $|\mathcal{L}| \geq 1$) because of equation 4.7.

As a final step, we need to assign the incoming arc to the output node corresponding to landfill, and this assignment is always feasible. □

Theorem 3. *In the graph obtained, each sorting unit $s \in \mathcal{S}$ is on a directed path originating from an input node $i \in \mathcal{I}$.*

Proof. Let's consider the graph formed by all the nodes in $\mathcal{S} \cup \mathcal{I}$ and the assigned arcs; let's augment it by adding an origin node that has outgoing arcs directed towards each of the input nodes $i \in \mathcal{I}$. The graph obtained has $N = S + I + 1$ nodes.

We show that the augmented graph is a tree rooted at the origin node. By definition, an undirected graph with N nodes is a tree if and only if it is connected and has $N - 1$ arcs.

By construction:

- The root node is the only node without an incoming arc;
- Each node $i \in \mathcal{I} \cup \mathcal{S}$ has exactly one incoming arc such that the start node is not among its descendants. Thus, we have an acyclic graph with $N - 1$ arcs, and therefore we have a tree.

By construction, the root node is directly connected only to nodes $i \in \mathcal{I}$. Thus, since each s is connected to the root node, there must be a path between a node $i \in \mathcal{I}$ and s. Since input units have only outgoing arcs, the connecting path must be directed from $i \in \mathcal{I}$ to $s \in \mathcal{S}$. □

Phase 3. Assign all remaining arcs obtaining a graph in which each input and sorting unit is on a directed path ending at an output node.

We assign destination nodes to the dangling arcs that remain in $\mathcal{L}$ by decoding the information contained in the alleles at positions $[S + I + 2, L]$ of chromosome c. Destination nodes can be either sorting units or the landfill output unit. Let k be an index that is used to iterate through the remaining alleles of the chromosome and is initially set as $k = S + I + 2$.

If $\mathcal{L} \neq \emptyset$:

- *Step 1:* Consider the first arc in list $\mathcal{L}$, arc $(i, a)_1$.
- *Step 2:* Set $j = 1 + c_k \% (S + 1)$.
- *Step 3:* If $j = S + 1$ or if $\bigcup_{\bar{a} \in \mathcal{A}_j} Descendants_{(j,\bar{a})}$ contains an output node $z \in \mathcal{Z}$:
  - Set $dest_{(i,a)_1} = j$;
  - Update the information in the system;
  - Remove $(i, a)_1$ from $\mathcal{L}$;
  - If $\mathcal{L} = \emptyset$: Stop. Otherwise: Increment $k = k + 1$ and go to Step 1.

Otherwise if $\bigcup_{\bar{a}\in\mathcal{A}_j} Descendants_{(j,\bar{a})}$ does not contain an output node $z \in \mathcal{Z}$:

- Increment j, $j = j + 1$.
- Go to Step 3.

Notice that if in *Step* 3 the assignment is infeasible, the algorithm increments the value of the destination node (i.e., $j = j+1$) until it is set to be the landfill. We allow multiple arcs originating from the same input unit to be directed to the landfill and thus this assignment is always feasible and the algorithm does not cycle indefinitely.

Theorem 4. *In the graph obtained, each input and sorting unit $i \in \mathcal{S} \cup \mathcal{I}$ is on a directed path ending at a destination node $z \in \mathcal{Z}$.*

Proof. At the beginning of *Phase* 3 each sorting unit is on a path originating from an input unit, and each input unit is connected to a sorting unit; thus, showing that there is a path from every sorting unit in the system to an output unit implies that there is a path from each input unit to an output unit as well.

Since each sorting unit has at least one dangling connection and there is one landfill unit, after *Phase* 2 there are only two possible options: from each sorting unit either there is a path ending to the landfill or there is a path ending to a unit with a dangling connection.

Since in this phase we assign dangling connections in such a way that these connections lead to a path ending to an output unit, all sorting units are on a path ending at an output node (landfill is considered an output node). □

Example

Let's consider a system separating aluminum and HDPE from a mixture of aluminum, HDPE, and other materials. The system has one input unit, three sorting units, two output collection units (one for aluminum and one for HDPE), and landfill output unit. Each sorting unit has two output streams. The first sorting unit is an eddy-current separator and collects aluminum; the second is a DAR and collects HDPE; the third is a DAR that can send its output streams either to other sorting units or to landfill. Table 4.1 summarizes this information.

Node Type	Node ID	Unit type	Outgoing Arcs
Sorting Units	1	Eddy Current	Arc $(1,1)$ - Dangling Arc $(1,2)$ - Connected to unit 6
	2	DAR	Arc $(2,1)$ - Dangling Arc $(2,2)$ - Connected to unit 7
	3	DAR	Arc $(3,1)$ - Dangling Arc $(3,2)$ - Dangling
Output Units	4	Landfill	-
	6	Aluminum	-
	7	HDPE	-
Input Unit	5	-	Arc $(5,1)$ - Dangling

Table 4.1: Nodes and arcs in the graph.

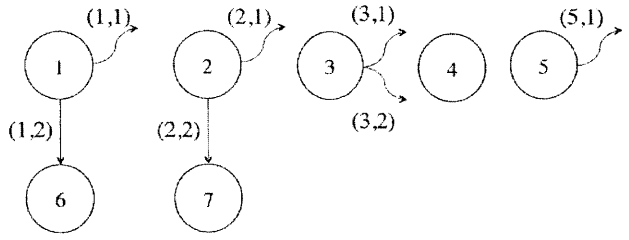

Figure 4-4: Nodes and outgoing arcs.

Figure 4-4 shows the nodes and the respective outgoing arcs. The list of dangling connections is $\mathcal{L} = \{(1,1),\ (2,1),\ (3,1),\ (3,2)\}$, containing all dangling connections originating from sorting units; dangling connections originating from input units are not included. In this example, we have $I = 1$ input node and $L = 4$ dangling connections, thus the chromosome is constituted of $I + L + 1 = 6$ alleles, each taking values in $[1, 4]$ (i.e., each taking value in $[1, L]$). In this example, we consider the chromosome shown in Figure 4-5.

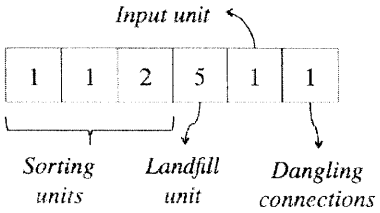

Figure 4-5: Representation of the chromosome in the example. Alleles 1-3 contain information about sorting units, allele 4 about landfill unit, allele 5 about input unit, and allele 6 about the remaining dangling arc.

Phase 1. Determine the root set.

We take node $i = 1 + c_5 \% S$ as the destination node of $(5, 1)$ and add it to the root set. In this case, $i = 1 + 1\%3 = 2$. Then: $Root = \{2\}$. Figure 4-6 shows the resulting graph.

We then update the information in the system:

- Update the information of arc $(5, 1)$:
  - $dest_{(5,1)} = 2$;
  - $Descendants_{(5,1)} = \{2, 7\}$.
- Update the information of the origin unit 5:
  - $Dangling_5 = \emptyset$;
  - $Assigned_5 = \{(5, 1)\}$.
- Update the information of the destination unit 2:
  - $Ancestors_2 = \{5\}$.
- Update the information of other units in the system:
  - $Ancestors_7 = \{2, 5\}$.

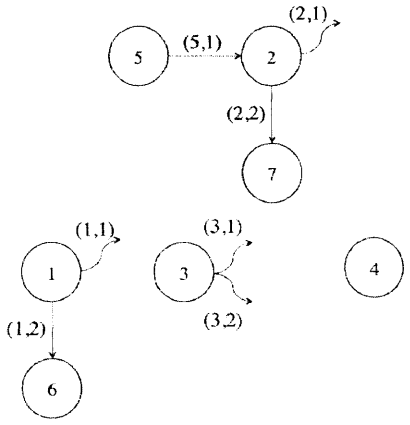

Figure 4-6: State of the graph.

Phase 2. Generate a graph in which each sorting unit is on a directed path originating from an input node.

Start by assigning an incoming arc to node 1:

- Consider allele $c_1 = 1$;
- Pick $(i, a)_j \in \mathcal{L}$, where:

$$j = c_1 \% |\mathcal{L}| + 1 = 1\%4 + 1 = 2.$$

Thus the incoming connection is $(2, 1)$. Since node 2 is not among the descendants of node 1 we finalize the assignment. Figure 4-7 shows the state of the graph after the assignment. We then update the information in the graph.

- Update the list of dangling arcs:
  - $\mathcal{L} = \{(1,1),\ (3,1),\ (3,2)\}$.
- Update the information of arc $(2,1)$:
  - $dest_{(2,1)} = 1$;
  - $Descendants_{(2,1)} = \{1\}$.
- Update the information of the origin unit 2:
  - $Dangling_2 = \emptyset$;
  - $Assigned_2 = \{(2,1),(2,2)\}$.
- Update the information of the destination unit 1:
  - $Ancestors_1 = \{2,5\}$.
- Update the information of other units in the system:
  - $Descendants_{(5,1)} = \{1,2,6,7\}$;
  - $Ancestors_6 = \{1,2,5\}$.

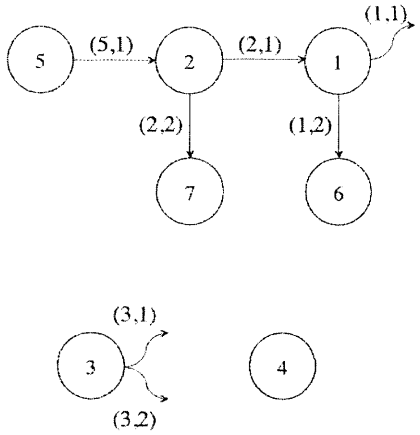

Figure 4-7: State of the graph.

We skip node 2 since it is in the *Root* set and proceed to node 3.

- Consider allele $c_3 = 2$.
- Pick $(i,a)_j \in \mathcal{L}$, where $j = 2\%3 + 1 = 3$. Thus the incoming connection is $(3,2)$. This connection cannot be incoming because it is self-reentrant.
- Set $j = 0$. Pick connection $(1,1)$. Since node 1 is not among the descendants of node 3 we finalize the assignment. Figure 4-8 shows the resulting graph.

We update the information in the graph:

- Update the list of dangling arcs:
  - $\mathcal{L} = \{(3,1),\ (3,2)\}$.

- Update the information of arc $(1,1)$:
  - $dest_{(1,1)} = 3$;
  - $Descendants_{(1,1)} = \{3\}$.
- Update the information of the origin unit 1:
  - $Dangling_1 = \emptyset$;
  - $Assigned_1 = \{(1,1),(1,2)\}$.
- Update the information of the destination unit 3:
  - $Ancestors_3 = \{1,2,5\}$.

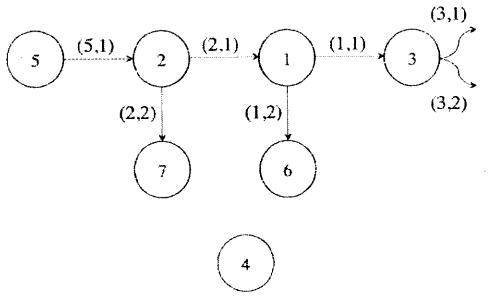

Figure 4-8: State of the graph.

- Update the information of other units in the system:
  - $Descendants_{(2,1)} = \{1,3,6\}$
  - $Descendants_{(5,1)} = \{1,2,3,6,7\}$

Finally, we move to the landfill unit and repeat the process.

- Consider allele $c_4 = 5$.
- Pick $(i,a)_j \in \mathcal{L}$, where $j = 5\%2+1 = 2$. Thus the incoming connection is $(3,2)$. We finalize the assignment. Figure 4-9 shows the resulting graph.

We update the information in the graph:

- Update the list of dangling arcs:
  - $\mathcal{L} = \{(3,1)\}$.
- Update the information of arc $(3,2)$:
  - $dest_{(3,2)} = 4$
  - $Descendants_{(3,2)} = \{4\}$
- Update the information of the origin unit 3:
  - $Dangling_3 = \{(3,1)\}$

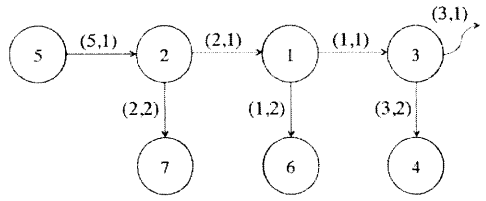

Figure 4-9: State of the graph.

- $Assigned_3 = \{(3,2)\}$.

- Update the information of the destination unit 4:

  - $Ancestors_4 = \{1,2,3,5\}$.

- Update the information of other units in the system:

  - $Descendants_{(1,1)} = \{3,4\}$

  - $Descendants_{(2,1)} = \{1,3,4,6\}$

  - $Descendants_{(5,1)} = \{1,2,3,4,6,7\}$

Phase 3. Assign all remaining arcs obtaining a graph in which each input and sorting unit is on a directed path ending at an output node.

As a final step, we iterate through the remaining connections in $\mathcal{L}$.

- Pick $(i,a)_1 = (3,1)$.

- Consider allele $c_6 = 1$.

- Consider node $i = 1 + c_6 \% (S+1) = 1 + 1 \% 4 = 2$ and try to assign it as the destination node of $(i,a)_1$. Since unit 2 is connected to output units $4,6,7$, we can finalize the assignment.

We update the information in the graph:

- Update the list of dangling arcs:

  - $\mathcal{L} = \emptyset$.

- Update the information of arc $(3,1)$:

  - $dest_{(3,1)} = 2$;

  - $Descendants_{(3,1)} = \{1,2,3,4,6,7\}$.

- Update the information of the origin unit 3:

  - $Dangling_3 = \emptyset$;

  - $Assigned_3 = \{(3,1),(3,2)\}$;

- $Ancestors_3 = \{1, 2, 3, 5\}$

- Update the information of the destination unit 2:

  - $Ancestors_2 = \{1, 2, 3, 5\}$;

- Update the information of other units in the system:

  - $Descendants_{(1,1)} = \{1, 2, 3, 4, 6, 7\}$
  - $Descendants_{(2,1)} = \{1, 2, 3, 4, 6, 7\}$
  - $Ancestors_1 = \{1, 2, 3, 5\}$
  - $Ancestors_6 = \{1, 2, 3, 5\}$
  - $Ancestors_7 = \{1, 2, 3, 5\}$.

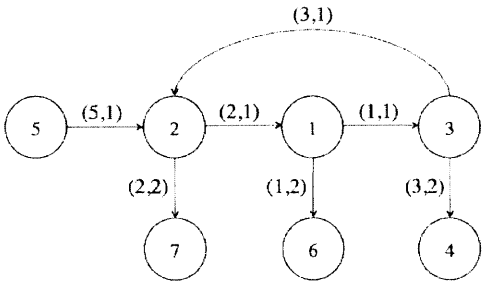

Figure 4-10: Final graph.

Figure 4-10 shows the final state of the graph.

4.3.2 Compute Material Flows

As seen in Section 3.2, to compute the material flows we need the system-level sorting matrix Q^m, for every material $m \in \mathcal{M}$, and use equation 3.26. After having determined the configuration of the MRF, the elements of matrix Q^m are given by:

$$q_{i,j}^m = \begin{cases} w_{(i,a)}^m & \text{if } dest_{(i,a)} = j \\ 0 & \text{otherwise.} \end{cases} \tag{4.8}$$

Let's continue with the example presented in Section 4.3.1, and let's assume that the weights $W_{(i,a)} = \{ w_{(i,a)}^{HDPE}, w_{(i,a)}^{Al}, w_{(i,a)}^{Other} \}$ of each arc are the ones in Table 4.2.

Arc	Weight $W_{(i,a)}$
(1,1)	{0.87, 0.1, 0.95}
(1,2)	{0.13, 0.9, 0.05}
(2,1)	{0.1, 0.15, 0.95}
(2,2)	{0.9, 0.85, 0.05}
(3,1)	{0.9, 0.85, 0.1}
(3,2)	{0.1, 0.15, 0.9}
(5,1)	{1, 1, 1}

Table 4.2: Weight vector $W_{(i,a)} = \{ w^{HDPE}_{(i,a)}, w^{Al}_{(i,a)}, w^{Other}_{(i,a)}\}$ for all arcs in the graphs.

The corresponding system-level sorting matrix for HDPE is given by:

$$Q^{HDPE} = \begin{pmatrix} 0 & 0 & 0.87 & 0 & 0 & 0.13 & 0 \\ 0.1 & 0 & 0 & 0 & 0 & 0 & 0.9 \\ 0 & 0.9 & 0 & 0.1 & 0 & 0 & 0 \\ 0 & 0 & 0 & 0 & 0 & 0 & 0 \\ 0 & 1 & 0 & 0 & 0 & 0 & 0 \\ 0 & 0 & 0 & 0 & 0 & 0 & 0 \\ 0 & 0 & 0 & 0 & 0 & 0 & 0 \end{pmatrix}.$$

Taking as input vector $\bar{\mu}^{HDPE} = \begin{pmatrix} 0 & 0 & 0 & 0 & 10 & 0 & 0 \end{pmatrix}^T$ (quantities in $\frac{Kg}{hour}$), the flow of HDPE $\bar{f}^{HDPE}$ in each unit is given by equation 3.26:

$$\bar{f}^{HDPE} = (I - (Q^{HDPE})^T)^{-1}\bar{\mu}^{HDPE}.$$

Thus:

$$\bar{f}^{HDPE} = \begin{pmatrix} 1.0850 \\ 10.8495 \\ 0.9439 \\ 0.0944 \\ 10.0000 \\ 0.1410 \\ 9.7646 \end{pmatrix}.$$

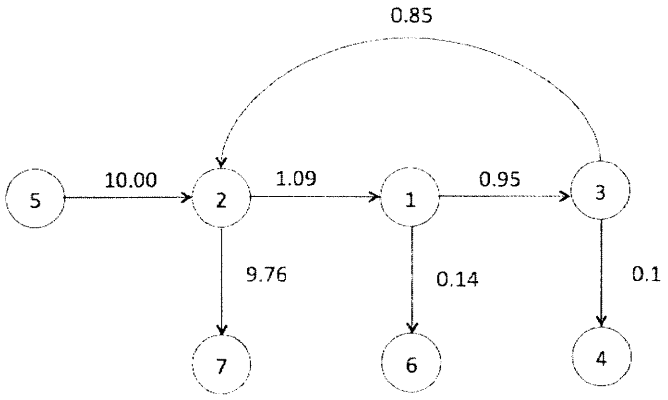

Figure 4-11: Material flow in the final configuration of the system. Quantities expressed in $\frac{Kg}{hour}$.

4.3.3 Assign Personnel

In this Section, we propose a heuristic to allocate hand-pickers in a MRF. Hand-pickers can improve the quality of the output streams and increase the revenues. Hand-pickers can either work on regular time or on overtime at an extra-cost and can be allocated to two different tasks: removal of impurities at quality control stations, or extraction of valuable materials at hand-sorting cabins. In the first task, workers remove contaminants and increase the stream purity (in the so called "negative sorting"); in the second task, workers extract desirable materials from a stream (in the so called "positive sorting"). We want to determine the workers assignment that maximizes profits.

Model of hand-sorting cabins and quality control units

Before presenting the algorithm, we clarify the effect of assigning personnel to a unit. Quality control units (QC) are located at the end of the sorting process, in correspondence to output collection units that follow mechanical sorting units. For example, a QC unit may be located on the conveyor carrying aluminum after an eddy-current unit. At QC units, material is carried on a conveyor belt and the personnel, located at the sides of the conveyor, removes contaminants from the stream. That is, if the conveyor to QC is carrying an initial quantity of non-valuable material n equal to α_n and we assign one person to perform QC, the quantity of material n after QC is reduced to $(1-r)\alpha_n$. Here, r indicates the fraction of material that the worker correctly removes from the stream. We model the effect of adding extra personnel to a unit as having a "train" of identical workers in sequence: after adding a second person, the quantity of non-valuable material n in the stream is $(1-r)^2\alpha_n$, and after adding the k^{th} worker it is reduced to $(1-r)^k\alpha_n$. Figure 4-12 shows a schematic of the quality control units.

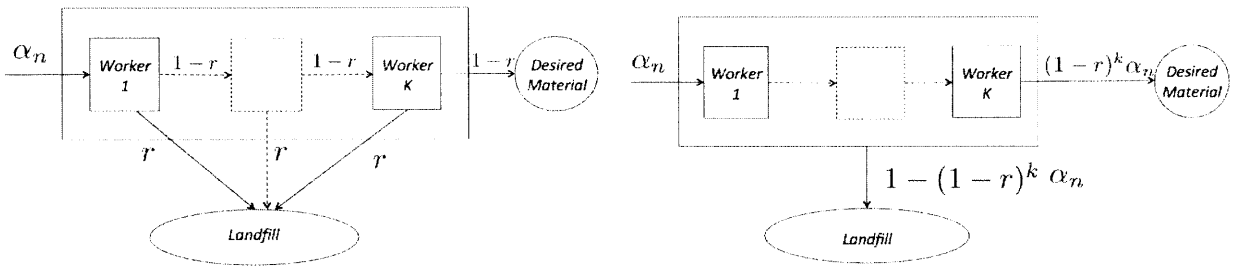

(a) Effect of each additional worker added.

(b) Aggregate unit performance.

Figure 4-12: Representation of quality control units.

Hand-sorting centers can be placed at any stage of the process and are usually located at positions in which the waste stream is composed of items that can be easily separated (e.g., streams containing packaging containers, or cardboard in a stream of large objects). In these units, sorters are located on the sides of the conveyor belt carrying the material and remove the desired items. The quantity of valuable material v that a single operator extracts from a stream containing α_v is $r\alpha_v$. The effect of adding multiple workers corresponds to having a sequence of identical steps: a second operator extracts an additional quantity of $r(1-r)\alpha_v$, and the k^{th} operator extracts an additional quantity of $(1-r)^{(k-1)}r\alpha_v$. Figure 4-13 shows a schematic for the hand-sorting cabins.

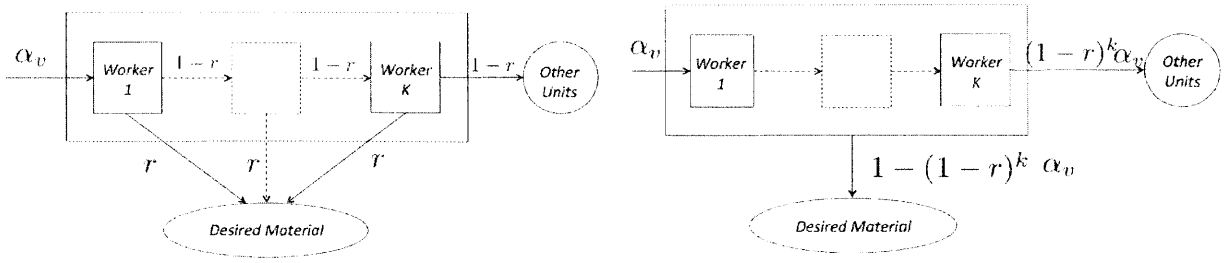

(a) Effect of each additional worker added.

(b) Aggregate unit performance.

Figure 4-13: Representation of hand-sorting cabins.

In a MRF, quality control units are located at the end of the process, corresponding output collection units, while hand-sorting cabins are located at any point in the process. For this reason, assigning personnel to a hand-sorting cabin may have a large effect on the system, changing the performance of downstream units; this can be further complicated if the system uses recirculation. In the heuristic, we consider only the local effects of the assignment and assign personnel only considering the immediate impact on the streams generated by the unit. That is, we measure the effect of assigning personnel to a hand-sorting cabin considering only the added revenues produced by removing valuable material from the stream, without considering the effect produced by the removal of the material to the downstream process.

Heuristic

At each iteration:

- For each hand-sorting cabin:
  - Compute the marginal profit from adding one person to the hand-sorting cabin;
- For each QC unit not meeting the concentration requirements:
  - Determine the number of people needed to meet the requirements.
  - If there are enough people available:
    * Determine the resulting increase in profit.
    * Divide the profit by the number of people to get the marginal profit (i.e., the average profit per person).

    Otherwise:
    * Do not consider the unit.
- Find the unit with the largest marginal profit:
  - If it is a hand-sorting cabin, then add a person to this unit as long as the profit exceeds the cost of the person.
  - If it is a QC unit, then add the number of people required as long as the total profit exceeds the cost of adding these people. If it is not economical to add these people to the unit, then move to the unit with the next highest marginal profit.
- If in either case you add people and there are more people available:
  - Continue to the next iteration.

  Otherwise:
  - Stop.

Recompute material flows and verify capacity constraints

Since hand-sorting cabins may be located at any stage in the process, assigning personnel to these units can affect the flows of material throughout the system. Therefore, after the personnel allocation is completed, we recompute the sorting parameters of hand-sorting cabin, update the system-level sorting matrices accordingly, and determine the resulting material flows.

Quality control units, instead, affect only the composition of the output collection units to which they are associated. Their effect on the output stream can be computed either:

- As hand-sorting cabins, modifying the system sorting matrix and the compute the flows.
- By considering the effect on output collection units after the flows is computed.

Once the personnel is assigned and the final material flows are computed, we verify that the flow of material through each unit is below unit capacity. If the capacity constraint is not satisfied, the solution is discarded.

4.3.4 Compute Efficiency and Profit

Once we have computed the flow of material in each unit and have assigned the personnel in overtime and in regular time, we can compute the profit and the efficiency as illustrated in Section 3.2.4.

Chapter 5

Implementation and Results

In this chapter, we apply the proposed model to a MRF operating in Spain. We describe the overall sorting process, and then we focus on a subsystem of the plant. The subsystem considered offers an interesting case study: it has all the elements of a general configuration, while being simple enough to illustrate the results. We explain how to estimate the parameters to populate the model, and we analyze the performance of the current configuration. We then apply the genetic algorithm to generate and select alternative configurations of the plant.[1]

5.1 MRF Description

In this work, we analyze the operations of a MRF with capacity to process 60 tons per hour of MSW. The plant operates five days per week: in summer, it operates on two shifts of eight hours each; in winter, it operates on two shifts of seven hours each. Maintenance occurs in a third night shift. Figure 5-1 shows the destination of input material; the plant uses a combination of manual and mechanical units to separate:

- Biological material to produce compost-like output. Compost-like-output is a product similar to compost but with restricted use due to its content of contaminant material;
- Combustibles to produce residue-derived fuel (RDF);
- Plastics (HDPE, PET, PP, PS, and EPS), tetra brik, ferrous, aluminum, plastic and industrial film, paper, cardboard, and glass to be sold to recyclers.

[1] Inconsistencies in the numbers reported in this section are due to rounding procedure.

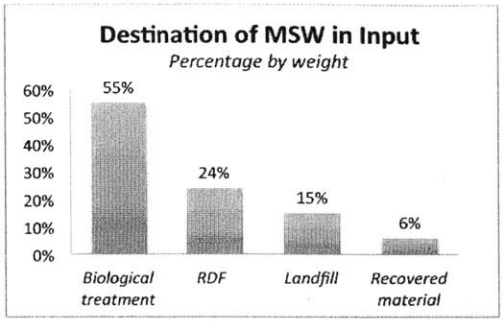

Figure 5-1: Destination of input material by weight. 2013 data.

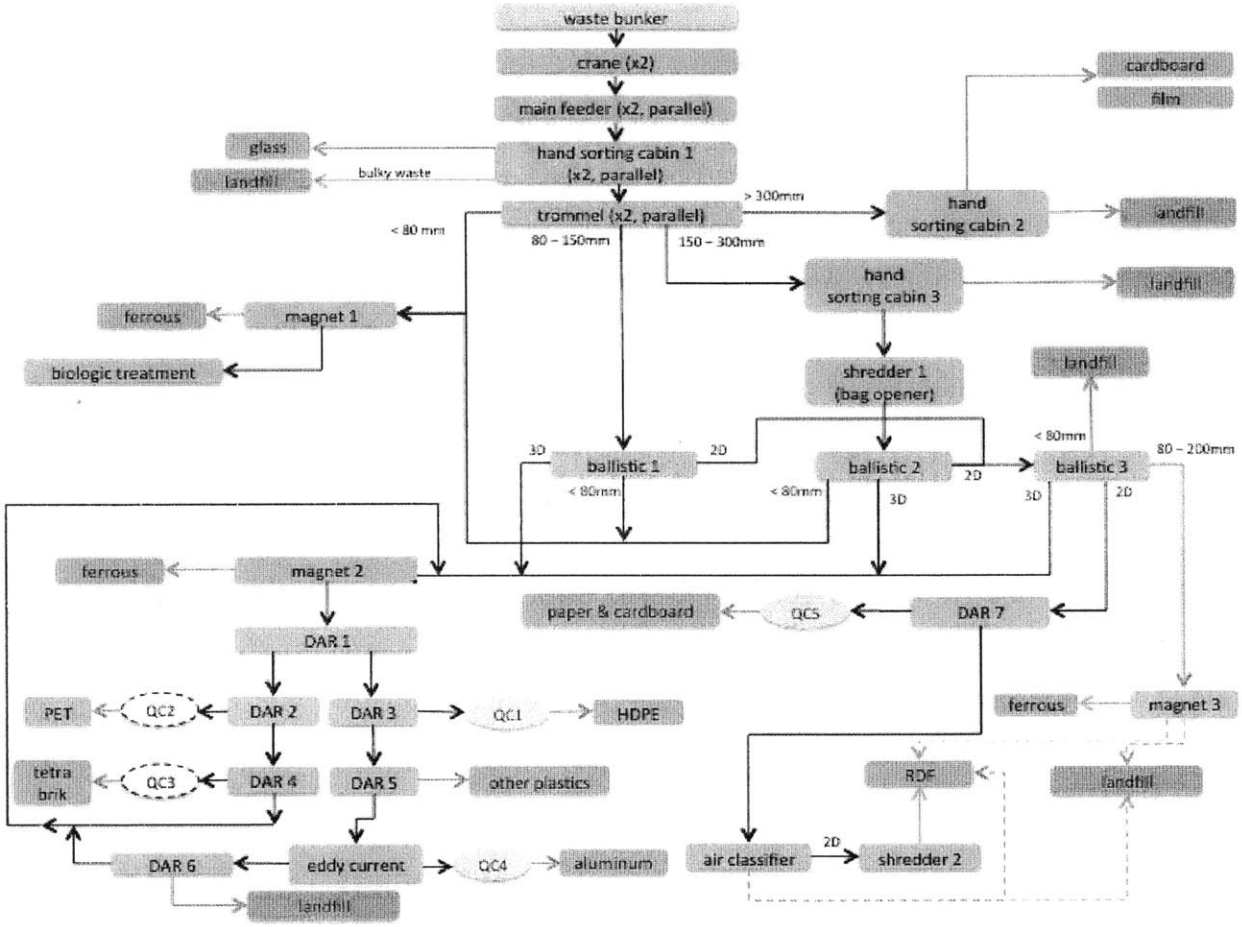

Figure 5-2: Representation of the sorting plant. Gray units represent sorting units, green units represent output collection units for valuable materials, and orange units represent output collection units for landfill. Arrows represent material flows; dashed arrows represent interchangeable material flows. For example, if we look at the output stream of *magnet* 3, the conveyor can be directed either to the RDF production or to landfill, depending on the settings. "QC" indicates quality control units: yellow and solid QCs are active, while white and dashed QCs are inactive.

Figure 5-2 shows the current configuration of the facility. The system works as follows:

1. MSW is collected daily and is stored in a reception bunker.

2. A crane controlled by an operator collects material from the bunker and places it on two conveyors. A second crane is available to guarantee regular plant operations.

3. The two conveyors are directed to a hand-sorting cabin, where two operators (one per conveyor) remove large bulky items that could damage following pieces of equipment and glass objects that could break, reducing the efficiency of following operations.

4. Two trommels in parallel divide the material by size, generating four combined output streams: one for materials below 80 mm, one for materials between 80 mm and 150 mm, one for materials between 150 mm and 300 mm, and one for larger materials.

   Trommels are primarily used to:

   - Isolate biodegradable material, which is mainly concentrated in the fraction below 80 mm. After going through a magnet that removes ferrous contaminants, the biodegradable fraction is sent to biological treatment.
   - Generate two streams of equal mass that are then processed by ballistic separators. Plastic bags contained in the $150 - 300mm$ stream are opened by a shredder. A worker in a hand-sorting cabin removes harmful materials that could damage the shredder.
   - Generate a stream of large objects that can be sorted manually. The stream of materials above $300mm$ is sent to a hand-sorting cabin, where three operators remove plastic and industrial film and large cardboard from the waste stream.

5. The two streams between $80 - 300mm$ are sent to ballistic separators, which sort:

   - Organic material below $80mm$. Material below $80mm$ is then sent to the magnet and to biological treatment.
   - Light packaging containers, called "$3D$". These materials include, for example, cans and plastic bottles, which are sent to the light packaging recovery section (LPRS) of the plant.
   - Light flat material, called "$2D$". This category includes, for example, paper and plastic film.

6. The light-packaging section of the system is constituted of a magnet, DAR units using near-infrared sensors, and an eddy-current separator. The materials collected include ferrous, PET, HDPE, tetra brik, other plastics (PP, PS, EPS), and aluminum. The output streams generated are sold to recyclers, except for the output stream collecting *other plastics* which is not currently exploited, but in the future will be possibly used to produce RDF. Two quality-control units are located in correspondence of the HDPE and the aluminum output streams. In these units, a worker (one for each cabin) removes contaminants from the aluminum and HDPE output streams. Other quality control (QC) stations are located at the PET and tetra brik output streams but are not currently used.

7. The light and flat material is sent to a DAR unit using near-infrared sensors that separates paper and cardboard from the material flow. A worker in a QC unit removes contaminants from the paper and cardboard stream. The remaining material is then sent to an air classifier that generates two output streams; one stream is sent to a shredder and used to produce RDF, and the other can either be sent to the RDF output collection stream or to landfill. This is possible because the conveyor can be programmed to be directed either to one unit or the other (in Figure 5-2 this is represented with a dotted line).

8. Ballistic separator 3 generates an output stream containing materials of $80 - 200mm$, which are sent to a magnet. The magnet generates two output streams, one collecting ferrous and one that can be directed either to the RDF output or to landfill.

5.1.1 Revenues and Costs

Local municipalities pay the MRF a fee of 29.74 € per ton of material processed. The MRF operates a landfill, and an estimate of the MRF's variable cost associated with using the landfill is 15.49 € for each ton sent to the landfill. This cost includes the depreciation of the landfill, the cost of personnel, and the cost for various operations, like waste compaction, waste transport from the MRF to the landfill, biogas and leachate treatment, and environmental analysis. The cost of each manual sorter is 36,311 € per year. We considered that each manual sorter works an average of 7.5 $hours/day$, 5 $days/week$, 48 $weeks/year$; thus we obtain an hourly cost of $20.17\frac{€}{hour}$ per person. In this work, we do not consider the cost of energy and the cost of maintenance associated with the operation of the MRF.

Ecoembes is an organization that since the introduction of the *Law 11/97 on Packaging and Packaging Waste* is responsible for overseeing the Spanish recycling industry for packaging goods, primarily made of PET, HDPE, tetra brik, paper and cardboard, ferrous, and aluminum. As a part of its activity, Ecoembes subsidizes the MRF by paying a *recovery-based price* p_m^{rec} on the top of the *market price* p_m^{mkt} per ton of material extracted. The total price is determined according to equations 2.2 and 2.3. In the case of aluminum, ferrous, HDPE, and PET, p_m^{rec} can take two values depending on the quantity of material recovered; the higher value is assigned if the ratio of the recovered material and the total material processed in one year, ρ_m, is above a threshold $\overline{\rho}_m$:

$$p_m^{rec} = \begin{cases} p_{m,1} & \text{if } \rho_m \geq \overline{\rho_m} \\ p_{m,2} & \text{Otherwise .} \end{cases} \tag{5.1}$$

For tetra brik and for paper and cardboard, instead, p_m^{rec} is independent of the quantity of material collected. Other materials, like glass, film, RDF, and compost-like output are not subsidized by Ecoembes, and the selling price is given only by p_m^{mkt}. Tables 5.1-5.3 report the selling prices for different materials as of May 2015.

	Aluminum	**Ferrous**	**HDPE**	**PET**
p_{mkt} $\frac{€}{ton}$	700	170	360	170
$\overline{\rho}$	0.06 %	1.17 %	0.27 %	0.20%
p_1^{rec} $\frac{€}{ton}$	9	6	45	118
p_2^{rec} $\frac{€}{ton}$	27	9	90	150

Table 5.1: Prices for aluminum, ferrous, HDPE and PET in $\frac{€}{ton}$. If $\rho \geq \overline{\rho}$ the *recovery based* price assigned is p_2^{rec}, p_1^{rec} otherwise. ρ is the ratio of the amount of material recovered and the total material processed in input; $\overline{\rho}$ is specified by Ecoembes. Prices as of May 2015.

	Tetra brik	**Paper & cardboard**
p_{mkt} $\frac{€}{ton}$	7	60
$\overline{\rho}$	0.00%	0.00%
p^{rec} $\frac{€}{ton}$	150	3

Table 5.2: Prices for tetra brik and paper and cardboard as of May 2015.

	Glass	Film	RDF	Compost-like output
p_{mkt} $\frac{€}{ton}$	42.00	47.25	14.00	5.00

Table 5.3: Prices for glass, film, RDF, and compost-like output as of May 2015.

Tables 5.4 - 5.7 show the composition requirements on aluminum, ferrous, tetra brik, HDPE, PET, paper and cardboard, and RDF.

Ferrous

Material	Min	Max
Ferrous	80.00%	100.00%
All other materials	0.00%	20.00%

Tetra brik

Material	Min	Max
Tetra brik	95.00%	100.00%
HDPE and PET	0.00%	3.00%
All other materials	0.00%	2.00%

Table 5.4: Concentration requirements on ferrous and tetra brik output streams as of May 2015.

HDPE

Material	Min	Max
HDPE	85.00%	100.00%
PET and other plastics	0.00%	8.00%
Ferrous and aluminum	0.00%	0.50%
All other materials	0.00%	6.50%

PET

Material	Min	Max
PET	92.00%	100.00%
PVC	0.00%	0.50%
Ferrous and aluminum	0.00%	0.50%
All other materials	0.00%	7.00%

Table 5.5: Concentration requirements on HDPE and PET output streams as of May 2015.

Paper & cardboard

Material	Min	Max
Paper & cardboard	97.00%	100.00%
All other materials	0.00%	3.00%

Table 5.6: Concentration requirements on paper and cardboard output stream as of May 2015.

Aluminum

Material	Min	Max
Aluminum	80.00%	100.00%
Paper & cardboard	0.00%	2.00%
HDPE	0.00%	2.00%
PET	0.00%	2.00%
PP	0.00%	2.00%
Tetra brik	0.00%	2.00%
Ferrous	0.00%	0.00%
HDPE, PET, PP, other plastics, plastic film, tetra brik, paper & cardboard	0.00%	4.00%
All other materials	0.00%	6.00%

RDF

Material	Min	Max
PET,HDPE, PP, other plastics	70.00%	100.00%
Paper & cardboard	0.00	18%
Organic matter	0.00%	10.00%
Other materials	0.00%	4.00%

Table 5.7: Concentration requirements on aluminum and RDF output streams as of May 2015.

5.2 Light Packaging Recovery Section

For illustrative purposes, we focus on the light packaging recovery section represented in Figure 5-3, but the approach outlined in this section can be applied to the entire facility. This subsystem processes a mixture of ferrous, HDPE, PET, tetra brik, other plastics, aluminum, and other materials, and uses a magnet, six DAR separators with near-infrared sensors, and an eddy current separator to isolate the different components. We label input units with letter "E", sorting units with letter "U", quality control units with "QC", output units collecting valuable materials with "V", and landfill unit with "L".

To apply the mathematical model and the GA, we need to know the composition of the input stream to the LPRS and the separation parameters of each unit. To estimate these parameters, we conducted three Tests (explained in detail in Appendix A):

- **Test 1:** We sampled the streams at the output collection units with recirculation active.
- **Test 2:** We sampled the streams at the output collection units with recirculation inactive.
- **Test 3:** We sampled the input stream to the LPRS.

We carried out the measurements with all quality control units deactivated, thus the data gathered does not account for the effect of personnel. Due to the costs and the time necessary to conduct waste characterizations, we could carry out Test 1 and Test 2 only once, and Test 3 twice.

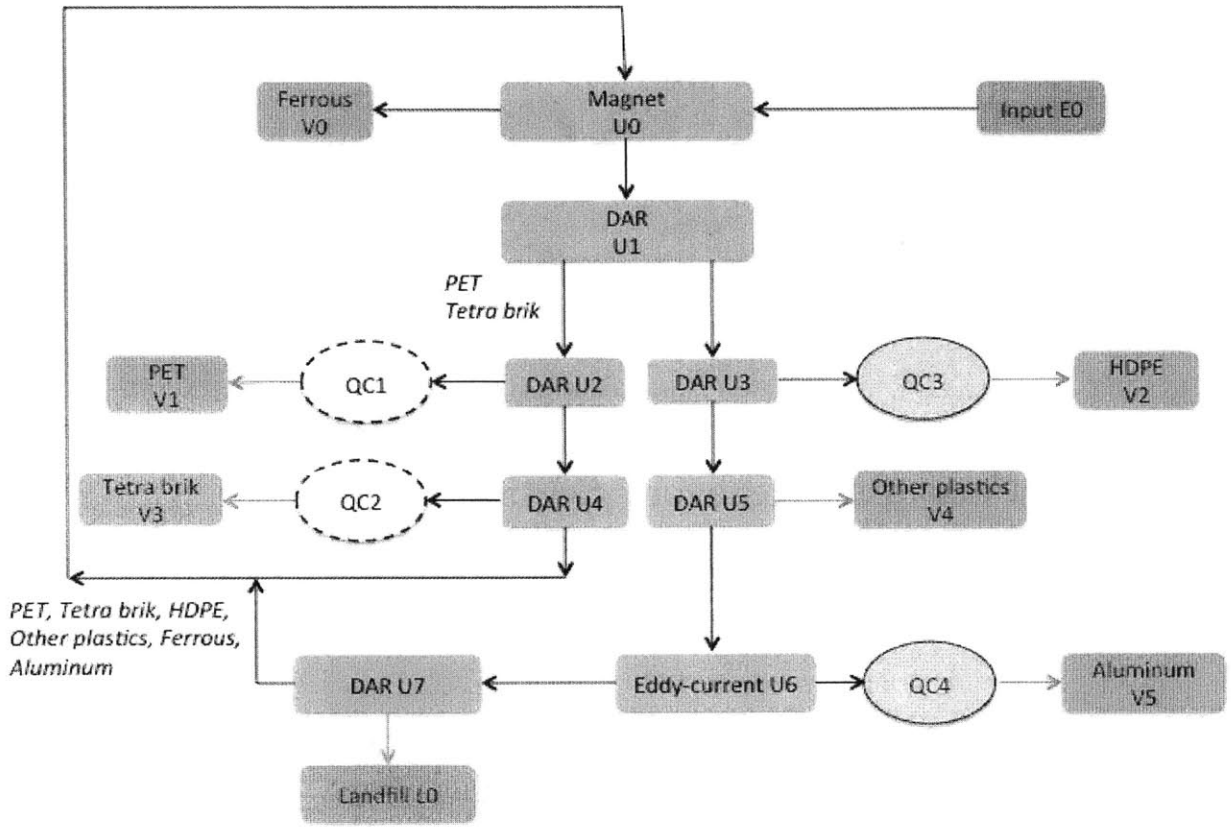

Figure 5-3: Representation of the light packaging section of the facility. The blue unit represents the input flow, gray units represent sorting units, green units represent output units collecting valuable materials, orange units represent landfill units, and round units represent quality control units. Yellow and solid QCs are active, while white and dashed QCs are inactive. Unit U1 sends tetra brik and PET to unit U2 and all other materials to unit U3; unit U7 sends all materials except for *other materials* to unit U0.

5.2.1 Output Characterization

Table 5.8 and Figure 5-4 report the composition of the output streams based on the characterizations from Test 1 and the inferred input stream, equal to the sum of the output streams. For a more detailed explanation of the characterization procedure see Appendix A.

Flow composition

Material	*E0* *Input*	*V0* *Fe*	*V1* *PET*	*V2* *HDPE*	*V3* *Tetra brik*	*V4* *Other plastics*	*V5* *Al*	*L0* *Landfill*
PET	445.7	0.8	438.6	0.3	0.2	0.5	0.1	5.2
HDPE	145.5	0.1	0.1	129.0	0.0	0.6	0.0	15.7
Aluminum	55.7	0.1	0.2	0.1	0.1	1.4	45.1	8.7
Ferrous	475.4	438.1	0.0	0.0	0.0	0.5	0.0	36.8
Tetra brik	146.1	0.3	6.3	0.1	132.4	0.1	2.4	4.5
Other plastics	135.5	0.3	1.3	0.6	0.7	126.7	0.3	5.6
Other	2683.2	17.3	13.5	23.0	9.6	110.2	6.1	2503.5
Total	4,087.1	457.0	460.0	153.1	143.0	240.0	54.0	2,580.0

Table 5.8: Mass of material in the output units. Quantities are in Kg and refer to the material collected from one half-hour of operations. The input column is inferred from the outputs, and just set equal to the sum over all of the output streams.

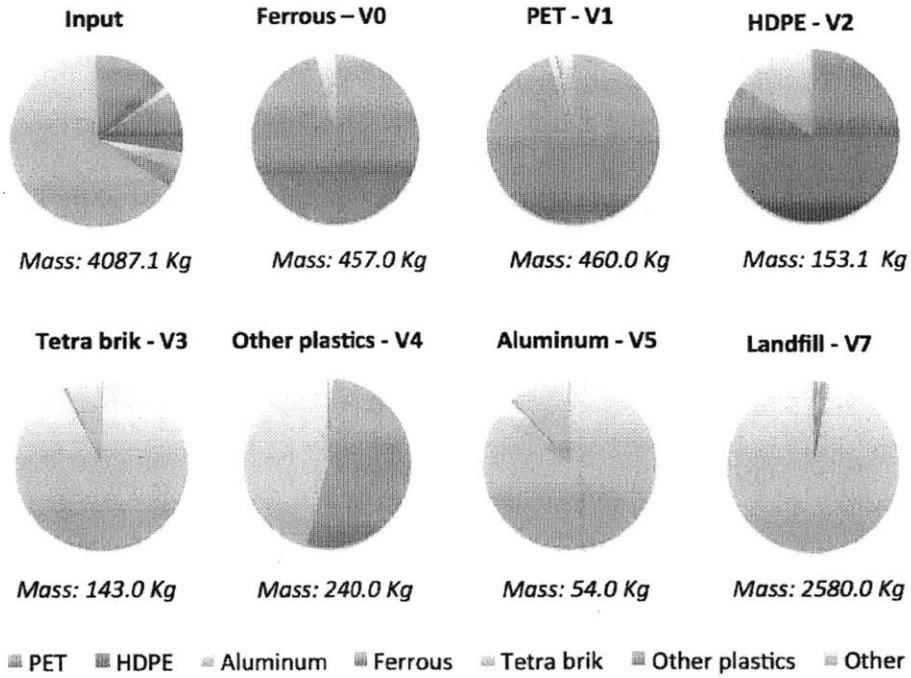

Figure 5-4: Composition of the input and output streams of the light packaging recovery section from Test 1. Quantities are in Kg processed in one half hour.

5.2.2 Input Characterization

To determine the composition of the input stream to the LPRS, we:

1. **Estimated the average input composition:** We took the average of four observations: the input composition of the two characterizations from Test 3, the inferred input compositions from Test 1, and the inferred input composition from Test 2. Input composition from Test 1 and Test 2 are given by the sum of the output streams. Table 5.9 reports the sample mean and the sample standard deviation of the input composition.

Input Composition		
Material	*Average*	*Standard Deviation*
PET	10.5%	2.0%
HDPE	3.6%	0.2%
Aluminum	1.2%	0.2%
Ferrous	11.2%	0.6%
Tetra brik	5.6%	1.4%
Other plastics	4.1%	0.8%
Other	63.8%	2.5%

Table 5.9: Sample mean and sample standard deviation of the concentration of different materials in the input stream to the LPRS, computed over 4 observations.

2. **Estimated the average size of the input stream**: From Test 1 the input stream to the LPRS is $8,174\frac{Kg}{hour}$ and from Test 2 it is $7,988\frac{Kg}{hour}$. Thus, the average input flow is $8,081\frac{Kg}{hour}$.

Combining the two results, we obtained the average input stream reported in Table 5.10.

Material	**Average input stream** $(\frac{Kg}{hour})$
PET	849.0
HDPE	292.4
Aluminum	97.4
Ferrous	902.9
Tetra brik	453.6
Other plastics	332.4
Other	5,153.2
Total	8,080.9

Table 5.10: Average input stream.

If the LPRS could perfectly sort the input stream into its components, the resulting efficiency would be 100% and the profit $787.6\frac{€}{hour}$. Table 5.11, shows revenues and costs in this case, and Figure 5-5 shows the value generated by different materials. Notice that this profit is not the

absolute highest profit that can be generated by the LPRS; in fact, the presence of a small content of impurities in the output streams can reduce the quantity of material sent to landfill and increase the revenues from sold materials.

Profit from ideal separation ($\frac{€}{hour}$)	
Revenues from processing materials	240.3
Revenues from recovered materials	706.9
Cost of landfill	79.8
Profit	**867.4**

Table 5.11: Breakdown of revenues and costs in the case of perfect separation.

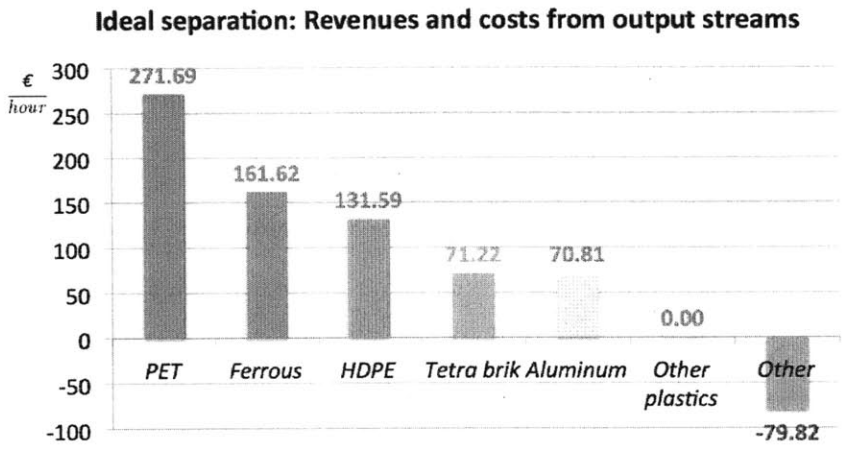

Figure 5-5: Value generated by the output streams of the LPRS in the case of perfect separation.

5.2.3 Separation Parameters of Mechanical Units

Reliably estimating the separation parameters with the little data available is a challenging task; ideally, we would use independent data sets to estimate the parameters and to validate the model, but currently this is not possible. Therefore, we used all available data to train the model, computing the separation parameters that minimize the weighted sum of the absolute errors between the output streams from Test 1 and Test 2 and the predicted output streams. We define:

- $\mathcal{M}$: Set of materials in the system.
- $\mathcal{E}_t$: Set of connections in the system in Test t, $t = 1, 2$. The system in Test 1 and in Test 2 is the same; the only difference is the presence of recirculation. That is, the stream that DAR

unit U4 directs towards magnet U0 in Test 1 is directed towards the collected recirculation stream R0 in Test 2; and the output stream that DAR unit U7 directs towards the magnet U0 in Test 1 is directed towards the collected recirculation stream R1 in Test 2 (see Figures A-1 and A-1 in Appendix A reporting the sampling locations).

- $\mathcal{S}$: Set of sorting units in the system.

- $\mathcal{Z}_t$: Set of output streams sampled in Test t, $t = 1, 2$.

- $\bar{f}^m_{z,t}$: Measured quantity of material m in output unit z, for all $z \in \mathcal{Z}_t$, for all materials $m \in \mathcal{M}$, and for all tests $t = 1, 2$.

- $\mu^m_{i,t}$: Quantity of external input of material m entering into unit i at Test t, for all $m \in \mathcal{M}$ and $t = 1, 2$. In the LPRS, the only unit receiving external input is the magnet. $\mu^m_{i,t}$ is given by the sum of the output streams in Test t. That is:

$$\mu^m_{i,t} = \sum_{z \in Z_t} \bar{f}^m_{z,t}, \qquad \forall m \in \mathcal{M}. \tag{5.2}$$

- $f^m_{i,t}$: Decision variable for the flow of material m in unit i in Test t, for all $m \in \mathcal{M}$,$i \in \mathcal{Z}_t \cup \mathcal{S}$, and $t = 1, 2$.

- $q^m_{i,j,t} \in [0, 1]$: Decision variable for the quantity of material m that unit i sends to unit j in Test t, with $\sum_{j|(i,j)\in\mathcal{E}_t} q^m_{i,j,t} = 1$. Under the assumption that the input flow does not affect the separation parameters, the separation parameters of each unit are the same in all tests. Thus, $q^m_{i,j,1} = q^m_{i,j,2}$, $\forall m \in \mathcal{M}$, $\forall (i, j) \in \mathcal{E}_1 \cap \mathcal{E}_2$. For the tests considered, we have that $q^m_{U4,U0,1} = q^m_{U4,R0,2}$ and $q^m_{U7,U0,1} = q^m_{U7,R1,2}$, $\forall m \in \mathcal{M}$.

- $\beta^m_{z,t} \in [0, 1]$: Weight of the error term $|\bar{f}^m_{z,t} - f^m_{z,t}|$, $\forall m \in \mathcal{M}$, $z \in \mathcal{Z}_t$, and $t = 1, 2$.

The optimization problem is then given by:

$$
\begin{aligned}
\min_{q,f} \quad & \sum_{t=1,2} \sum_{m \in \mathcal{M}} \sum_{z \in \mathcal{Z}_t} \beta_{z,t}^m |\bar{f}_{z,t}^m - f_{z,t}^m| \\
\text{s.t.} \quad & f_{j,t}^m = \sum_{(i,j) \in \mathcal{E}_t} f_{i,t}^m q_{i,j,t}^m + \mu_{j,t}^m && \forall m \in \mathcal{M},\ \forall j \in \mathcal{Z}_t, t = 1,2 \\
& \sum_{j|(i,j) \in \mathcal{E}_t} q_{i,j,t}^m = 1 && \forall m \in \mathcal{M},\ \forall i \in \mathcal{S},\ t = 1,2 \\
& q_{i,j,1}^m = q_{i,j,2}^m && \forall m \in \mathcal{M},\ \forall (i,j) \in \mathcal{E}_1 \cap \mathcal{E}_2 \\
& q_{U4,U0,1}^m = q_{U4,R0,2}^m && \forall m \in \mathcal{M} \\
& q_{U7,U0,1}^m = q_{U7,R1,2}^m && \forall m \in \mathcal{M} \\
& q_{i,j,t}^m \in [0,1] && \forall m \in \mathcal{M},\ \forall (i,j) \in \mathcal{E}_t, t = 1,2.
\end{aligned}
\tag{5.3}
$$

We introduce the auxiliary variables $g_{z,t}^m$ to obtain an optimization problem with linear objective and quadratic constraints, given by:

$$
\begin{aligned}
\min_{q,f} \quad & \sum_{t=1,2} \sum_{m \in \mathcal{M}} \sum_{z \in \mathcal{Z}_t} \beta_{z,t}^m g_{i,t}^m \\
\text{s.t.} \quad & f_{j,t}^m = \sum_{(i,j) \in \mathcal{E}_t} f_{i,t}^m q_{i,j,t}^m + \mu_{j,t}^m && \forall m \in \mathcal{M},\ \forall j \in \mathcal{Z}_t,\ t = 1,2 \\
& g_{z,t}^m \geq \bar{f}_{z,t}^m - f_{z,t}^m && \forall m \in \mathcal{M},\ \forall z \in \mathcal{Z}_t, t = 1,2 \\
& g_{z,t}^m \geq f_{z,t}^m - \bar{f}_{z,t}^m && \forall m \in \mathcal{M},\ \forall z \in \mathcal{Z}_t, t = 1,2 \\
& \sum_{j|(i,j) \in \mathcal{E}_t} q_{i,j,t}^m = 1 && \forall m \in \mathcal{M},\ \forall i \mathcal{S}, t = 1,2 \\
& q_{i,j,1}^m = q_{i,j,2}^m && \forall m \in \mathcal{M},\ \forall (i,j) \in \mathcal{E}_1 \cap \mathcal{E}_2 \\
& q_{U4,U0,1}^m = q_{U4,R0,2}^m && \forall m \in \mathcal{M} \\
& q_{U7,U0,1}^m = q_{U7,R1,2}^m && \forall m \in \mathcal{M} \\
& q_{i,j,t}^m \in [0,1] && \forall m \in \mathcal{M},\ \forall (i,j) \in \mathcal{E}_t,\ t = 1,2.
\end{aligned}
\tag{5.4}
$$

Since the LPRS has only binary units, we have one separation parameter for each material in each unit (i.e., if a separation parameter is $q_{i,j}^m \in [0,1]$, the other is $1 - q_{i,j}^m$). Thus, we have to estimate seven independent separation parameters for each material. Under the assumption that the separation parameters are independent from the input composition, the problem can be decoupled and solved independently for each material.

The quantity of material m in different streams varies greatly. For example, in Test 1, there are $438.6Kg$ of PET in the desired output stream V1, but only $0.1\frac{Kg}{hour}$ in the output stream collecting *other plastics* V5. Looking at other output streams, the average PET flow in V0,V2,V3,V4,V5 is $0.4Kg$ and $5.2Kg$ in L0. Thus, if we don't assign proper weights to the objective function, the optimization considers only the observations from the streams where there is a higher quantity of a given material and disregards the others. One possible approach to solve this problem would be that of considering the absolute percentage error; but this is not a viable option because most of the observations are either close to zero or zero. Thus, we added the weight terms $\beta^m_{z,t}$ to reduce the relative weight of the streams with higher material (i.e., the higher the quantity of a material in a stream, the lower its weight). Defining $\alpha^m_{z,t}$ to be the quantity of material m in stream z at Test t:

$$\tilde{\beta}^m_{z,t} = 1 - \frac{\alpha^m_{z,t}}{\sum_{z \in \mathcal{Z}_t} \alpha^m_{z,t}}, \qquad m \in \mathcal{M},\ t = 1, 2. \tag{5.5}$$

We then normalized the weights as follows:

$$\beta^m_{z,t} = \frac{\tilde{\beta}^m_{z,t}}{\sum_{z \in \mathcal{Z}_t} \tilde{\beta}^m_{z,t}}, \qquad m \in \mathcal{M},\ t = 1, 2. \tag{5.6}$$

The resulting problem has 392 decision variables and 504 constraints; we formulated it in Julia and solved it on a personal computer using the JuMP package with Gurobi Solver. The minimum weighted absolute deviation found was $11.2\frac{Kg}{hour}$; the results are reported in Appendix A; we see that most of the units sort materials with more than 90% accuracy. The only notable exception is DAR U7 (see Table 5.12), which has an accuracy of less than 25% for aluminum and less than 2% for ferrous. This is consistent with the high quantity of ferrous and aluminum in landfill in Test 1. In theory, all accuracies should be greater than or equal to 50%; thus, this result is either due to errors in the sampling procedure or to a misclassification error in DAR U7. This result is inconsistent with the results obtained for other DAR units, which all sort aluminum with more than 95% accuracy and ferrous with more than 98% accuracy. For this reason, we corrected the separation parameters for aluminum and ferrous by computing the average of the sorting parameters of all DAR units in the system for the corresponding material. Tables 5.13 reports the results.

DAR - U7

Material	End node	
	U0	*L0*
PET	7.187%	92.813%
HDPE	29.873%	70.127%
Aluminum	75.120%	24.880%
Ferrous	98.875%	1.125%
Tetra brik	2.356%	97.644%
Other plastics	12.191%	87.809%
Other	97.164%	2.836%

Table 5.12: Estimated separation parameters for unit U7.

DAR U7: Parameters Correction

Material	DAR U1	DAR U2	DAR U3	DAR U4	DAR U5	DAR U7	Average
Aluminum	95.407%	94.110%	99.912%	96.548%	97.595%	24.880%	84.742%
Ferrous	99.898%	100.000%	100.000%	100.000%	98.708%	1.125%	83.289%

Table 5.13: Estimation of the separation parameter for ferrous in DAR U7 as the average of the separation parameters of all DAR units in the system.

Comparison between the predicted output composition and that from the tests

We compared the output composition predicted by the model and that resulting from the tests. Detailed results are reported in Appendix A.4.1. Figure 5-6 shows the average absolute deviation in each output stream, and the average absolute deviations divided by the mass of the output stream. We can see that the ferrous, landfill, recirculation R1, and aluminum output streams have the highest absolute deviation; for landfill and for R1, this is primarily due to the large quantity of material in the streams. If we look more in detail at the results, we see that in the landfill output stream, the deviation is due to discrepancies in the quantity of HDPE and *other materials*; in the R1 output stream, the deviation is due to discrepancies in the quantity of ferrous; in the ferrous output stream, the deviation is due to discrepancies in the content of ferrous; and in the aluminum output stream the deviation is due to discrepancies in the content of aluminum.

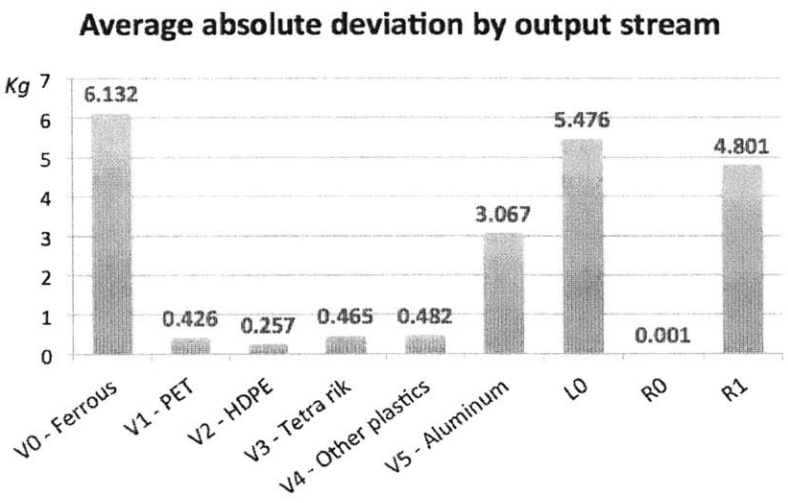

(a)

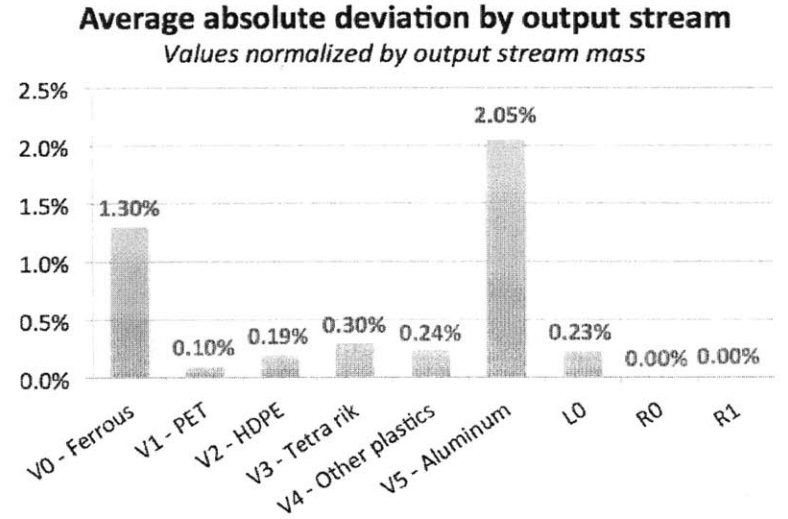

(b)

Figure 5-6: Average absolute error between the output composition from Test 1 and Test 2 and that predicted from the mathematical model. a) Average error per output stream. b) Errors were divided by the mass of material in each output stream.

We repeated the deviation analysis considering the absolute average and deviation per material type and the same metric divided by the corresponding mass of material in input. Figure 5-7 reports the results. The high deviation for ferrous and aluminum is consistent with the fact that the separation parameters for these two materials in DAR U7 are given by the average of the separation parameters of all DAR units.

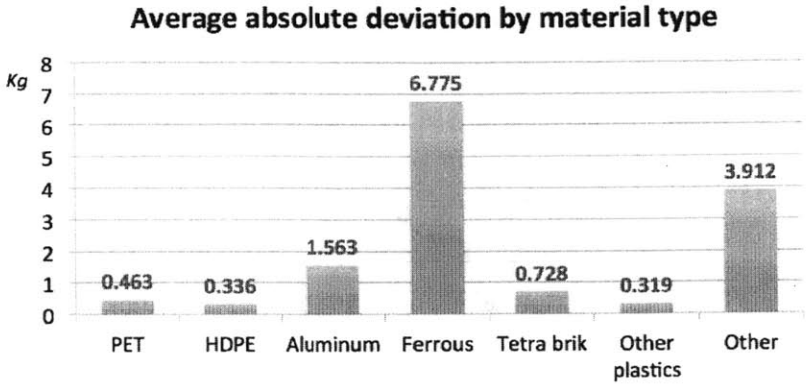

(a)

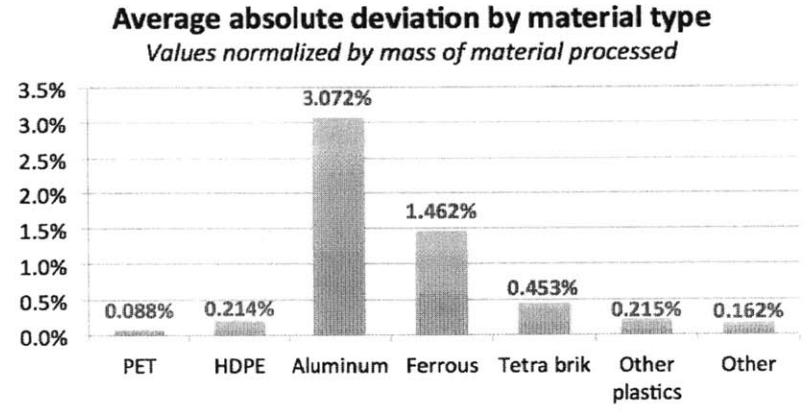

(b)

Figure 5-7: Average absolute error by material type between the output composition from Test 1 and Test 2 and that predicted from the mathematical model. a) Average absolute deviation by material type. b) Deviations are divided by the mass of a material in the system.

5.2.4 Performance of the current configuration without QC

We evaluate the performance of the current configuration as predicted by the mathematical model with estimated separation parameters. The input stream is given by the estimate in Table 5.10. Table 5.14 reports the economic and material performance of the system, and Appendix A.5 reports the composition of the output streams.

Looking at the data in Appendix A.5 we can see that:

- The configuration has a profit that is 30.9% lower than the profit from perfect separation.
- The output streams collecting HDPE, tetra brik, and aluminum don't meet the requirements but are very close to meeting them.

Performance of the current configuration	
Revenues from processing material ($\frac{€}{hour}$)	240.3
Revenues from recovered material ($\frac{€}{hour}$)	448.2
Costs of landfill ($\frac{€}{hour}$)	89.0
Profit ($\frac{€}{hour}$)	***599.5***
Efficiency (%)	***90.42***

Table 5.14: Economic performance and efficiency for the current configuration without QC.

- **HDPE:** The predicted concentration of HDPE in the corresponding output stream is 84.8%, which is slightly below the minimum concentration required of 85%.
- **Tetra brik:** The predicted concentration of tetra brik in the corresponding output stream is 95.337%, which is above the required minimum concentration of 95%; but the concentration of *other materials* is 4.2%, which is above the maximum allowed concentration of 2%.
- **Aluminum:** The predicted concentration of aluminum in the corresponding output stream is 81.9%. This value is above the 80% required, but the concentration of other impurities in the stream is too high. For example, the concentration of tetra brik is 6.7%, when the maximum concentration allowed is 2%.

5.2.5 Separation Efficiency of Manual Operations at QC Stations

In the light packaging recovery section there are four QC stations, two of which are currently used with one worker separating waste, while the others are inactive. We do not have any experimental data about the efficiency of workers in QC units, and thus we rely on the data obtained from literature and reported in Section 2.2, in Table 2.6. Table 2.6 reports a range of separation efficiencies per person per stream type (i.e., $[r_i^{min}, r_i^{max}]$) and a range of material flows (i.e., $[f_i^{min}, f_i^{max}]$) for which the efficiencies are valid. We assume a linear relationship between separation efficiency and material flow; the separation efficiency r_i of a worker at unit i is given by:

$$r_i = \begin{cases} r_i^{max} & \text{if } f_i \leq f_i^{min} \\ \frac{r_i^{max} - r_i^{min}}{f_i^{min} - f_i^{max}}(f_i - f_i^{min}) + r_i^{max} & \text{if } f_i \in (f_i^{min}, f_i^{max}) \\ r_i^{min} & \text{if } f_i \geq f_i^{max} \ . \end{cases} \tag{5.7}$$

Here, f_i is the flow of material entering QC i. We assume that multiple workers assigned to a station have the same sorting efficiency r_i. Figure 5-8 shows the efficiency of QC personnel for aluminum and plastic containers.

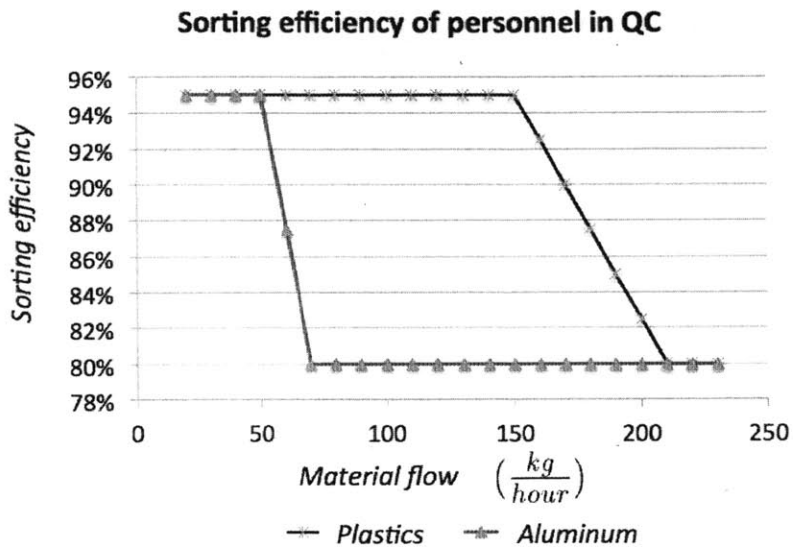

Figure 5-8: Linear approximation of personnel sorting efficiencies on the basis of Table 2.6.

For example:

- If QC3 receives $300\frac{kg}{hour}$ of material, the sorting efficiency of every worker is 80.0%.
- If QC3 receives $170\frac{kg}{hour}$ of material, the sorting efficiency of every worker is 87.5%.
- If QC3 receives $100\frac{kg}{hour}$ of material, the sorting efficiency of every worker is 95.0%.

This is a very simple model, which we used since no better data was available; additional analysis should be conducted to obtain better estimates of personnel sorting efficiencies.

5.2.6 Effect of QC on the current configuration

In Section 5.2.3 we evaluated the performance of the current configuration considering only mechanical units; in this section, we account for the effect of QC. We applied the model to the LPRS with HDPE and aluminum QC active, using the estimated parameters and the input stream from Table 5.10: the predicted profit is $754.2\frac{€}{hour}$ and the efficiency 90.97%. This corresponds to an

increase in profit of 25.8% and an increase in the efficiency of 0.6% with respect to the case without QC. The high impact that QC has on profit is due to the fact that QC makes the HDPE and aluminum output streams profitable; while the little improvement on efficiency derives only from the additional *Other material* sent to landfill. Figure 5-9 shows the economic performance of the LPRS with QC, and Tables A.21 and A.22 in Appendix A.6 show the variation in the composition of the output streams of HDPE and aluminum. The profit obtained is 13.1% lower than that of the ideal separation.

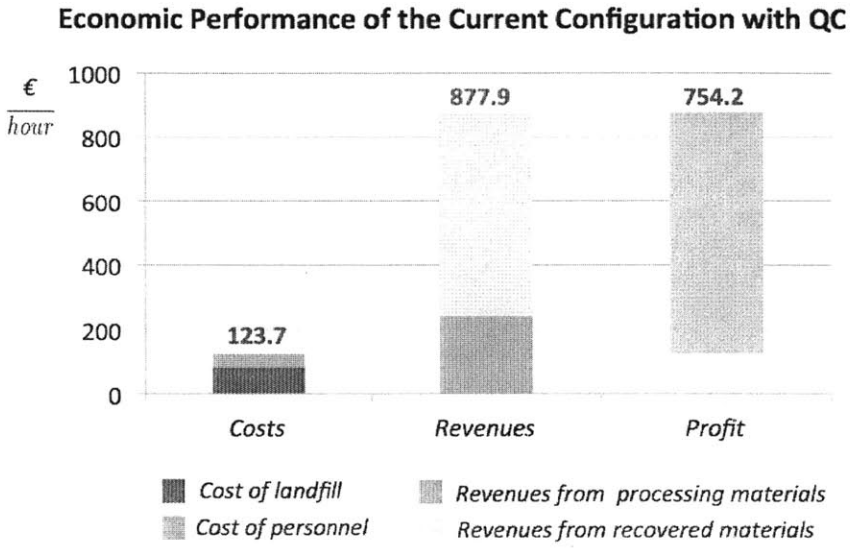

Figure 5-9: Revenues, costs, and profits for the current configuration with QC.

5.3 Software

We developed a software program in Java to:

- Compute material flows and evaluate the performance of a given configuration;
- Identify alternative configurations of a facility using the GA with personnel allocation.

We developed the code internally and used the external library Apache Commons Math (available at http://commons.apache.org/) to solve the system of linear equations. The code is flexible, and allows the user to specify:

- The materials processed.

- The requirements on the collected materials and the selling price (i.e., the market-based and the recovery-based components and the threshold on the recovery).
- The list of sorting units in the system. For each unit the user can specify the destination unit of the output streams if known. If the user wants to find alternative configurations, a solution is guaranteed to be found only if all sorting units have at least one unassigned output stream. Moreover, for each unit the user specifies the sorting parameters associated to a specific output stream. In the case of DAR units without the primary output stream assigned, the user has to specify the set of targetable materials (see Section 5.4.1).
- The list of output units in the system and the materials collected at each unit.
- The list of input units and the corresponding material flows.
- The list of QC and hand-sorting units. The user specifies the minimum and maximum number of workers to be assigned to each manual unit, the minimum and maximum sorting efficiency per person, and the material flows for which the recovery range is valid. The user also specifies the total number of people available in regular time and in overtime, and the respective cost.
- Cost of landfill.
- The user can also specify constraints on the system, such as capacity constraints and precedence constraints between units.

When the model is used to identify different configurations, the software outputs the list of the N configurations with the highest fit, where N is defined by the user. For each configuration, the software reports detailed information regarding:

- The efficiency;
- The economic performance: Revenues from processing and recovering materials, costs of personnel and of landfill, and profit;
- For each mechanical unit and hand-sorting cabin in the system: Material flows and concentrations, and destination node of the output streams.
- For each QC and hand-sorting cabin: Personnel assigned.

- For each output collection unit: Material flows and concentrations, selling price, and whether it meets the requirements or not.

- For DAR units: Set of target materials.

This information is provided also for an predefined configuration for which the user wants to estimate the performance. The results described in the following sections have been obtained running this software on a personal computer.

5.4 Tuning and Evaluation of the Genetic Algorithm

We apply the genetic algorithm presented in Section 4.3 to the LPRS of the facility. As explained in Section 5.2.3, we use separation parameters from error minimization and input from Table 5.10. In this section, we first make a clarification on the way in which DAR units are treated in the algorithm. We then discuss the general characteristics of the algorithm: the sensitivity to the initial population generated, the effect of the parameters selected, and the typical run-times; finally, we compare the algorithm to random generation of configurations. In the next section, we apply the model to the design of the LPRS.

5.4.1 LPRS Configuration: Detect and Route Units

The light packaging recovery section uses six DAR units; two of them, DAR U1 and DAR U7, generate two output streams that are directed to other sorting units. Depending on the characteristics of the configuration and on the specifications of the decision maker, each DAR unit will send materials to one stream or the other. This choice affects the sorting performance of the system and has to be incorporated in the GA. That is, for a given configuration the GA needs to determine which materials are sent to which output stream. Before explaining how the assignment takes place, we further specify the characteristics of DAR units.

Each DAR unit has two output streams, a *primary* and a *secondary* output stream, and can potentially target a set of materials (*targetable materials*): a subset of these materials (*target materials*) is detected, removed from the stream, and sent to the primary output stream, while the remaining materials are sent to the secondary output stream. In the system considered, the

targetable materials of DAR units are PET, HDPE, tetra brik, other plastics, aluminum, and ferrous. The GA needs to determine which of the output streams is the primary output stream and what subset of the targetable materials is the set of target materials. In our algorithm, we first assign each targetable material to the stream that maximizes the value of material collected. After assigning each targetable material to an output stream for each of the sorting units, we then designate the primary stream to be the stream that recovers a higher value of material. Finally, for each sorting unit, we designate the target materials to be the materials sent to the primary output stream.

We determine the primary output stream and the set of target materials of DAR units after *Phase* 3 of the algorithm, when the configuration of the MRF is defined. Let $\mathcal{U}$ be the set of DAR units for which we have to make the assignment. We can treat each material m independently. For each material m, we need to assign its output stream for each unit u, element of $\mathcal{U}$. We make this assignment one unit at a time. For each unit $u \in \mathcal{U}$, we assign material m to the output stream that maximizes the value of material m collected. To compute the value of material m collected, we need to determine the flow of material m in the output streams by solving the system of linear equations 3.24 for the entire configuration. We know how all units $i \notin \mathcal{U}$ sort materials; for the unit u that we are considering we evaluate both cases in which m is sent to one stream or the other; and for other units in $\mathcal{U}$ for which we haven't made the assignment yet, we assume that material m is sent equally to the output streams, i.e., exactly 50% of the input flow goes to each output stream.

Once we have assigned all potentially targetable materials of all units in $\mathcal{U}$, we designate the primary output stream to be the stream that collects a higher value of material and the target materials to be the targetable materials sent to that stream. Determining the primary output stream is important because all unassigned materials are sent to the secondary output stream.

In this application, we can easily enumerate all possible assignments because there are only two units in $\mathcal{U}$. For larger instances where each material is collected at only one output node, one could formulate a dynamic program where node i with outgoing arcs (i, i_1) and (i, i_2) sends

material m as to maximize the value collected:

$$V(i) = \max\{\bar{q}_i^m V(i_1), \bar{q}_i^m V(i_2)\}. \tag{5.8}$$

Here, $V(i)$ is the value collected at unit i and $\bar{q}_i^m \in [0.5, 1]$ is the separation parameter corresponding to the quantity of material m that unit i sends to the desired output stream. This assumes that we can evaluate $V(i_1)$ and $V(i_2)$ before $V(i)$, where $V(i_1)$ and $V(i_2)$ are closer to the output node collecting m. If there is no connection between node i and the output node, then $V(i) = 0$. This is just the outline of the algorithm and further refining is left to future research.

5.4.2 GA: Effect of Initial Population

In this section, we evaluate the sensitivity of the algorithm to the initial population. To do so, we apply the genetic algorithm using the same set of parameters 50 different times; each time we generate the initial population at random. We applied the GA setting a population size of 50, a number of iterations of 50, a swap-mutation rate of 0.7, a one-point and a two-point crossover rate of 0.3, and a weight of profit of 0.9. Figure 5-10 shows the results for each of the 50 iterations; the profit and the efficiency have been divided by the respective mean value (the average profit is $808.8\frac{€}{hour}$ and the average efficiency is 90.84%). Table 5.15 reports the sample mean, the sample standard deviation, and the coefficient of determination of the results. We see that the algorithm is sensitive to the initial population, but the fluctuations are not too consistent. This effect can be reduced by trying different initial populations at random, or by including specific configurations in the initial population. In the next section, we evaluate the GA starting with an initial random population that is kept constant by setting a random seed.

Metric	**Mean** μ	**Stdev** σ	**Coefficient of Determination** $\frac{\sigma}{\mu}$
Profit ($\frac{€}{hour}$)	808.8	18.2	0.0
Efficiency (%)	90.84	5.87	0.07

Table 5.15: Sample mean, sample standard deviation, and coefficient of determination of profit and efficiency of the configuration with the highest fit found by the GA applied to different initial populations.

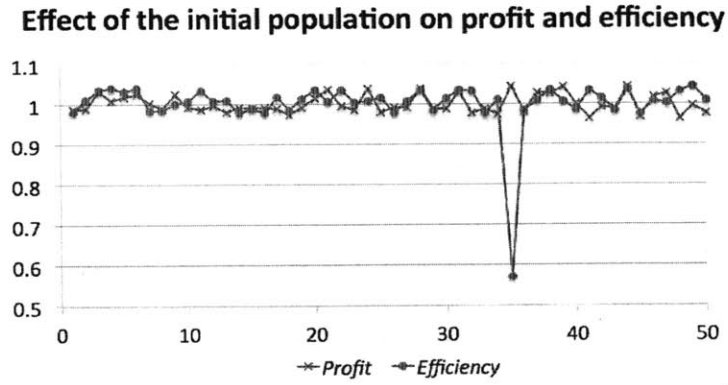

Figure 5-10: Profit and efficiency obtained running the GA on 50 different initial populations randomly generated. Quantities have been divided by the mean. Configuration 35 has a particularly low efficiency; but this seems and outlier.

5.4.3 GA: Parameters Selection

Before applying the GA to the LPRS, we want to see how the parameters of the algorithm affect efficiency and profit of the configuration with the highest fit. We consider the case in which there are three people that can be assigned to QC units. The parameters evaluated are:

- Probability (or rate) of single-allele mutation and of swap mutation.
- Probability (or rate) of one-point, two-point, and mask crossover.
- Population size and number of iterations.
- Weight of profit and of efficiency.

Table 5.16 reports the initial value of each parameter, chosen after experimenting with the algorithm. To further refine the selection, we will be varying one parameter at a time keeping the others constant to these initial values.

Mutation rate		**Crossover rate**			**Population size**	**Iterations**	**Objectives**	
single-allele	*swap*	*one-point*	*two-point*	*mask*			*profit*	*eff.*
0.3	0.7	0.3	0.3	0.4	100	100	0.9	0.1

Table 5.16: Initial parameters value.

Mutation Rate

The results show that the genetic algorithm has a small sensitivity to mutation rate. We take as base values the profit and the efficiency of the configuration with the highest fit for a swap-mutation rate of 0. Figure 5-11 shows that when swap-mutation rate ranges in [0.2, 0.8], the configuration with the highest measure of fit has a profit that is 1.02 times higher than the base profit and an efficiency that is 0.97 times lower than the base efficiency; when swap-mutation rate is above 0.8, both metrics increase (the profit increases by a factor of 1.04 and the efficiency by a factor of 1.02 with respect to their base performance). The fact that an increase in the swap-mutation rate generates configurations with higher profit and efficiency could be associated to the fact that, all other parameters being equal, swap-mutation changes more alleles than single-allele mutation (we say that swap-mutation is more *disruptive* than single-allele mutation). For this reason, swap-mutation rate is more likely to generate solutions that encode different configurations.

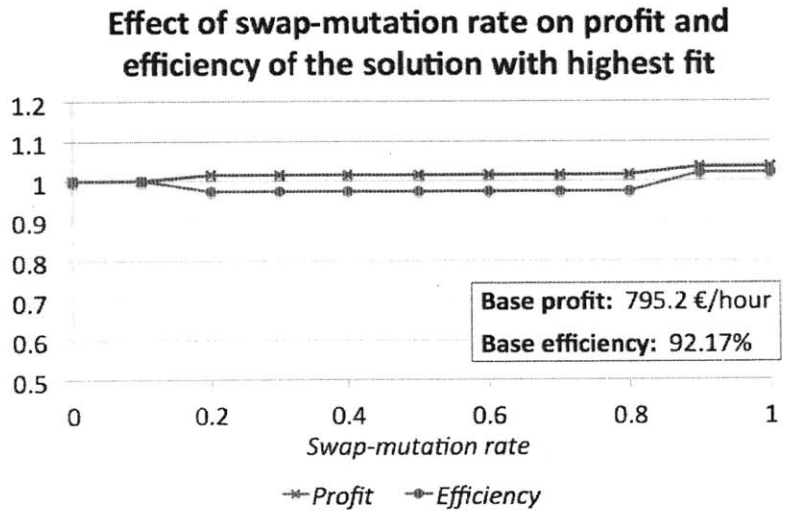

Figure 5-11: Variation in profit and efficiency due to variations in the swap mutation rate p_{swap}. Values reported to a base of $p_{swap} = 0$, with a profit of $795.2\frac{€}{hour}$ and an efficiency of 92.17 %. At $p_{swap} = 1$ the profit is $823.2\frac{€}{hour}$ and the efficiency 94.09%.

Crossover Rate

We varied probabilities of one-point, two-point, and swap crossover one at a time; when we varied one probability we considered the other two to be equal. The objectives are not affected by these variations, with a constant profit of $832.9\frac{€}{hour}$ and a constant efficiency of 91.15%.

Population Size and Number of Iterations

The population size and the number of iterations of a genetic algorithm are related, and both impact on the number of different configurations generated: if we apply the GA with a population size of P and N iterations, we generate at most $P(3N + 1)$ different individuals. At every iteration, crossover generates P additional individuals and mutation generates $2P$ additional individuals; since every time we accept only individuals with new chromosomes, the number of distinct individuals is in the range $[P, P(3N + 1)]$. For example, with a population of 100 individuals and 250 iterations, we generate at most 75,100 different individuals. Since the number of configurations generated grows with NP, we expect the algorithm to behave similarly with respect to these two parameters; but since the algorithm is sensitive to the composition of the initial population, this is difficult to verify. Figures 5-12 and 5-13 show how the objectives of the configuration with the highest fit vary for different population sizes and number of iterations. As expected, the effect of population size on the results is difficult to evaluate. The highest profit of $841.4\frac{€}{hour}$ is obtained for a population of 50 individuals; the highest efficiency of 94.07% is obtained for a population of 40 individuals.

Looking at Figure 5-13, we see that when we increase the number of iterations from 1 to 50, the profit increases by a factor of 1.15 and the efficiency reduces by a factor of 0.99. The fact that the profit increases while the efficiency decreases is consistent with the fact that the profit has a higher weight in the measure of fit used by the GA. The objectives do not change when we increase the number of iterations from 50 to 1,000.

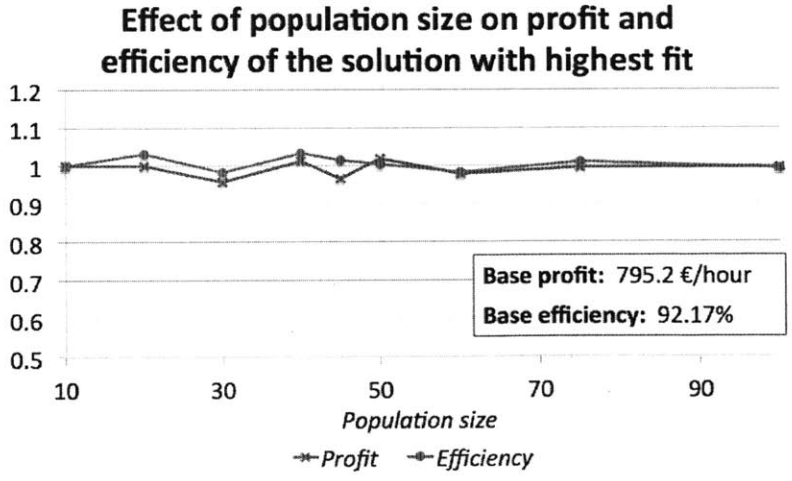

Figure 5-12: Variation in profit and efficiency due to variations in population size.

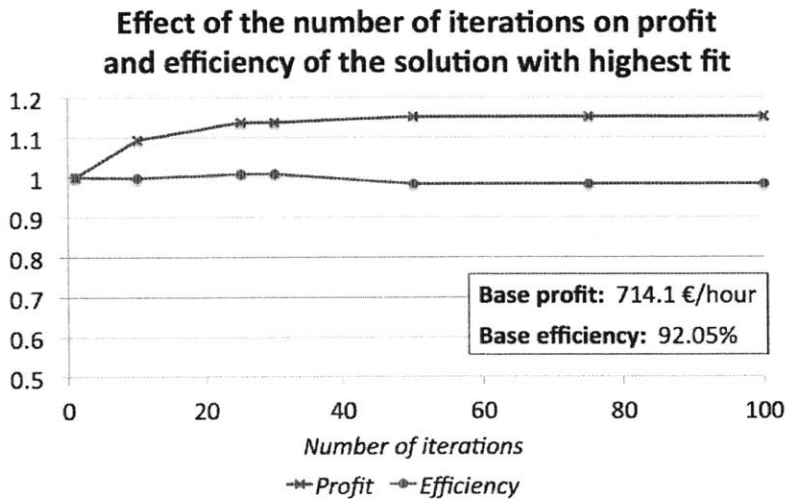

Figure 5-13: Variation in profit and efficiency of the configuration with the highest measure of fit due to variations in the number of iterations N. For$N = 1$ the profit is $714.1\frac{€}{hour}$ and the efficiency is 92.05%; from $N = 50$ to $N = 1,000$ (not reported), the profit is $822.3\frac{€}{hour}$ and the efficiency 90.43%.

Weight of Profit and Efficiency

Figure 5-14 shows how profit and efficiency vary by varying the weight of profit in the measure of fit.

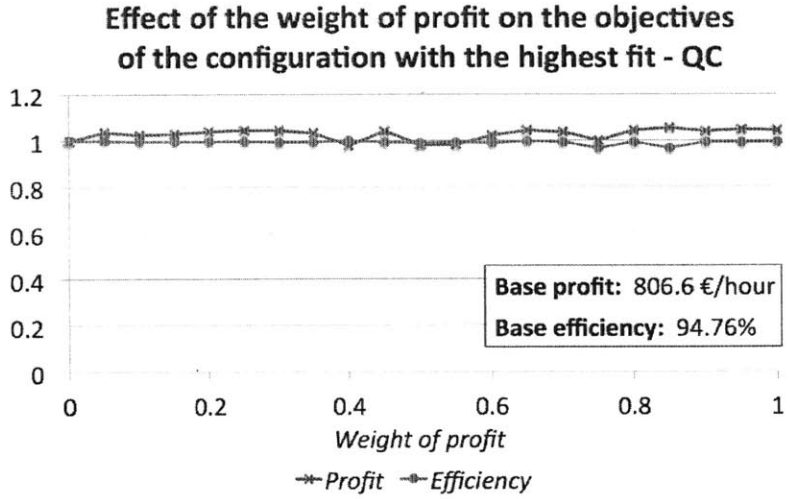

Figure 5-14: Variation in profit and efficiency due to variations in the weights in the measure of fit. Values reported to a base at a weight of profit of 0. At $\alpha_{profit} = 0$ the profit is $806.6\frac{€}{hour}$ and the efficiency is 94.76%; at $\alpha_{profit} = 1$ the profit is $839.8\frac{€}{hour}$ and the efficiency 94.10%.

The absence of a clear pattern in the results is surprising; we investigated this result further and repeated the analysis in absence of QC. In this case, the behavior of the algorithm matches the

expectations, and an increase in the weight of profit produces an increase in profit and a reduction in efficiency. The higher sensitivity of the GA to the objective weights in absence of QC could be due to the fact that the presence of QC improves all configurations and levels their performance.

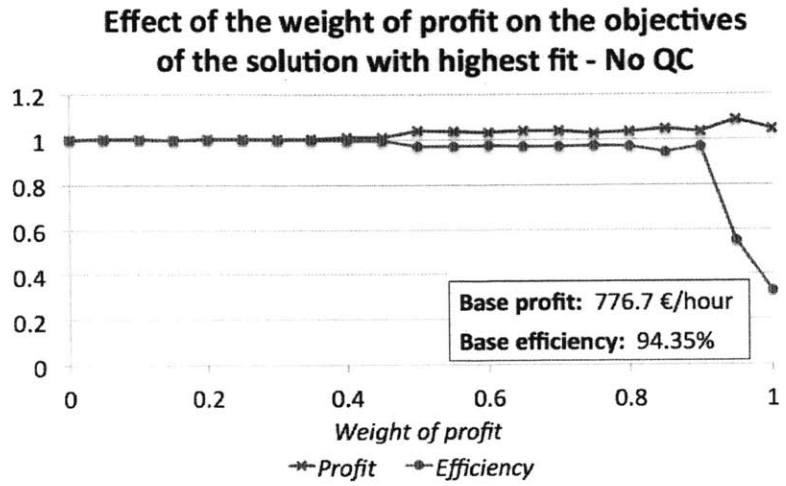

Figure 5-15: Variation in profit and efficiency due to variations in the weight assigned to profit in the measure of fit. In this case the GA cannot assign personnel to QC units. Values reported to a base at a weight of profit of 0. At $\alpha_{profit} = 0$ the profit is $776.7\frac{€}{hour}$ and the efficiency is 94.35%; at $\alpha_{profit} = 1$ the profit is $811.8\frac{€}{hour}$ and the efficiency 31.05%.

Final Considerations

The results on the parameters selection show how, for the facility considered, swap-mutation rate and the number of iterations have the highest effect on the algorithm performance. These two parameters impact on the capacity of the algorithm to explore the search-space; a high probability of single-allele mutation and a low number of iterations reduce the ability of generating different configurations. When QC is active, the relative weight of profit and efficiency does not have a clear effect on the results, with performances that oscillate around an average profit of $827.5\frac{€}{hour}$ and an average efficiency of 93.90%. When QC is inactive, this behavior changes and an increase in the weight of profit produces an increase of profit a reduction of efficiency. Table 5.17 shows the final parameters adopted in the optimization.

Mutation rate		**Crossover rate**			**Population size**	**Iterations**	**Objectives**	
single-allele	*swap*	*one-point*	*two-point*	*mask*			*profit*	*eff.*
0.1	0.9	0.3	0.3	0.4	50	150	0.9	0.1

Table 5.17: Final parameters selected.

5.4.4 GA: Typical Run-time

The run-time of the algorithm is affected by the number of iterations and the population size, which determine the number of individuals generated. With a population of 50 individuals and 150 iterations, the GA takes 18.96 seconds to run. Figure 5-16 shows that the runtime increases a little more than linearly with the potential number of individuals generated.

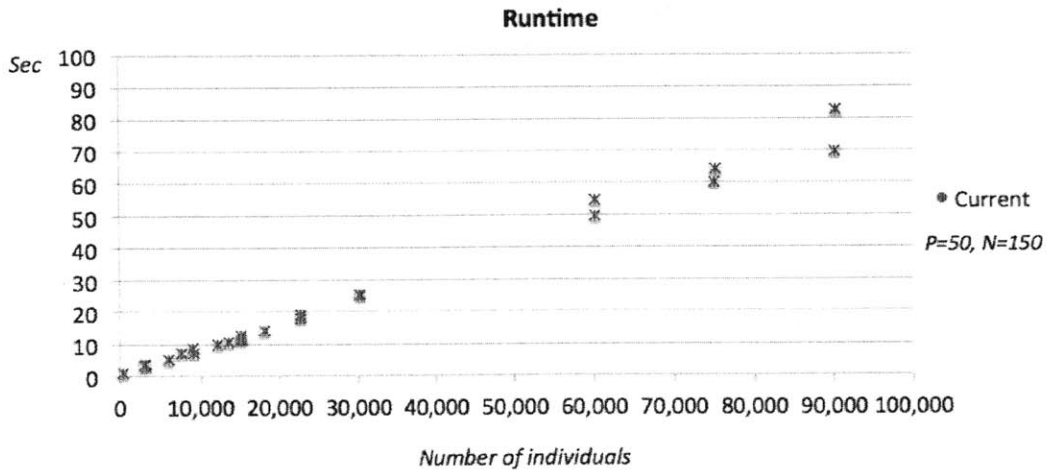

Figure 5-16: Runtime (*sec*) as a function of the maximum number of different individuals in the population. N is the number of iterations and P the number of individuals; the maximum number of configurations is given by $P(3N+1)$.

5.4.5 Genetic Algorithm and Random Generation

In this section, we compare the performance of the genetic algorithm (GA) to that of random generation (RG). In RG, we first generate the chromosome of each individual at random; we then decode the chromosome, assign target materials to DAR units and personnel at QC stations as we do in the GA. The only difference with the GA is that in RG we do not perform crossover, mutation, and the selection of the fittest. We compare the performance of RG with $K = 22,550$ individuals to the performance of the GA with $N = 150$ and $P = 50$. The two approaches have comparable run-times: RG takes 45.32 seconds to execute, while GA 18.96 seconds. Figure 5-17 shows the ten individuals with the highest measure of fit generated by RG and by GA. We see that with the exception of the configuration with the highest measure of fit, which is generated by the GA, configurations generated by RG perform generally better: only 5 of the 50 configurations with the highest measure of fit out of all 22,600 configurations are generated by the GA. Examining the

different configurations found, we did not identify any underlying pattern that could be associated to the difference in the performance of the two searching techniques. Looking at the clusters of configurations with the ten highest fit for RG and GA:

- **Random generation**: In the cluster, the sample mean of profit is $835.4\frac{€}{hour}$ and the sample standard deviation is $3.9\frac{€}{hour}$; the sample mean of efficiency is 92.96% and the sample standard deviation is 1.26%.

- **Genetic algorithm**: in the cluster, the sample mean of profit is $811.1\frac{€}{hour}$ and the sample standard deviation is $16.1\frac{€}{hour}$; the sample mean of efficiency is 91.05% and the sample standard deviation is 1.59%.

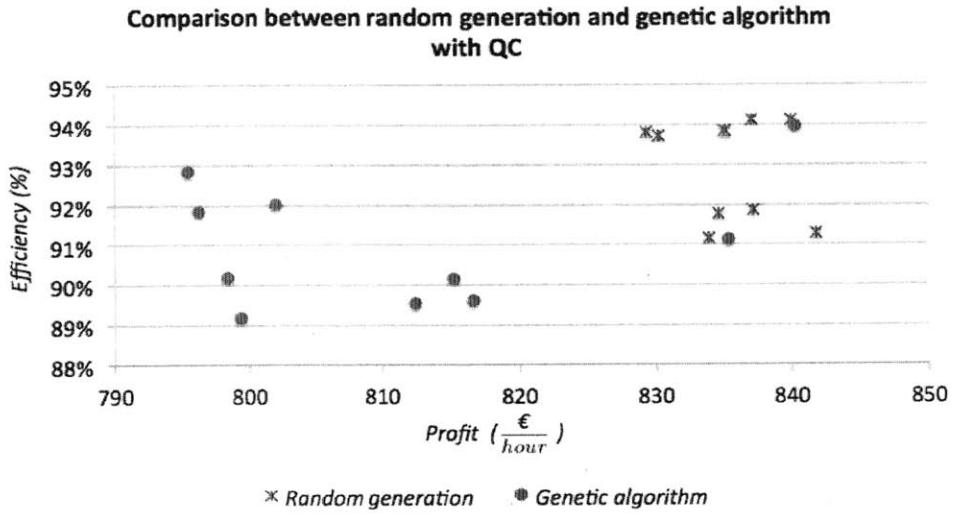

Figure 5-17: Profit and efficiency of the ten configurations with highest measure of fit found by random generation and by the genetic algorithm with quality control units.

We then compared the GA to RG in the case without quality control (QC). Figure 5-18 shows the profit and the efficiency of the ten configurations with the highest measure of fit generated with the two methods. In this case, we see that the GA performs better than RG and finds configurations with higher profits. If we consider the 50 configurations performing better out of all 55,600 configurations generated, 46 of these are generated by GA. Moreover, looking at the clusters of configurations with the ten highest measures of fit generated from RG and GA, we see that:

- **Random generation**: In the cluster, the sample mean of profit is $788.5\frac{€}{hour}$ and the sample standard deviation is $6.5\frac{€}{hour}$; the sample mean of efficiency is 90.30% and the sample standard deviation is 3.80%.
- **Genetic algorithm**: In the cluster, the sample mean of profit is $797.6\frac{€}{hour}$ and the sample standard deviation is $1.7\frac{€}{hour}$; the sample mean of efficiency is 91.40% and the sample standard deviation is 0.97%.

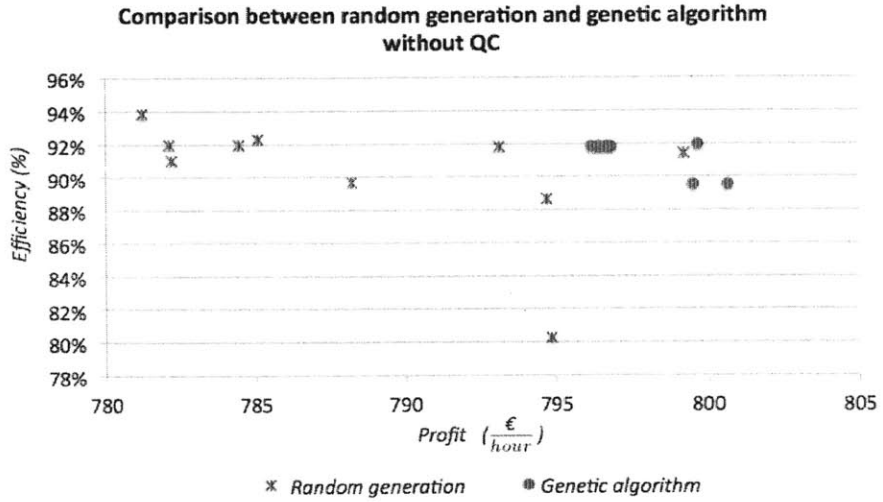

Figure 5-18: Profit and efficiency of the ten configurations with highest measure of fit found by random generation and by the genetic algorithm without quality control units.

Effect of Quality Control

The different performance of GA and RG with and without QC is consistent with the results seen in Section 5.4.3: the presence of QC makes solutions less sensitive to the selection process of the GA. This is due to the fact that the presence of QC increases the ability of different configurations to extract materials in a profitable way, and thus, when QC is active, there are more configurations that lead to good solutions. The case with QC is conceptually analogous to one with "overcapacity": systems with high sorting capacity (either due to the presence of many mechanical units with high efficiencies or to QC) can be arranged in a higher number of configurations with high profit and efficiency. For this reason, RG obtains good results: more of the possible configurations have performances close to the maximum performance obtainable. In conclusion, the results suggest that GA performs better than RG when it is more difficult to obtain output streams that meet concentration requirements.

5.5 LPRS Design

In this section, we evaluate the configurations with the highest measure of fit considering both the case with QC and without QC. Even though the LPRS uses QC, we believe that it is interesting to look at the best configurations in the case without QC, when it is more difficult to generate output streams that meet the requirements. We consider the best configurations found using both the genetic algorithm and random generation.

5.5.1 LPRS Design With Quality Control

We begin our analysis by considering the two configurations with the highest measure of fit in the case with quality control. The configuration with the highest measure of fit, C1, was generated by GA, while the configuration with the second highest measure of fit, C2, was generated by RG. Appendix B reports the composition of the output streams of all configurations found.

C1: Configuration With the Highest Fit

C1, shown in Figure 5-19, has a profit of $840.1\frac{€}{hour}$ and an efficiency of 93.98%, achieving a profit 3.2% lower than the one achieved by perfect separation. Table 5.18 reports the economic performance and the efficiency of the configuration, and Figure 5-20 shows the percentage improvement of the proposed configuration on the current one. Appendix B reports the composition of each output stream.

Metric	Performance
Revenues from processing materials ($\frac{€}{hour}$)	240.3
Revenues from recovered materials ($\frac{€}{hour}$)	704.1
Costs of personnel ($\frac{€}{hour}$)	20.2
Costs of landfill ($\frac{€}{hour}$)	84.1
Profit ($\frac{€}{hour}$)	840.1
Efficiency (%)	93.98

Table 5.18: Economic performance and efficiency of the configuration with highest fit for the LPRS with quality control. This configuration was found with the genetic algorithm.

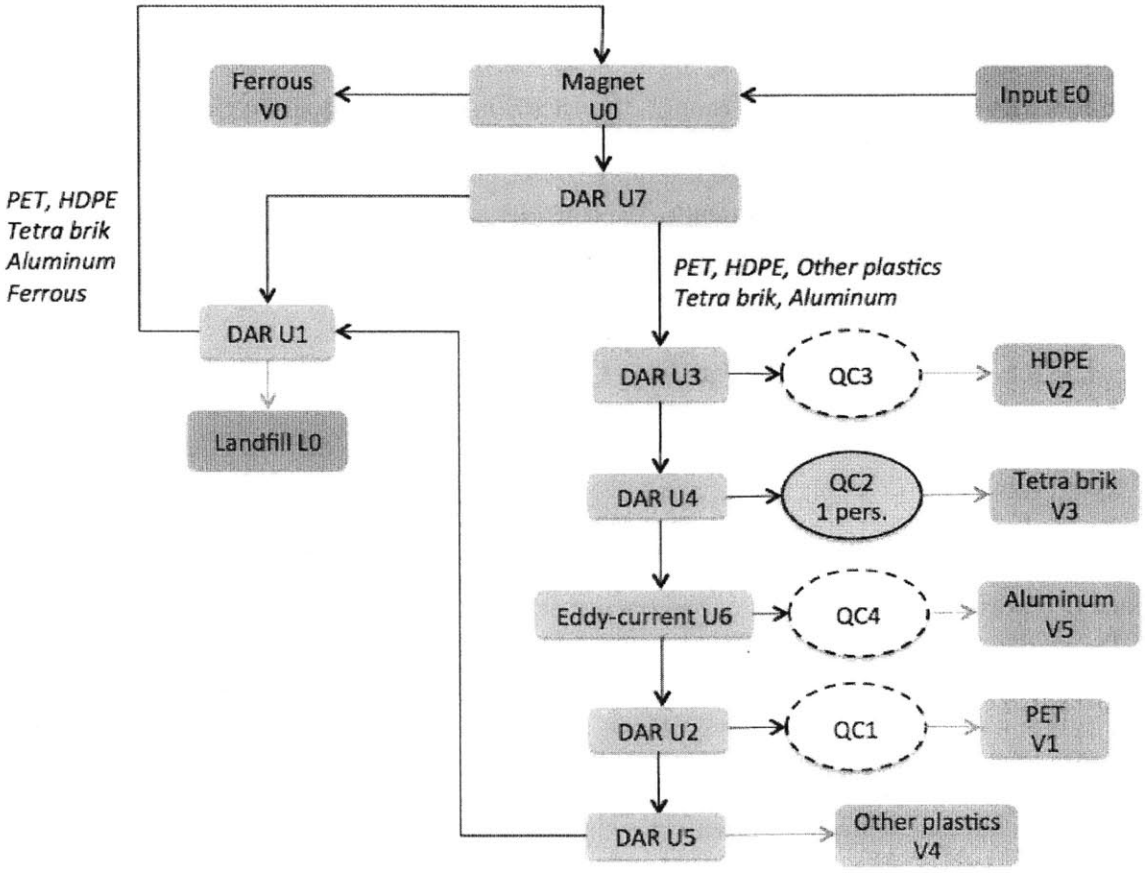

Figure 5-19: C1: Configuration with the highest fit. The algorithm assigns one person at the quality control station QC2 in correspondence of the tetra brik output stream.

We can see that:

- All output streams of C1 meet the requirements.
- The fact that C1 generates a higher profit than the current configuration is due to the fact that:
  - C1 assigns one hand sorter, while the current configurations assigns two.
  - The tetra brik output stream in C1 meets the requirement, while in the current configuration not.
- Mechanical sorting units in C1 form long subsequences of units in series (see the subsystem formed by DAR U2, DAR U3, DAR U4, DAR U5, eddy-current U6), which reduce the quantity of impurities in the collected output streams.

- DAR U1 sends *other plastics* to landfill, reducing the impurities of *other plastics* in other output streams. For example, in the ferrous output stream the content of *other plastics* is decreased by 17.4% with respect to the current configuration.
- In both C1 and in the current configuration all units are located on a recirculating stream.
- In both C1 and in the current configuration, each unit is connected to landfill.
- Both configurations locate the magnet at the beginning of the LPRS; this could be due to the fact that the requirements on ferrous are less stringent than those on other materials.

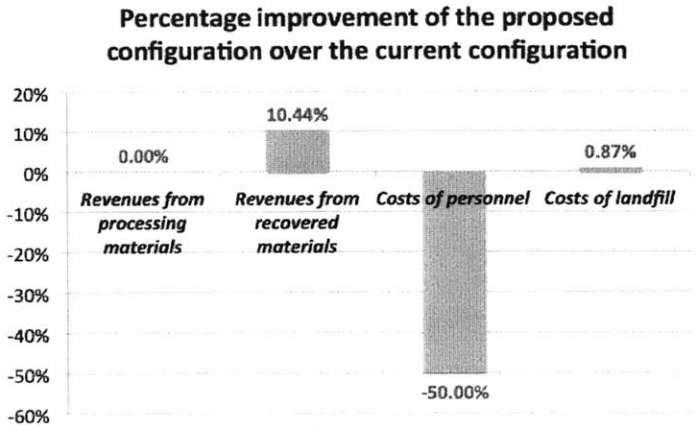

(a) Revenues and costs performance

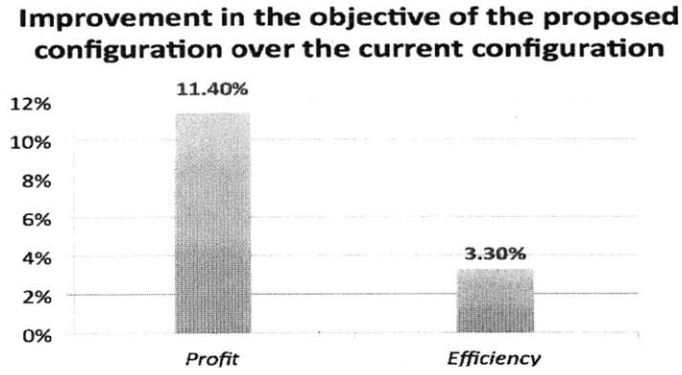

(b) Profit and efficiency

Figure 5-20: Improvement of the proposed configuration over the current one. Percentages are computed as $\frac{P-C}{C}$, where P stands for proposed and C for current.

C2: Configuration With the Second Highest Fit

Figure 5-21 shows C2, the configuration of the LPRS with the second highest measure of fit.

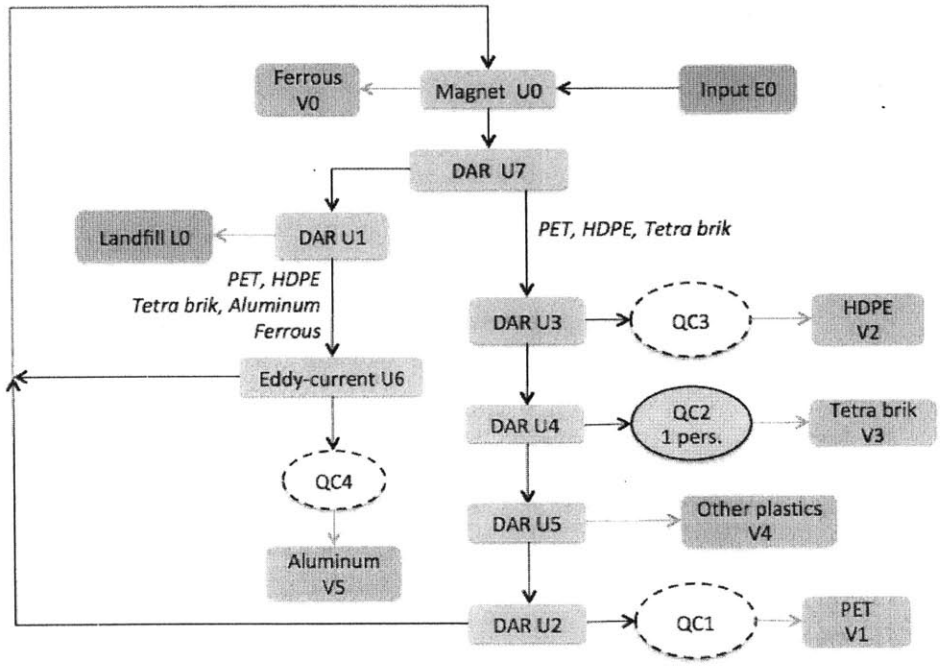

Figure 5-21: C2: Configuration with the second highest fit. The algorithm assigns one person at the quality control station QC2 in correspondence of the tetra brik output stream.

C2 has a profit of $839.8\frac{€}{hour}$, which is 11.4% higher than that of the current configuration and 3.2% lower than that of the perfect separation. The efficiency of C2 is 94.13%, which is 3.5% higher than the efficiency of the current configuration. Table 5.19 reports the economic performance and the efficiency of the configuration.

Metric	Performance
Revenues from processing materials ($\frac{€}{hour}$)	240.3
Revenues from recovered materials ($\frac{€}{hour}$)	703.6
Costs of personnel ($\frac{€}{hour}$)	20.2
Costs of landfill ($\frac{€}{hour}$)	83.9
Profit ($\frac{€}{hour}$)	839.8
Efficiency (%)	94.13

Table 5.19: Economic performance and efficiency of the configuration with the second highest fit for the LPRS with quality control. Configuration found with the random generation.

Looking at the results, we note the following:

- The higher profit of configuration C2 is due to the fact that in C2 the tetra brik output stream meets the requirements, while in the current configuration it does not. This reduces the cost of landfill by $7.5\frac{€}{hour}$ and increases the revenues from recovered materials by $71.8\frac{€}{hour}$. Moreover, C2 assigns only one person to the QC of tetra brik, while the current configuration assigns one person to the aluminum and one person to the HDPE output streams; this reduces the cost of personnel by $20.2\ \frac{€}{hour}$. Minor performance improvements are due to a 1.40% increase in the revenues from ferrous and to a 2.91% increase in the revenues from tetra pack.

- The fact that the output stream collecting tetra brik in C2 meets the requirements is primarily due to a reduction of 70.10% in the content of *other materials* in the stream.

- C2 sends *other plastics* to landfill, reducing the impurities of *other plastics* in other output streams, like in those collecting aluminum and HDPE.

First, we note that all units are connected to landfill and all units are on a recirculating stream. Second, if we compare C2 to C1, we see that the composition of the output streams of the two configurations are similar. The only remarkable difference is that C2 sends 1.2% more aluminum to landfill, and this is due to the fact that DAR U7 sends aluminum towards DAR U1. This loss impacts mainly the PET output stream, which sees a 15.0% reduction in the content of aluminum. The content of aluminum in the desired output stream in C2 is 0.1% higher than that in C1.

5.5.2 LPRS Design Without Quality Control

In this section, we consider the two configurations with the highest measure of fit in the case without quality control. Both configurations have been found with the GA.

C3: Configuration With the Highest Fit

C3, shown in Figure 5-22, has a profit of $799.6\frac{€}{hour}$ and an efficiency of 91.98%, improving the profit of the current configuration (without quality control) by 33.4% and the efficiency by 1.7%. This increase in profit is due to the fact that in C3, the output streams of HDPE, tetra brik, and aluminum meet the requirements. The profit of C4 is 7.8% lower than that of perfect separation.

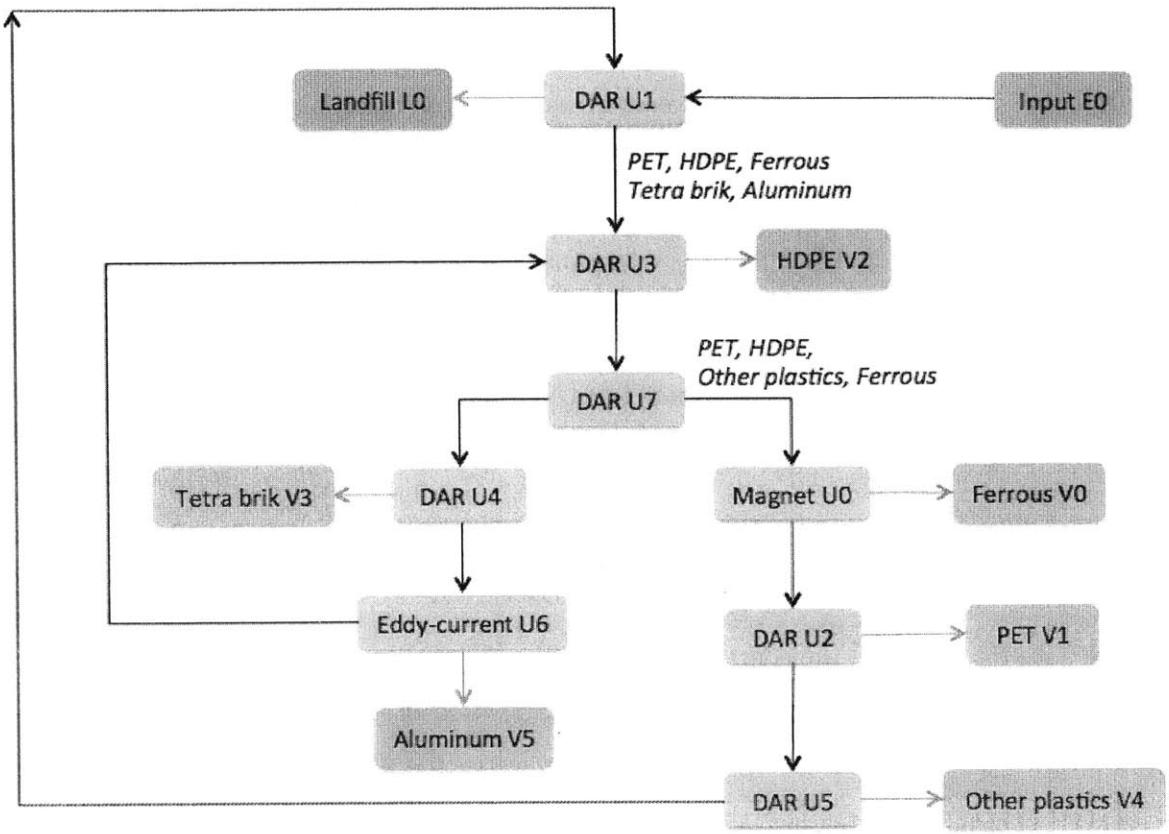

Figure 5-22: C3: Configuration with the highest fit without QC.

Looking at the output streams of HDPE, tetra brik, and aluminum we see that:

- **HDPE:** The HDPE output stream in the current configuration does not meet the requirements because of the low concentration of HDPE. C3 improves this performance in two ways. First, it reduces the quantity of *other materials* and *other plastics* in the stream by connecting DAR U1 to landfill. Second, it increases the amount of HDPE in the stream of 5.8% by placing DAR U3 right after DAR U1 and by recirculating one of the output streams of the eddy-current separator.

- **Tetra brik:** The tetra brik output stream in C3 has a lower content of impurities than the corresponding output stream in the current configuration. This is a consequence of connecting DAR U1 to landfill and directing *other plastics* to that stream.

- **Aluminum:** In C3, the quantity of tetra brik, *other plastics*, and *other materials* in the aluminum output stream is reduced by factors of 13.5, 42.0, and 1,703.1 respectively. This is due to the fact that DAR U1 sends *other plastics* and *other materials* to landfill and that DAR U4, which collects tetra brik, is placed right before the eddy-current.

Moreover, we see that all units are on a recirculating stream and that all units are connected to landfill. The results also show that directing one of the output streams of DAR U1, located at the beginning of the system, to landfill increases the total mass of disposed material by 16.6% with respect to the current configuration; this negative effect is outweighed by the positive effect that a reduction in the content of impurities has on the tetra brik, HDPE, and aluminum output streams. Table 5.20 summarizes the performance of C3; in Appendix B we report the output composition.

Metric	Performance
Revenues from processing materials ($\frac{€}{hour}$)	240.3
Revenues from recovered materials ($\frac{€}{hour}$)	647.5
Costs of personnel ($\frac{€}{hour}$)	-
Costs of landfill ($\frac{€}{hour}$)	88.2
Profit ($\frac{€}{hour}$)	799.6
Efficiency (%)	91.98

Table 5.20: Economic performance and efficiency of the configuration with the highest fit without quality control. Configuration found with the genetic algorithm.

C4: Configuration With the Second Highest Fit

C4, shown in Figure 5-23, has a profit of $793.6\frac{€}{hour}$ that is 33.5% higher than the profit of the current configuration and 8.5% lower than that of the ideal separation; the profit of C4 is also 0.1% higher than the profit of C3. The efficiency is 89.57%, which is 0.9% lower than that of the current configuration and 2.6% lower than that of C3. Table 5.21 reports the economic performance and efficiency of C4.

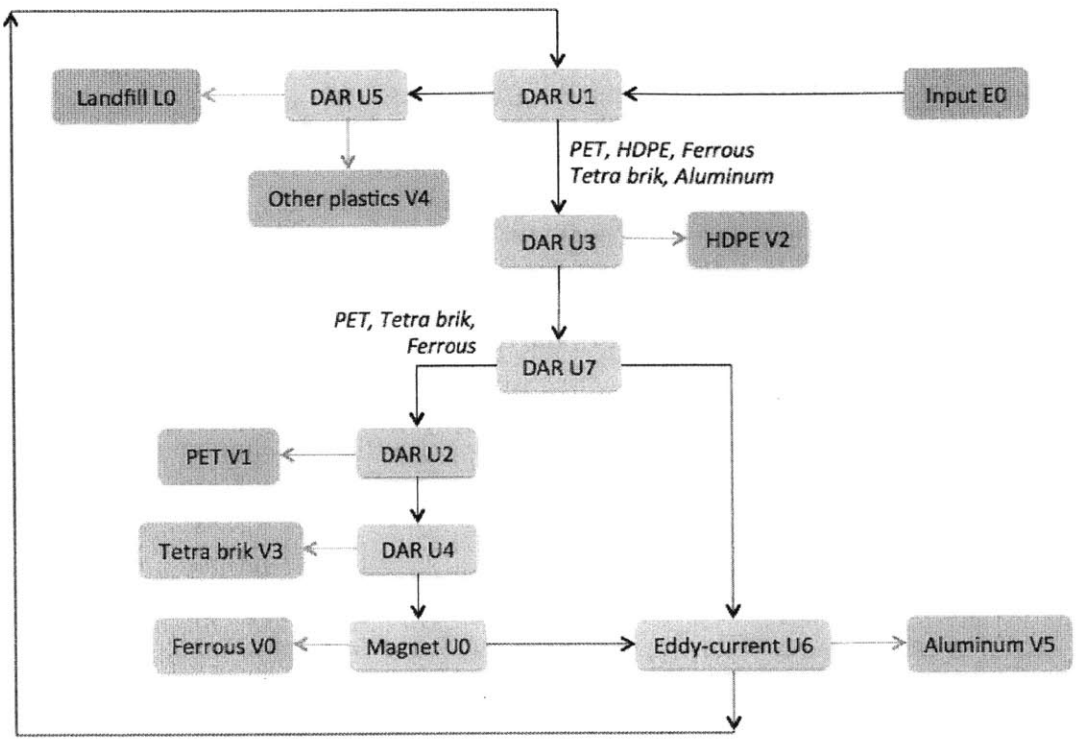

Figure 5-23: C4: Configuration with the second highest fit without QC.

Metric	Performance
Revenues from processing materials ($\frac{€}{hour}$)	240.3
Revenues from recovered materials ($\frac{€}{hour}$)	642.3
Costs of personnel ($\frac{€}{hour}$)	-
Costs of landfill ($\frac{€}{hour}$)	89.0
Profit ($\frac{€}{hour}$)	793.6
Efficiency (%)	89.57

Table 5.21: Economic performance and efficiency of the configuration with the second highest fit in the case without quality control. Configuration found with the genetic algorithm.

The results show the following:

- The lower efficiency of C4 with respect to the current configuration is primarily due to an increase of valuable materials sent to landfill; in fact, C4 sends 76.8% more valuable materials to disposal; consequently, the quantities of PET, tetra brik, and other plastics sent to desired streams are reduced (the reduction is of 14.4%, 26.5%, and 21.8% respectively).

- The increase in profit with respect to the current configuration is due to the fact that the PET, tetra brik, and aluminum output streams of C4 meet the requirements and contribute to the revenues.

- As in C3, the fact that DAR U1 sends *other plastics* and *other materials* to DAR U5 and landfill reduces the impurities in the output streams of HDPE and tetra brik.

- The aluminum output stream of C4 has a lower content of PET, tetra brik, *other plastics*, and *other materials*. This is due to the fact that in C4, aluminum is extracted at the end of the sequence and all other materials have been targeted before. Moreover, the quantity of aluminum collected in the desired output stream in C4 is 4.3% higher than the quantity of aluminum collected in C3. This is due to the fact that the eddy current separator processes a material mixture containing a higher quantity of aluminum because it receives a stream from the magnet and a stream from DAR U3.

- Comparing the performance of C4 to the performance of C3, we see that the higher profit of C4 is a consequence of the lower cost of landfill (the cost of C4 is 7.0% lower than that of C3). This is due to the fact that, in configuration C4, DAR U5 is placed before the landfill and compensates a reduction in the revenues from recovered materials, which are 0.8% lower for C3.

- Like in all other configurations found, all units are on a recirculating stream and are connected to landfill.

Chapter 6

Conclusion

In this work, we built upon existing mathematical models to describe the operations of material recovery facilities. We proposed a genetic algorithm to generate and evaluate alternative configurations of a MRF and allocate personnel to manual operations. We coded the model in Java and used it to analyze a real MRF, finding configurations that improve the current performance.

When input material and unit separation parameters are known, our model defines a system of linear equations to determine material flows. We proved that the only necessary requirement for the system to be solvable is to have an output stream going from each sorting and input unit to an output unit. Like previous models, the proposed model can be used to describe facilities processing any number of materials using any number of units, each unit having any number of output streams which can be directed downstream or upstream (i.e., with recirculation). Moreover, the proposed model of manual operations distinguishes between positive and negative sorting and is based on the observation of real sorting systems.

We represent the configurations of a MRF using a sequence of integer numbers, and we use a genetic algorithm to generate alternative configurations of the system and select solutions with the highest profit and efficiency. To the best of our knowledge, this is the first work that systematically generates possible MRF configurations with a generic number of sorting units, multiple output streams, and recirculation. Previous works either employed full enumeration of solutions for systems of binary units connected in series or relied on manual generation of different configurations, which limited the analysis to small problems of two or three binary-units. Our model

allows analyzing problems that occur in real situations in an efficient amount of time on a personal computer. Our algorithm finds feasible configurations, computes material flows, and compares the profit and the efficiency of different configurations. We included constraints that are not necessary from a mathematical point of view, but that are relevant to real operations of MRFs: the respect of flow capacity, the existence of a path from an input node to each sorting unit, and precedence constraints between different units. The GA incorporates personnel allocation using an embedded heuristic.

We developed a Java code in which the user can define the elements of a MRF, and we applied it to the analysis of an existing MRF. We compared different ways of determining the sorting parameters of mechanical units; with the data available, the preferred method is minimizing the error between the composition of output flows from material characterization and from the mathematical model. We estimated the sorting efficiencies of personnel using data available in the literature. We found that the most relevant parameters of the GA are the probability of mutation, which should guarantee the generation of different solutions and the number of iterations. The GA works better than random generation in those cases in which it is more difficult to separate materials and generate output streams that meet the concentration requirements.

The configurations found without personnel assignment improved the profit of the current configuration (with no additional personnel) by 33.4% and the efficiency by 1.7%. When including personnel assignment, the configuration with the highest measure of fit increases the profit by 6.7% and efficiency by 3.9%, compared to the current configuration with personnel added. We noted that the best configurations share common properties: they employ recirculation loops that include most of the units collecting valuable materials, they connect each unit to landfill, and they remove contaminant materials at the first stages of the sequence.

This work provides insights on MRF operations and could be developed further. Areas of future research could include parameter estimation and the definition of specific sorting unit models, relating separation parameters to operational settings. Moreover, additional work should include the analysis of input composition and the way in which its variation over time affects the performance of the facility.

Appendix A

Testing Procedures and Parameters Estimation

In this appendix, we illustrate the testing procedures used to characterize waste streams and report the results.[1]

A.1 Test 1: LPRS Output Stream Characterization

To determine the composition of the output streams in the light packaging recovery section (LPRS) of the plant, we conducted the following test:

1. The plant was completely emptied from previous material.
2. No hand sorting operation was performed.
3. A regular quantity of input collected from the reception bunker was processed for 30 minutes (approximately 60 t/h input to the entire plant).
4. When all input material was collected the plant was stopped.
5. The output streams from the light packaging recovery section were weighed and sampled.
6. The samples were characterized by material type to determine the concentration of different materials in the stream (see Table A.2).

Figure A-1 shows the locations sampled in the LPRS.

[1]Inconsistencies in the numbers reported in this section are due to rounding procedure.

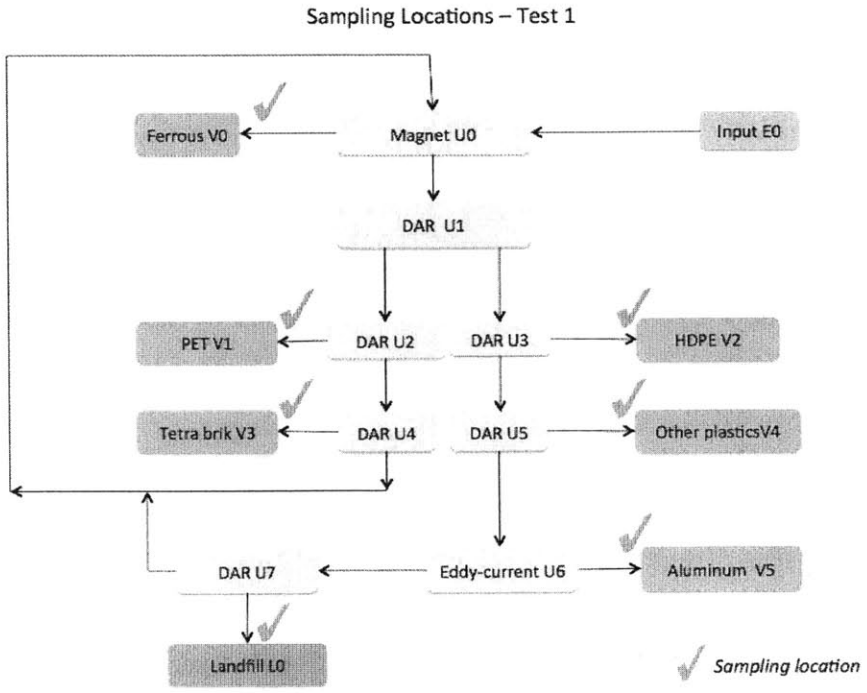

Figure A-1: Sampling locations in Test 1. Blue units represent input units, gray units sorting units, green units valuable output streams, and orange units landfill.

Table A.1 shows how the quantity of input material is directed towards each output stream (mass-balance) and the mass sampled from each stream.

Stream	**Stream mass** *(mass balance)* *Kg*	**Sampled material quantity** *Kg*
Input to the entire plant	31,600	-
V0 - Ferrous	457	148.34
V1 - PET	460	166.90
V2 - HDPE	153	150.01
V3 - Tetra brik	143	158.56
V4 - Other plastics	240	152.77
V5 - Aluminum	54	45.87
L0 - Landfill	2580	147.99

Table A.1: Quantity of material in each stream and quantity of material sampled.

The quantity of material in input to the LPRS ($4,087Kg$) is the 13.36% of the material in input to the entire plant ($30,600Kg$).

The quantity of sampled material from stream V3 is greater than the total mass of material in the stream. This is a consequence of the fact that different scales were used to weight the two

quantities: the total mass of the stream (*mass balance*) was weighed at the plant during the tests. The sampled stream was then divided into the different materials categories and weighed (*material characterization*); these results were summed to determine the mass sampled. To overcome the resulting discrepancy, we considered the mass-balance data to determine the total mass of material in the stream and the stream-characterization data to determine the stream composition.

Composition of characterized material

Material	*V0* *Ferrous*	*V1* *PET*	*V2* *HDPE*	*V3* *Tetra Brik*	*V4* *Other plastics*	*V5* *Aluminum*	*L0* *Landfill*
PET	0.26	159.12	0.31	0.23	0.29	0.09	0.3
HDPE	0.03	0.05	126.47	0.03	0.4	0	0.9
Aluminum	0.02	0.06	0.05	0.1	0.89	38.34	0.5
Ferrous	142.21	0.00	0.00	0.00	0.31	0.00	2.11
Tetra brik	0.09	2.29	0.08	146.8	0.08	2.01	0.26
Other plastics	0.11	0.47	0.57	0.72	80.65	0.26	0.32
Other	5.62	4.91	22.53	10.68	70.15	5.17	143.6
Total	148.34	166.9	150.01	158.56	152.77	45.87	147.99

Table A.2: Breakdown of sampled material by material type. Quantities expressed in Kg.

We combined stream-characterization and mass-balance data to determine the composition of the output streams reported in A.3.

Flow composition

Material	*E0* *Input*	*V0* *Ferrous*	*V1* *PET*	*V2* *HDPE*	*V3* *Brik*	*V4* *Other plastics*	*V5* *Aluminum*	*L0* *Landfill*
PET	0.316	0.207	438.557	0.456	0.106	0.801	5.230	445.673
HDPE	128.991	0.027	0.138	0.628	0.000	0.092	15.690	145.566
Aluminum	0.051	0.091	0.165	1.398	45.135	0.062	8.717	55.619
Ferrous	0.000	0.000	0.000	0.487	0.000	438.115	36.785	475.387
Tetra brik	0.082	132.394	6.312	0.126	2.366	0.277	4.533	146.090
Other plastics	0.581	0.649	1.295	126.700	0.307	0.339	5.579	135.450
Other	22.979	9.632	13.533	110.205	6.086	17.314	2503.466	2683.215
Total	153.000	143.000	460.000	240.000	54.000	457.000	2580.000	4087.000

Table A.3: Mass of material in the output units and derived input composition as resulted from stream characterization. Quantities are in Kg and refer to the material collected in half-hour of operations.

A.2 Test 2: Output characterization with recirculation inactive

To characterize the output composition with recirculation inactive, we conducted the following test:

1. The plant was completely emptied from previous material.
2. Recirculation (i.e., the streams sending material from $U4$ and from $U7$ to $U0$) was deactivated. No quality control was present.
3. Input collected from the reception bunker was processed for 30 minutes (i.e., approximately 60 t/h input to the entire plant).
4. When all input material was processed and sorted towards an output stream the plant was stopped.
5. The output streams from the light packaging recovery section (including the two recirculation streams) were weighed and sampled.
6. The samples were characterized by material type to determine the concentration of different materials in the stream.

Figure A-2 shows the sampled location in the LPRS.

Table A.4 shows how input material was sorted into each output and recirculation stream (*mass balance*) and the quantity of material sampled from each stream. Table A.5 reports the composition of each sample.

The quantity of material in input to the LPRS ($3,994Kg$) is 12.97% of the total input material ($30,800Kg$).

As in Test 1, also in Test 2 we have inconsistencies between the quantity of material sampled and the total quantity of material in the streams. As we did for Test 1, we used mass-balance data to estimate the total mass of material in each stream and the stream-characterization data to determine the stream composition.

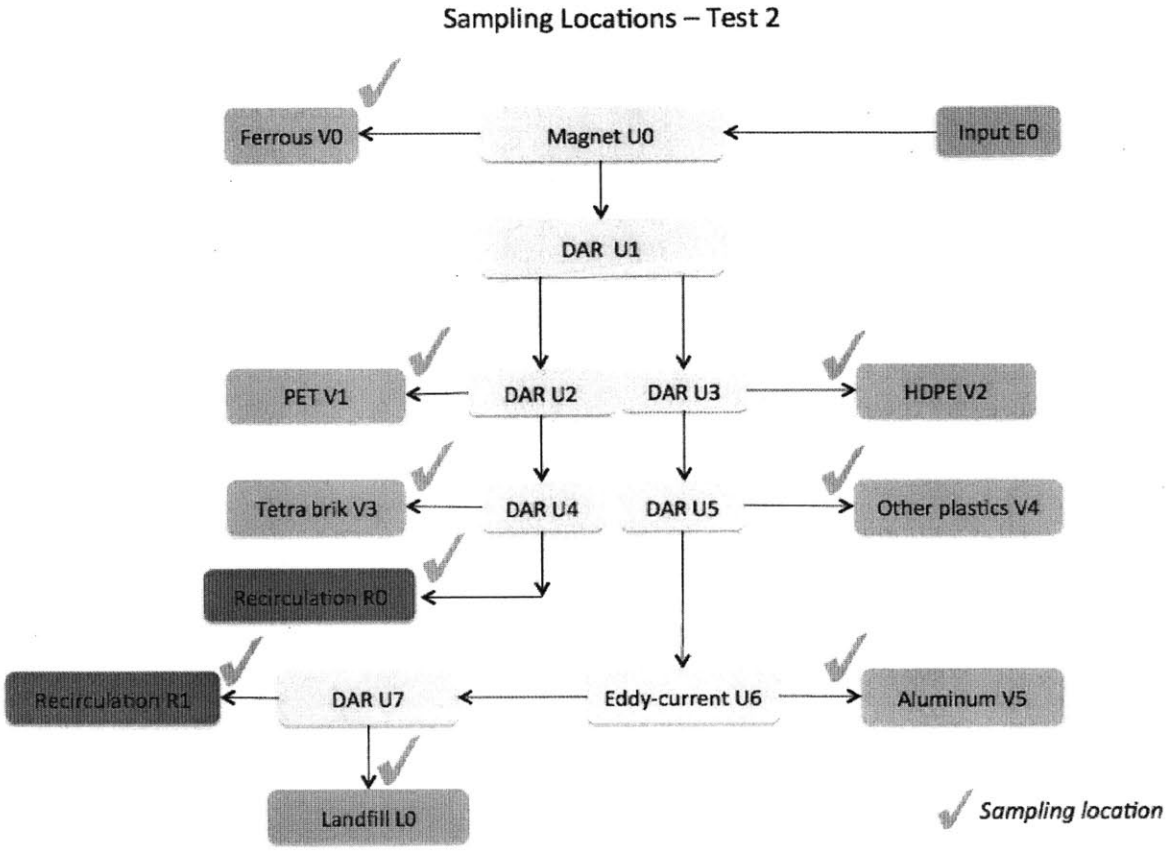

Figure A-2: Sampling locations in Test 2. Blue units represent input units, gray units sorting units, green units valuable output streams, orange units landfill, and purple units recirculating streams interrupted for the purpose of the test.

Stream	**Stream mass** *(mass-balance)* *Kg*	**Sampled material quantity** *Kg*
Input to the entire plant	30,800	-
V0 - Ferrous	480	152.04
V1 - PET	440	158.25
V2 - HDPE	135	143.81
V3 - Tetra brik	185	212.90
V4 - Other plastics	200	136.91
V5 - Aluminum	50	46.52
L0 - Landfill	2160	165.00
R1 - Recirculation after $U4$	84	70.10
R2 - Recirculation after $U7$	260	153.32

Table A.4: Quantity of material in each stream, as obtained from the test on the light packaging section of the plant.

Composition of characterized material

Material	*V0* *Ferrous*	*V1* *PET*	*V2* *HDPE*	*V3* *Brik*	*V4* *Other plastics*
PET	0.16	151.96	39.80	0.28	0.17
HDPE	0.02	0.00	140.15	0.21	0.03
Aluminum	0.01	0.01	38.88	0.07	0.42
Ferrous	139.35	0.00	0.52	0.01	0.05
Tetra brik	0.14	2.18	42.46	200.30	0.13
Other plastics	0.17	0.35	91.18	0.24	70.18
Other	12.19	3.75	292.57	11.79	65.93
Total	152.04	158.25	143.81	212.90	136.91

Composition of characterized material

Material	*V5* *Aluminum*	*L0* *Landfill*	*R1* *Recirculation after U4*	*R2* *Recirculation after U7*
PET	0.24	0.62	25.65	38.61
HDPE	0.29	0.90	0.22	18.69
Aluminum	37.14	0.01	1.56	1.25
Ferrous	0.00	0.24	0.03	0.23
Tetra brik	3.57	0.12	5.58	38.39
Other plastics	0.44	0.20	6.39	19.00
Other	4.84	162.91	30.67	37.15
Total	46.52	165.00	70.10	153.32

Table A.5: Composition of the sampled quantity of material. Quantities expressed in Kg.

A.3 Test 3: Input Stream Characterization

We sampled and characterized the input to the LPRS adopting a similar approach to the one used in Test 1 and Test 2. That is:

1. The plant was completely emptied from previous material.
2. No hand sorting operation was performed.
3. A regular quantity of input collected from the reception bunker was processed for 30 minutes (approximately 60 t/h input to the entire plant).
4. When the plant was at regime, a sample of the material in input to the LPRS was collected.
5. The sample were characterized by material type in order to determine the concentration of different materials in the stream (see Table A.2).

We conducted two characterizations. Table A.6 reports the sampled input stream.

Material	Input C1 *Kg*	Input C2 *Kg*
PET	11.610	11.220
HDPE	4.530	4.370
Aluminum	1.220	1.770
Ferrous	14.520	13.480
Tetra brik	8.020	7.820
Other plastics	6.400	5.610
Other	79.680	84.990
Total	125.980	129.260

Table A.6: Composition of the input stream to the LPRS as resulted from the tests.

We used the results from Test 3 and the results from Test 1 and Test 2 to estimate the average concentration of different materials in the input stream. Table A.7 reports the results.

	Input Composition					
Material	**Input C1** *(%)*	**Input C2** *(%)*	**Test 1** *(%)*	**Test 2** *(%)*	**Average** *(%)*	**Standard Deviation** *(%)*
PET	9.216	8.680	10.905	13.226	10.507	2.046
HDPE	3.596	3.381	3.562	3.936	3.619	0.232
Aluminum	0.968	1.369	1.361	1.122	1.205	0.195
Ferrous	11.526	10.429	11.632	11.106	11.173	0.546
Tetra brik	6.366	6.050	3.575	6.464	5.614	1.371
Other plastics	5.080	4.340	3.314	3.718	4.113	0.771
Other	63.248	65.751	65.652	60.427	63.770	2.511

Table A.7: Columns C1, C2, Test 1, and Test 2 report the observations for concentration of each material in the input stream. The last two columns report the sample mean and the sample standard deviation per material type.

A.4 Separation Parameters

As explained in Section 5.2.3, we estimated the separation parameters by solving an optimization problem to minimize the weighted absolute deviation between the flows from Test 1 and Test 2 and the flows predicted by the model. The objective function is given by:

$$\sum_{t=1,2} \sum_{m \in \mathcal{M}} \sum_{z \in \mathcal{Z}_t} \beta^m_{z,t} |\bar{f}^m_{z,t} - f^m_{z,t}|, \tag{A.1}$$

where, $\bar{f}^m_{z,t}$ is the quantity of material m in output unit z at test t, $f^m_{z,t}$ the corresponding predicted quantity, and $\beta^m_{z,t} \in [0, 1]$ the weight.

Weights for the error terms

Tables A.8 and A.9 report the normalized weights of the objective function.

Weights used for Test 1

Material	*V0*	*V1*	*V2*	*V3*	*V4*	*V5*	*L0*
PET	0.166	0.003	0.167	0.167	0.166	0.167	0.165
HDPE	0.167	0.167	0.019	0.167	0.166	0.167	0.149
Aluminum	0.166	0.166	0.167	0.166	0.162	0.031	0.141
Ferrous	0.013	0.167	0.167	0.167	0.166	0.167	0.154
Tetra brik	0.166	0.159	0.167	0.016	0.167	0.164	0.161
Other plastics	0.166	0.165	0.166	0.166	0.011	0.166	0.160
Other	0.166	0.166	0.165	0.166	0.160	0.166	0.011

Table A.8: Weights for the deviations in Test 1. For example, the element in the PET row and V0 column corresponds to the weight $\beta_{V0,1}PET$.

Weights used for Test 2

Material	*V0*	*V1*	*V2*	*V3*	*V4*	*V5*	*L0*	*R0*	*R1*
PET	0.125	0.025	0.125	0.125	0.125	0.125	0.123	0.118	0.110
HDPE	0.125	0.125	0.035	0.125	0.125	0.125	0.116	0.125	0.100
Aluminum	0.125	0.125	0.125	0.125	0.123	0.014	0.125	0.120	0.119
Ferrous	0.001	0.125	0.125	0.125	0.125	0.125	0.124	0.125	0.125
Tetra brik	0.125	0.122	0.125	0.041	0.125	0.123	0.124	0.122	0.093
Other plastics	0.125	0.124	0.124	0.125	0.039	0.125	0.123	0.119	0.098
Other	0.123	0.124	0.124	0.124	0.120	0.125	0.015	0.123	0.122

Table A.9: Weights for the deviations in Test 2. For example, the element in the PET row and V0 column corresponds to the weight $\beta_{V0,2}PET$.

Separation parameters

Tables A.10 - A.13 report the estimated separation parameters of the mechanical units; for unit U7, we report the separation parameters corrected as explained in Section 5.2.3.

Magnet - U0

Material	End node	
	V0	*U1*
PET	0.147%	99.853%
HDPE	0.050%	99.950%
Aluminum	0.102%	99.898%
Ferrous	92.071%	7.929%
Tetra brik	0.137%	99.863%
Other plastics	0.182%	99.817%
Other	0.619%	99.381%

DAR - U1

Material	End node	
	U2	*U3*
PET	13.536%	86.464%
HDPE	99.742%	0.258%
Aluminum	95.407%	4.593%
Ferrous	99.898%	0.102%
Tetra brik	27.134%	72.866%
Other plastics	93.78%	6.218%
Other	97.635%	2.365%

Table A.10: Separation parameters of unit U0 and unit U1.

DAR - U2

Material	End node	
	V1	*U4*
PET	93.217%	6.783%
HDPE	29.249%	70.751%
Aluminum	5.890%	94.110%
Ferrous	0.000%	100.000%
Tetra brik	3.794%	96.206%
Other plastics	11.267%	88.733%
Other	20.571%	79.429%

DAR - U3

Material	End node	
	V3	*U5*
PET	0.429%	99.571%
HDPE	70.819%	29.181%
Aluminum	0.088%	99.912%
Ferrous	0.000%	100.000%
Tetra brik	0.105%	99.850%
Other plastics	0.335%	99.665%
Other	0.846%	99.154%

Table A.11: Separation parameters of unit U2 and unit U3.

DAR - U4

Material	End node	
	V3	*U0*
PET	0.649%	99.351%
HDPE	8.089%	91.911%
Aluminum	3.452%	96.548%
Ferrous	0.000%	100.000%
Tetra brik	96.301%	3.699%
Other plastics	6.364%	93.636%
Other	18.433%	81.567%

DAR - U5

Material	End node	
	V4	*U6*
PET	0.622%	99.378%
HDPE	1.182%	98.818%
Aluminum	2.405%	97.595%
Ferrous	1.292%	98.708%
Tetra brik	0.230%	99.770%
Other plastics	73.335%	26.665%
Other	4.093%	95.907%

Table A.12: Separation parameters from of unit U4 and unit U5.

Eddy-current - U6		
Material	End node	
	V5	*U7*
PET	0.145%	99.855%
HDPE	0.000%	100.000%
Aluminum	79.548%	20.452%
Ferrous	0.000%	100.000%
Tetra brik	4.331%	95.669%
Other plastics	0.666%	99.334%
Other	0.236%	99.764%

DAR - U7		
Material	End node	
	U0	*L0*
PET	7.187%	92.813%
HDPE	29.873%	70.127%
Aluminum	15.258%	84.742%
Ferrous	16.711%	83.289%
Tetra brik	2.356%	97.644%
Other plastics	12.191%	87.809%
Other	97.164%	2.836%

Table A.13: Separation parameters of unit U6 and unit U7.

A.4.1 Comparison Between Output Composition

We compared the predicted flow and the flows from Test 1 and Test 2. Tables A.14 -A.20 report the results.

Comparison with the output streams of Test 1

	V0 - Ferrous			V1 - PET		
	Test 1	**Model**	**AD**	**Test 1**	**Model**	**AD**
PET	0.801	0.801	0.000	438.557	438.557	0.000
HDPE	0.092	0.091	0.001	0.138	0.138	0.000
Aluminum	0.062	0.071	0.009	0.165	0.189	0.024
Ferrous	438.115	468.222	30.107	0.000	0.000	0.000
Tetra brik	0.277	0.277	0.000	6.312	5.587	0.725
Other plastics	0.339	0.339	0.000	1.295	1.295	0.000
Other	17.314	17.325	0.011	13.533	13.533	0.000
Total	457.000	487.127	30.129	460.000	459.297	0.750
MAD			4.304	**MAD**		0.107
$\widetilde{\textbf{MAD}}$			0.942%	$\widetilde{\textbf{MAD}}$		0.023%

Table A.14: Composition of the V0 and V1 output streams from Test 1 and the model. The table shows the absolute deviation (AD) per material type, the mean absolute deviation (MAD) per stream, and the MAD divided by the mass in the stream ($\widetilde{\text{MAD}}$).

	V2 - HDPE			V3 - Tetra brik		
	Test 1	**Model**	**AD**	**Test 1**	**Model**	**AD**
PET	0.316	0.316	0.000	0.207	0.207	0.000
HDPE	128.991	128.992	0.001	0.027	0.027	0.000
Aluminum	0.051	0.059	0.008	0.091	0.104	0.013
Ferrous	0.000	0.000	0.000	0.000	0.000	0.000
Tetra brik	0.082	0.082	0.000	132.394	136.421	4.027
Other plastics	0.581	0.581	0.000	0.649	0.649	0.000
Other	22.979	22.976	0.003	9.632	9.632	0.000
Total	457.000	487.127	30.129	460.000	459.297	0.750
MAD			0.002	**MAD**		0.577
$\widetilde{\textbf{MAD}}$			0.001%	$\widetilde{\textbf{MAD}}$		0.404%

Table A.15: Composition of the V2 and V3 output streams from Test 1 and the model. The table shows the absolute deviation (AD) per material type, the mean absolute deviation (MAD) per stream, and the MAD divided by the mass in the stream ($\widetilde{\text{MAD}}$).

	V4 - Other plastics			V5 - Aluminum			L0 - Landfill		
	Test1	**Model**	**AD**	**Test1**	**Model**	**AD**	**Test1**	**Model**	**AD**
PET	0.456	0.456	0.000	0.106	0.106	0.000	5.230	5.230	0.000
HDPE	0.628	0.628	0.000	0.000	0.000	0.000	15.690	15.690	0.000
Al.	1.398	1.598	0.200	45.135	51.576	6.441	8.717	2.023	6.694
Ferrous	0.487	0.520	0.033	0.000	0.000	0.000	36.785	6.644	30.141
Tetra brik	0.126	0.126	0.000	2.366	2.366	0.000	4.533	1.231	3.302
Other plastics	126.700	126.701	0.001	0.307	0.307	0.000	5.579	5.579	0.000
Other	110.205	110.217	0.012	6.086	6.095	0.009	2503.466	2503.438	0.028
Total	240.000	240.246	0.246	54.000	60.449	6.450	2580.000	2539.836	40.165
MAD			0.035	**MAD**		0.921	**MAD**		5.738
$\widetilde{\textbf{MAD}}$			0.015%	$\widetilde{\textbf{MAD}}$		1.706%	$\widetilde{\textbf{MAD}}$		0.222%

Table A.16: Composition of the V4, V5, and L0 output streams from Test 1 and the model. The table shows the absolute deviation (AD) per material type, the mean absolute deviation (MAD) per stream, and the MAD divided by the mass in the stream ($\widetilde{\text{MAD}}$).

Comparison with the output streams of Test 2

	V0 - Ferrous			V1 - PET		
	Test 2	**Model**	**AD**	**Test 2**	**Model**	**AD**
PET	0.505	0.777	0.272	422.511	425.133	2.622
HDPE	0.063	0.079	0.016	0.000	0.119	0.119
Aluminum	0.032	0.046	0.014	0.028	0.121	0.093
Ferrous	439.937	408.415	31.522	0.000	0.000	0.000
Tetra brik	0.442	0.354	0.088	6.061	7.128	1.067
Other plastics	0.537	0.272	0.265	0.973	1.038	0.065
Other	38.484	14.939	23.545	10.427	11.669	1.242
Total	480.000	424.881	55.721	440.000	445.207	5.207
MAD			7.960	**MAD**		0.744
$\widetilde{\textbf{MAD}}$			1.658%	$\widetilde{\textbf{MAD}}$		0.169%

Table A.17: Composition of the V0 and V1 output streams from Test 2 and the model. The table shows the absolute deviation (AD) per material type, the mean absolute deviation (MAD) per stream, and the MAD divided by the mass in the stream ($\widetilde{\text{MAD}}$). Quantities in Kg.

	V2 - HDPE			V3 - Tetra brik		
	Test 2	**Model**	**AD**	**Test 2**	**Model**	**AD**
PET	0.150	0.306	0.156	0.243	0.201	0.042
HDPE	112.874	110.995	1.879	0.182	0.023	0.159
Aluminum	0.056	0.038	0.018	0.061	0.067	0.006
Ferrous	0.000	0.000	0.000	0.009	0.000	0.009
Tetra brik	0.235	0.105	0.130	174.051	174.051	0.000
Other plastics	1.277	0.466	0.811	0.209	0.520	0.311
Other	20.408	19.812	0.596	10.245	8.305	1.940
Total	135.000	131.721	3.591	185.000	183.167	2.467
MAD			0.513	**MAD**		0.352
$\widetilde{\textbf{MAD}}$			0.380%	$\widetilde{\textbf{MAD}}$		0.191%

Table A.18: Composition of the V2 and V3 output streams from Test 2 and the model. The table shows the absolute deviation (AD) per material type, the mean absolute deviation (MAD) per stream, and the MAD divided by the mass in the stream ($\widetilde{\text{MAD}}$). Quantities in Kg.

	V4 - Other plastics			V5 - Aluminum			L0 - Landfill		
	Test2	**Model**	**AD**	**Test2**	**Model**	**AD**	**Test2**	**Model**	**AD**
PET	0.248	0.442	0.194	0.258	0.102	0.156	8.116	5.070	3.046
HDPE	0.044	0.541	0.497	0.312	0.000	0.312	11.782	13.501	1.719
Aluminum	0.614	1.027	0.413	39.918	33.141	6.777	0.131	1.300	1.169
Ferrous	0.073	0.454	0.381	0.000	0.000	0.000	3.142	5.796	2.654
Tetra brik	0.190	0.161	0.029	3.837	3.018	0.819	1.571	1.571	0.000
Other plastics	102.520	101.592	0.928	0.473	0.246	0.227	2.618	4.473	1.855
Other	96.311	95.039	1.272	5.202	5.256	0.054	2132.640	2158.690	26.050
Total	200.000	199.255	3.714	50.000	41.764	8.343	2160.000	2190.401	36.493
	MAD		0.929	**MAD**		1.192	**MAD**		5.213
	$\widetilde{\textbf{MAD}}$		0.464%	$\widetilde{\textbf{MAD}}$		2.384%	$\widetilde{\textbf{MAD}}$		0.241%

Table A.19: Composition of the V4, V5, and L0 output streams from Test 2 and the model. The table shows the absolute deviation (AD) per material type, the mean absolute deviation (MAD) per stream, and the MAD divided by the mass in the stream ($\widetilde{\text{MAD}}$). Quantities in Kg.

	R0 - Recirculation from U4			R1 - Recirculation from U7		
	Test 2	**Model**	**AD**	**Test 2**	**Model**	**AD**
PET	30.736	30.734	0.002	65.475	65.477	0.002
HDPE	0.264	0.264	0.000	31.694	31.694	0.000
Aluminum	1.869	1.869	0.000	2.120	7.221	5.101
Ferrous	0.036	0.036	0.000	0.390	28.886	28.496
Tetra brik	6.686	6.685	0.001	65.102	65.102	0.000
Other plastics	7.657	7.657	0.000	32.220	32.220	0.000
Other	36.752	36.751	0.001	62.999	63.007	0.008
Total	84.000	83.996	0.004	260.000	293.607	33.608
	MAD		0.001	**MAD**		4.801
	$\widetilde{\textbf{MAD}}$		0.001%	$\widetilde{\textbf{MAD}}$		1.847%

Table A.20: Composition of the R0 and R1 recirculation streams from Test 2 and the model. The table shows the absolute deviation (AD) per material type, the mean absolute deviation (MAD) per stream, and the MAD divided by the mass in the stream ($\widetilde{\text{MAD}}$). Quantities in Kg.

A.5 Performance of the current configuration without QC

We applied the mathematical model to the current configuration without QC, input from Section A.3, and estimated parameters.

	V0 Ferrous		**V1 PET**		**V2 HDPE**	
Meet Requirements	TRUE		TRUE		FALSE	
Selling price $\frac{€}{ton}$	179		320		0	
Stream Mass	926.087		882.605		305.637	
Material Type	*Concentration* (%)	*Flow* ($\frac{kg}{hour}$)	*Concentration* (%)	*Flow* ($\frac{kg}{hour}$)	*Concentration* (%)	*Flow* ($\frac{kg}{hour}$)
PET	0.165	1.526	94.661	835.483	0.197	0.602
HDPE	0.020	0.184	0.031	0.277	84.782	259.126
Aluminum	0.014	0.125	0.037	0.330	0.034	0.102
Ferrous	96.026	889.287	0.000	0.000	0.000	0.000
Tetra brik	0.093	0.861	1.965	17.347	0.084	0.255
Other plastics	0.090	0.832	0.360	3.178	0.466	1.425
Other	3.593	33.274	2.945	25.990	14.437	44.126

	V3 Tetra brik		**V4 Other Plastics**		**V5 Aluminum**		**L1 Landfill**	
Meet Requirements	TRUE		TRUE		TRUE			
Selling price $\frac{€}{ton}$	0		0		0			
Stream Mass	444.334		528.890		110.323		5427.245	
Material Type	*Concentration* (%)	*Flow* ($\frac{kg}{hour}$)	*Concentration* (%)	*Flow* ($\frac{kg}{hour}$)	*Concentration* (%)	*Flow* ($\frac{kg}{hour}$)	*Concentration* (%)	*Flow* ($\frac{kg}{hour}$)
PET	0.197	0.602	0.089	0.395	0.182	0.201	0.204	9.964
HDPE	84.782	259.126	0.012	0.054	0.000	0.000	0.645	31.519
Aluminum	0.034	0.102	0.041	0.182	81.866	90.317	0.073	3.543
Ferrous	0.000	0.000	0.000	0.000	0.000	0.000	0.258	12.620
Tetra brik	0.084	0.255	95.337	423.613	6.659	7.346	0.078	3.823
Other plastics	0.466	1.425	0.358	1.593	0.682	0.753	0.280	13.690
Other	14.437	44.126	4.163	18.498	10.610	11.706	98.461	4807.966

A.6 Performance of the Current Configuration with QC

Tables A.21 and A.22 report the predicted composition of the output streams of HDPE and aluminum.

V2 HDPE

	No QC		**QC**	
Meet Requirements	No		Yes	
Material Type	*Concentration* %	*Flow* ($\frac{kg}{hour}$)	*Concentration* %	*Flow* ($\frac{kg}{hour}$)
PET	0.197	0.602	0.045	0.120
HDPE	84.782	259.126	96.535	259.126
Aluminum	0.034	0.102	0.008	0.021
Ferrous	0.000	0.000	0.000	0.000
Tetra brik	0.084	0.255	0.019	0.051
Other plastics	0.466	1.425	0.106	0.285
Other	14.437	44.126	3.288	8.825

Table A.21: Composition of the HDPE output stream in the current configuration with and without QC.

V2 HDPE

	No QC		**QC**	
Meet Requirements	No		Yes	
Material Type	*Concentration* %	*Flow* ($\frac{kg}{hour}$)	*Concentration* %	*Flow* ($\frac{kg}{hour}$)
PET	0.182	0.201	0.043	0.040
HDPE	0.000	0.000	0.000	0.000
Aluminum	81.866	90.317	95.758	90.317
Ferrous	0.000	0.000	0.000	0.000
Tetra brik	6.659	7.346	1.558	1.469
Other plastics	0.682	0.753	0.160	0.151
Other	10.610	11.706	2.482	2.341

Table A.22: Composition of the aluminum output stream in the current configuration with and without QC.

Appendix B

Proposed Configurations

In this appendix, we report the output composition associated to:

- **Configuration C1:** Configuration with highest measure of fit and QC active. Results in Appendix B.1.
- **Configuration C2:** Configuration with second highest measure of fit and QC active. Results in Appendix B.2.
- **Configuration C3:** Configuration with highest measure of fit and QC inactive. Results in Appendix B.3.
- **Configuration C4:** Configuration with second highest measure of fit and QC inactive. Results in Appendix B.4.

B.1 Configuration C1

Configuration with highest measure of fit and QC active.

	V0 Ferrous		V1 PET		V2 HDPE	
Meet Requirements	TRUE		TRUE		TRUE	
Selling price $\frac{€}{ton}$	179		320		450	
Stream Mass	901.832		878.36		260.179	
Material Type	*Concentration* (%)	*Flow* ($\frac{kg}{hour}$)	*Concentration* (%)	*Flow* ($\frac{kg}{hour}$)	*Concentration* (%)	*Flow* ($\frac{kg}{hour}$)
PET	0.15	1.411	93.251	819.077	1.467	3.816
HDPE	0.027	0.256	3.205	28.154	97.689	254.167
Aluminum	0.015	0.14	0.154	1.353	0.039	0.102
Ferrous	96.19	902.648	0	0	0	0
Tetra brik	0.069	0.648	0.07	0.619	0.266	0.692
Other plastics	0.069	0.644	0.51	4.476	0.055	0.144
Other	3.48	32.658	2.81	24.681	0.484	1.258

	V3 Tetra brik		V4 Other Plastics		V5 Aluminum		L1 Landfill	
Meet Requirements	TRUE		TRUE		TRUE			
Selling price $\frac{€}{ton}$	157		0		727			
Stream Mass	453.264		31.649		91.899		5427.245	
Material Type	*Concentration* (%)	*Flow* ($\frac{kg}{hour}$)	*Concentration* (%)	*Flow* ($\frac{kg}{hour}$)	*Concentration* (%)	*Flow* ($\frac{kg}{hour}$)	*Concentration* (%)	*Flow* ($\frac{kg}{hour}$)
PET	0.254	1.15	1.171	0.371	1.388	1.276	0.404	21.94
HDPE	0.374	1.694	2.543	0.805	0	0	0.135	7.345
Aluminum	0.177	0.803	1.643	0.52	97.21	89.335	0.095	5.144
Ferrous	0	0	0.53	0.168	0	0	0.001	0.079
Tetra brik	97.876	443.638	0.114	0.036	0.803	0.738	0.134	7.266
Other plastics	0.12	0.544	81.674	25.849	0.29	0.266	5.536	300.451
Other	1.199	5.436	12.324	3.901	0.309	0.284	93.694	5085.02

B.2 Configuration C2

Configuration with second highest measure of fit and QC active. Results in Appendix B.2

	V0 Ferrous		**V1 PET**		**V2 HDPE**	
Meet Requirements	TRUE		TRUE		TRUE	
Selling price $\frac{€}{ton}$	179		320		450	
Stream Mass $\frac{kg}{hour}$	877.98		920.02		260.316	
Material Type	*Concentration* (%)	*Flow* ($\frac{kg}{hour}$)	*Concentration* (%)	*Flow* ($\frac{kg}{hour}$)	*Concentration* (%)	*Flow* ($\frac{kg}{hour}$)
PET	0.152	1.424	93.731	822.935	1.48	3.852
HDPE	0.027	0.256	3.171	27.838	97.696	254.318
Aluminum	0.015	0.142	0.134	1.176	0.007	0.019
Ferrous	96.127	902.661	0	0	0	0
Tetra brik	0.07	0.655	0.074	0.652	0.269	0.699
Other plastics	0.071	0.662	0.141	1.234	0.057	0.147
Other	3.539	33.233	2.75	24.144	0.492	1.28

	V3 Tetra brik		**V4 Other Plastics**		**V5 Aluminum**		**L1 Landfill**	
Meet Requirements	TRUE		TRUE		TRUE			
Selling price $\frac{€}{ton}$	157		0		727			
Stream Mass	457.277		42.493		90.287		5413.616	
Material Type	*Concentration* (%)	*Flow* ($\frac{kg}{hour}$)	*Concentration* (%)	*Flow* ($\frac{kg}{hour}$)	*Concentration* (%)	*Flow* ($\frac{kg}{hour}$)	*Concentration* (	*Flow* ($\frac{kg}{hour}$)
PET	0.254	1.161	13.003	5.525	0.097	0.087	0.260	14.055
HDPE	0.371	1.695	2.679	1.138	0.000	0.000	0.133	7.176
Aluminum	0.032	0.146	1.158	0.492	99.044	89.424	0.111	5.997
Ferrous	0.000	0.000	0.395	0.168	0.000	0.000	0.001	0.066
Tetra brik	98.012	448.185	0.093	0.040	0.393	0.355	0.056	3.052
Other plastics	0.122	0.558	70.883	30.120	0.145	0.131	5.533	299.521
Other	1.210	5.531	11.788	5.009	0.320	0.289	93.907	5083.749

B.3 Configuration C3

Configuration with highest measure of fit and QC inactive.

	V0 Ferrous		V1 PET		V2 HDPE	
Meet Requirements	TRUE		TRUE		TRUE	
Selling price $\frac{€}{ton}$	179		320		450	
Stream Mass	902.877		760.243		280.375	
Material Type	*Concentration* (%)	*Flow* ($\frac{kg}{hour}$)	*Concentration* (%)	*Flow* ($\frac{kg}{hour}$)	*Concentration* (%)	*Flow* ($\frac{kg}{hour}$)
PET	0.126	1.139	94.905	721.511	1.283	3.598
HDPE	0.002	0.017	1.302	9.895	98.077	274.984
Aluminum	0.002	0.021	0.157	1.192	0.042	0.117
Ferrous	99.78	900.894	0	0	0	0
Tetra brik	0.001	0.011	0.041	0.31	0.186	0.522
Other plastics	0.004	0.038	0.306	2.327	0.028	0.079
Other	0.084	0.757	3.289	25.008	0.383	1.074

	V3 Tetra brik		V4 Other Plastics		V5 Aluminum		L1 Landfill	
Meet Requirements	TRUE		TRUE		TRUE			
Selling price $\frac{€}{ton}$	157		0		727			
Stream Mass	338.551		19.48		87.054		5692.42	
Material Type	*Concentration* (%)	*Flow* ($\frac{kg}{hour}$)	*Concentration* (%)	*Flow* ($\frac{kg}{hour}$)	*Concentration* (%)	*Flow* ($\frac{kg}{hour}$)	*Concentration* (%)	*Flow* ($\frac{kg}{hour}$)
PET	0.115	0.39	1.676	0.327	0.099	0.086	2.143	121.988
HDPE	1.899	6.427	1.452	0.283	0	0	0.014	0.815
Aluminum	1.147	3.883	2.351	0.458	99.247	86.399	0.094	5.327
Ferrous	0	0	5.146	1.002	0	0	0.018	0.999
Tetra brik	96.591	327.01	0.093	0.018	0.625	0.544	2.2	125.221
Other plastics	0.054	0.183	68.992	13.439	0.021	0.018	5.556	316.29
Other	0.194	0.658	20.289	3.952	0.008	0.007	89.975	5121.78

B.4 Configuration C4

Configuration with second highest measure of fit and QC inactive.

	V0 Ferrous		**V1 PET**		**V2 HDPE**	
Meet Requirements	TRUE		TRUE		TRUE	
Selling price $\frac{€}{ton}$	179		320		450	
Stream Mass	901.832		739.833		280.375	
Material Type	*Concentration* (%)	*Flow* ($\frac{kg}{hour}$)	*Concentration* (%)	*Flow* ($\frac{kg}{hour}$)	*Concentration* (%)	*Flow* ($\frac{kg}{hour}$)
PET	0.008	0.076	96.64	714.975	1.251	3.561
HDPE	0.001	0.011	1.359	10.058	98.136	279.364
Aluminum	0.002	0.016	0.14	1.033	0.036	0.101
Ferrous	99.985	901.694	0	0	0	0
Tetra brik	0.002	0.016	1.723	12.744	0.182	0.517
Other plastics	0	0.004	0.041	0.301	0.026	0.074
Other	0.002	0.014	0.098	0.722	0.371	1.055

	V3 Tetra brik		**V4 Other Plastics**		**V5 Aluminum**		**L1 Landfill**	
Meet Requirements	TRUE		TRUE		TRUE			
Selling price $\frac{€}{ton}$	157		0		727			
Stream Mass	314.739		455.333		91.6		5292.992	
Material Type	*Concentration* (%)	*Flow* ($\frac{kg}{hour}$)	*Concentration* (%)	*Flow* ($\frac{kg}{hour}$)	*Concentration* (%)	*Flow* ($\frac{kg}{hour}$)	*Concentration* (%)	*Flow* ($\frac{kg}{hour}$)
PET	0.107	0.338	0.177	0.808	0.176	0.161	2.439	129.122
HDPE	0.625	1.968	0.003	0.012	0	0	0.019	1.008
Aluminum	0.181	0.57	0.029	0.133	98.405	90.139	0.102	5.405
Ferrous	0	0	0.003	0.016	0	0	0.022	1.185
Tetra brik	98.875	311.199	0.065	0.295	0.948	0.868	2.418	127.997
Other plastics	0.048	0.151	53.423	243.253	0.156	0.143	1.671	88.448
Other	0.163	0.514	46.299	210.816	0.316	0.289	93.328	4939.826

Bibliography

[1] Pillai, R., & Shah, R. (2014). Municipal Solid Waste Management: Current Practices and Futuristic Approach. *SCMS Journal Of Indian Management*, 11(4), 72-78.

[2] The U.S. Environmental Protection Agency. (2015) Retrieved from http://www.epa.gov/epawaste/index.htm

[3] The United Nations Environment Programme, International Environmental Technology Center (2005). *Solid Waste Management* [Pdf]. Retrieved from http://www.unep.org/ietc/informationresources/solidwastemanagementpublication/tabid/79356/default.aspx

[4] World Bank (1992). *World Development Report 1992: Development and the Environment.* New York: Oxford University Press. Retrieved from https://openknowledge.worldbank.org/handle/10986/5975 License: CC BY 3.0 IGO.

[5] OECD (2010). Municipal Waste. *OECD Factbook 2010: Economic, Environmental and Social Statistics*, OECD Publishing, Paris. Retrieved from http://dx.doi.org/10.1787/factbook-2010-64-en

[6] OECD (2014)- Municipal Waste. in *OECD Factbook 2014: Economic, Environmental and Social Statistics*, OECD Publishing. Retrieved from http://dx.doi.org/10.1787/factbook-2014-70-en

[7] Key Note Global (2007). *Global Waste Management Market Assessment 2007.* Key Note Publications ltd.

[8] Giusti, L. (2009). A review of waste management practices and their impact on human health. *Waste Management*, 29(8), 2227 - 2239. http://www.sciencedirect.com/science/article/pii/S0956053X09001275

[9] EASUR(2005). Waste Management in China: Issues and Recommendations. *Urban Development Working Papers, East Asia Infrastructure Department*, World Bank, Working Paper No. 9, East Asia and Pacific Urban Development Sector Unit (EASUR), May 2005.

[10] OECD (2014). Municipal Waste. *OECD Environment Statistics (database).* DOI: http://dx.doi.org/10.1787/data-00601-en (Accessed on 17 February 2015)

[11] EPA (2012). Municipal Solid Waste Generation, Recycling, and Disposal in the United States: Facts and Figures for 2012 [Pdf]. Retrieved from http://www.epa.gov/epawaste/nonhaz/municipal/pubs/2012_msw_fs.pdf

[12] Stessel, R. I. (1996). Recycling and Resource Recovery Engineering, Principles of Waste Processing. Springer.

[13] "Waste hierarchy" by User:Drstuey, Stannered - File:Waste-hierarchy.png. Licensed under CC BY-SA 3.0 via Wikimedia Commons - http://commons.wikimedia.org/wiki/File:Waste_hierarchy.svg#mediaviewer/File:Waste_hierarchy.svg

[14] Wang, J. (2006). All in One: Do Single-Stream Curbside Recycling Programs Increase Recycling Rates?.

[15] Fishbein, B. K., Ehrenfeld, J. R., & Young, J. E. (2000). Extended Producer Responsibility. A Materials Policy for the 21st Century, New York: Inform Inc.

[16] Altimir, N. (2006). The ozone transfer between atmosphere and vegetation. A study on Scots pine in the field. Dissertationes Forestales.

[17] Wang, J. (2006). All in One: Do Single-Stream Curbside Recycling Programs Increase Recycling Rates?. Single-Stream Recycling.

[18] Connecticut Resources Recovery Authority, Hartford, CT (2013-03-28). "The Facts About Single-Stream Recycling." Retrieved from http://www.crra.org/pages/single-stream_recycling.htm

[19] "Sustainable Facilities Tool: Solid Waste System Overview". sftool.gov. Retrieved 1 July 2014. Retrieved from https://sftool.gov/explore/green-building/section/57/solid-waste/solid-waste#recycling_program.

[20] BARNES Reports: U.S. Materials Recovery Facilities Industry (NAICS 56292). (2013). United States Materials Recovery Facilities Industry Report, 1-140

[21] Albert,James G. (1977), "Aluminum Recovery: A Status Report," *NCRR Bulletin.* Reprint 7(2).

[22] Gitzhofer, Karl-Heinz (1991). "Construction of an Experimental Unit for the Mechanical Colour Sorting of Non-Crushed Recycled Container Glass". *Glastech Ber*, (64)1:9-15.

[23] Lewis, M.R., Newell, T.A. (1992). "Development of an Automated Color Sorting System for Recyclable Glass Containers," *Proceedings of the 1992 National Waste Processing Conference.* ASME. New Your, pp. 197-207.

[24] Wheeler P.A., Barton J.R., New R., 1989. An Empirical Approach to the Design of Trommel Screens for Fine Screening of Domestic Refuse. Resources, Conservation and Recycling, 2 261-273

[25] Alter H. 1981. Design Models of Trommels for Resource Recovery Processing. Resources and Conservation, 6 223-240

[26] Stessel R.I. 1991. A new Trommel Model. Resources, Conservation and Recycling, 6 1-22

[27] Sullivan J. W., Hill R. M., Sullivan, J. F. (1992). The Place of the Trommel in Resource Recovery.

[28] Hershaft, A. (1972). Solid waste treatment technology. Environmental Science & Technology, 6(5), 412-421.

[29] Representation of ballistic operations. [Graph illustration retrieved on April 20, 2015]. Retrieved from http://www.tinsleycompany.com/recycling/ballistic-separators/

[30] Representation of ballistic operations. [Graph illustration retrieved on April 20, 2015]. Retrieved from http://www.tinsleycompany.com/recycling/ballistic-separators/

[31] Diaz, Luis F., Savage, and Golueke. Resource Recovery from Municipal Solid Wastes, Volume I. Boca Raton, FL: CRC Press, Inc., 1982.

[32] Berenyi, Eileen Brettler. The Materials Recycling and Processing Industry in the United States. New York, NY: Governmental Advisory Associates, Inc., 1997.

[33] Palmer, James R. (1999). Concept Design and Optimization of MSW Management Systems. Master Thesis at the faculty of the Graduate School of Engineering of the Air Force Institute of Technology Air University Air Education and Training Command.

[34] Tchobanoglous, George, Hilary Theisen, and Sam A. Vigil. Integrated Solid Waste Management: Engineering Principles and Management Issues. New York, NY: McGraw-Hill Incorporated, 1993.

[35] Vesilind, P. Aarne and Alan E. Rimer. Unit Operations in Resource Recovery Engineering. Englewood Cliffs, NJ: Prentice-Hall, 1981.

[36] P. C. Rem, P. A. Leest, and A. J. van den Akker. A model for eddy current separation. International Journal of Mineral Processing, 49:193–200, 1997.

[37] P. C. Rem, E. M. Beunder, and A. J. van den Akker. Simulation of eddy-current separators. IEEE Transactions on Magnetics, 34(4):2280–2286, July 1998.

[38] Fabiano Maraspin, Paolo Bevilacqua, and Peter C. Rem. Modelling the throw of metals and nonmetals in eddy current separations. International Journal of Mineral Processing, 73:1–11, 2004.

[39] Shunli Zhang, Eric Forssberg, Bo Arvidson, and William Moss. Separation mechanisms and criteria of a rotating eddy-current separator operation. Resources, Conservation and Recycling, 25:215–232, 1999.

[40] Timothy G. Gutowski and Jeffrey B. Dahmus. (2005). Product recycling systems. In NSF Design Service and Manufacturing Grantees and Research Conference, Scottsdale, AZ, 3-6 January 2005.

[41] Dahmus, J. B., and T. G. Gutowski. What Gets Recycled: An Information Theory Based Model of Product Recycling, Environmental Science and Technology, 2007, 41, 7543 - 7550

[42] Timothy G. Gutowski, J. B. Dahmus, D. K. Albino, and Matthew S. Branham. (2007) Bayesian material separation model with applications to recycling. In International Symposium on Electronics and the Environment, Orlando, FL, 7-10 May 2007. IEEE.

[43] Gutowski, T. G., Wolf, M. I., Dahmus, J. B., & Albino, D. K. NSF GRANT# 0423484 NSF PROGRAM NAME: Design, Manufacturing, and Innovation.

[44] Wolf, M. I., Colledani, M., Gershwin, S. B., & Gutowski, T. G. (2010, May). Modeling and design of multi-stage separation systems. In Sustainable Systems and Technology (ISSST), 2010 IEEE International Symposium on (pp. 1-6). IEEE.

[45] Wolf, M. I. (2011). Modeling and design of material separation systems with applications to recycling (Doctoral dissertation, Massachusetts Institute of Technology).

[46] Wolf, M. I., Colledani, M., Gershwin, S. B., & Gutowski, T. G. (2013). A network flow model for the performance evaluation and design of material separation systems for recycling. Automation Science and Engineering, IEEE Transactions on, 10(1), 65-75.

[47] A. van Schaik, M. A. Reuter, and K. Heiskanen. The influence of particle size reduction and liberation on the recycling rate of end-of-life vehicles. Minerals Engineering, 17:331–347, 2004.

[48] ISRI Scrap Specifications, Circular 2008: Guidelines for Nonferrous Scrap, Ferrous Scrap, Glass Cullet, Paper Stock, Plastic Scrap, Electronics Scrap, Tire Scrap. Published by Institute of Scrap Recycling Industries.

[49] Deutsche Gesellschaft fur Kreislaufwirtschaft und Rohstoffe mbH. Plastics Recycling Current Product Specifications. Available at http://www.gruener-punkt.de/en/waste-management/downloads/plastics-recycling.html. Accessed on April 9, 2011.

[50] Holland, J. (1975) Adaptation in Natural and Artificial Systems. University of Michigan Press.

[51] De Jong, K. A. (1975). Analysis of the behavior of a class of genetic adaptive systems.

[52] Whitley, D. (1994). A genetic algorithm tutorial. Statistics and computing, 4(2), 65-85.

[53] H. Aytug , M. Khouja & F. E. Vergara (2003). Use of genetic algorithms to solve production and operations management problems: A review, International Journal of Production Research, 41:17, 3955-4009, DOI: 10.1080/00207540310001626319

[54] Reeves, C. R. (1997). Feature Article-Genetic Algorithms for the Operations Researcher. INFORMS journal on computing, 9(3), 231-250.

[55] Bean, J. C. (1994). Genetic algorithms and random keys for sequencing and optimization. ORSA journal on computing, 6(2), 154-160.

[56] Aravind, S. (2004). A fast elitist multiobjective genetic algorithm: NSGA-II. IEEE Transactions on Evolutionary Computation.

[57] Horn, J., Nafpliotis, N., & Goldberg, D. E. (1994, June). A niched Pareto genetic algorithm for multiobjective optimization. In Evolutionary Computation, 1994. IEEE World Congress on Computational Intelligence., Proceedings of the First IEEE Conference on (pp. 82-87). Ieee.

[58] Deb, K., Pratap, A., Agarwal, S., & Meyarivan, T. A. M. T. (2002). A fast and elitist multiobjective genetic algorithm: NSGA-II. Evolutionary Computation, IEEE Transactions on, 6(2), 182-197.

[59] Zitzler, E., & Thiele, L. (1999). Multiobjective evolutionary algorithms: a comparative case study and the strength Pareto approach. evolutionary computation, IEEE transactions on, 3(4), 257-271.

[60] Konak, A., Coit, D. W., & Smith, A. E. (2006). Multi-objective optimization using genetic algorithms: A tutorial. Reliability Engineering & System Safety, 91(9), 992-1007.

[61] Burdett, R. L., & Kozan, E. (2000). Evolutionary algorithms for flowshop sequencing with non-unique jobs. International Transactions in Operational Research, 7(4-5), 401-418.

[62] Chang, P. C., Chen, S. H., & Lin, K. L. (2005). Two-phase sub population genetic algorithm for parallel-machine scheduling problem. Expert Systems with Applications, 29(3), 705-712.

[63] Cai, X., & Li, K. N. (2000). A genetic algorithm for scheduling staff of mixed skills under multi-criteria. European Journal of Operational Research, 125(2), 359-369.

[64] Simaria, A. S., & Vilarinho, P. M. (2004). A genetic algorithm based approach to the mixed-model assembly line balancing problem of type II. Computers & Industrial Engineering, 47(4), 391-407.

[65] Hyun, C. J., Kim, Y., & Kim, Y. K. (1998). A genetic algorithm for multiple objective sequencing problems in mixed model assembly lines. Computers & Operations Research, 25(7), 675-690.

[66] Sabuncuoglu, I., Erel, E., & Tanyer, M. (2000). Assembly line balancing using genetic algorithms. Journal of intelligent manufacturing, 11(3), 295-310.

[67] Pierreval, H., & Tautou, L. (1997). Using evolutionary algorithms and simulation for the optimization of manufacturing systems. IIE transactions, 29(3), 181-189.

[68] Beasley, J. E., & Chu, P. C. (1996). A genetic algorithm for the set covering problem. European Journal of Operational Research, 94(2), 392-404.

[69] Altiparmak, F., Gen, M., Lin, L., & Paksoy, T. (2006). A genetic algorithm approach for multi-objective optimization of supply chain networks. Computers & Industrial Engineering, 51(1), 196-215.

[70] Farahani, R. Z., & Elahipanah, M. (2008). A genetic algorithm to optimize the total cost and service level for just-in-time distribution in a supply chain. International Journal of Production Economics, 111(2), 229-243.

[71] Gravel, M., Nsakanda, A. L., & Price, W. (1998). Efficient solutions to the cell-formation problem with multiple routings via a double-loop genetic algorithm. European Journal of Operational Research, 109(2), 286-298.

[72] Moon, C., & Gen, M. (1999). A genetic algorithm-based approach for design of independent manufacturing cells. International Journal of Production Economics, 60, 421-426.

[73] Plaquin, M. F., & Pierreval, H. (2000). Cell formation using evolutionary algorithms with certain constraints. International Journal of Production Economics, 64(1), 267-278.

[74] Srinivas, M., & Patnaik, L. M. (1994). Adaptive probabilities of crossover and mutation in genetic algorithms. Systems, Man and Cybernetics, IEEE Transactions on, 24(4), 656-667.